DEVELOPMENT AND VERIFICATION OF AN INTELLIGENT SENSOR SYSTEM FOR ROADWAY AND BRIDGE SURFACE CONDITION ASSESSMENTS

by

Mohammed Aljuboori

A Thesis Submitted in

Partial Fulfillment of the

Requirements for the Degree of

Master of Science

in Engineering

at

The University of Wisconsin-Milwaukee

August 2014

ABSTRACT

DEVELOPMENT AND VERIFICATION OF AN INTELLIGENT SENSOR SYSTEM FOR ROADWAY AND BRIDGE SURFACE CONDITION ASSESSMENTS

by

Mohammed Aljuboori

The University of Wisconsin-Milwaukee, 2014
Under the Supervision of Professor Habibollah Tabatabai

Surface ice formation on roadways and bridges has been a major safety issue in transportation. Surface ice, or black ice, is a layer of frozen water that can form on roadway surface. Surface ice can form when moisture comes in contact with a pavement surface that is at a temperature below freezing. On bridges, surface ice formation tends to occur more rapidly because bridges are elevated, and are therefore subjected to air circulation both above and below the concrete slab. Each year hundreds of people die in road accidents related to surface ice in the United States alone. Hazards associated with surface ice presence are greatest in the Midwestern United States.

In this thesis, an intelligent sensor system is developed for detection of surface ice on roads, runways, and bridges. The proposed sensor can also identify wet, dry, and frozen

conditions. A decision algorithm is also developed that utilizes sensor output and measured surface temperature to determine surface conditions.

The proposed sensor works by monitoring changes in electrical resistance between stainless steel poles embedded in the concrete sensor. The sensor consists of a 4-in-diameter, 1.5-in-high, concrete cylinder.

The concrete cylinder includes an opening on its bottom surface to house the electrical circuits, power supply, wireless transmission unit, surface temperature sensor, and electrical controller that implements the decision algorithm. Two sets of poles (two LUS poles and two LU poles) are embedded at a distance of 2 inches between them. The LUS poles are sensitive to both above-surface and near-surface conditions. LU poles are only sensitive to changes directly above the sensor's top surface. Resistance changes are measured using two Wheatstone bridge circuits.

A serious of laboratory experiments were performed on two sensor prototypes. The experimental results indicated that the proposed intelligent sensor can effectively detect various environmental conditions of interest including surface ice and wet conditions.

The sensor output can be transmitted wirelessly to activate side warnings (lights/sounds/messages), or signals can be relayed to a website, transportation control center, maintenance crews, or control systems in vehicles.

TABLE OF CONTENTS

LIST OF FIGURES

LIST OF TABLES

ACKNOWLEDGMENTS

I would like to thank Professor Habibollah Tabatabai for his great efforts, guidance and support in this research. This study could not been accomplished without his never-ending assistance, brilliant thoughts, and encouragement. I would like to also thank Professor Tabatabai for his advice and counseling throughout the course of this research. I am also grateful for the guidance and help from my committee, Professor Hani Titi and Professor Rani El-Hajjar. I would like to thank my family, especially my father who was the first source of inspiration for me to accomplish this study.

The experimental tests were conducted in Professor Tabatabai's laboratory at the University of Wisconsin, Milwaukee (UWM). I am also thankful to Professor Konstantin Sobolev who allowed me to use the freezer located in the concrete laboratory. I am appreciative for the help of the Director of the Structural Laboratory, Professor Ghorbanpoor and the help provided by Mr. Rahim Rashadi. Thanks are also due to all my friends for their unlimited support. Several undergraduate students helped with some of my laboratory work, including Kenneth Sosinski and Brian Mullen.

My research and study here at UWM was partially funded by the Department of Civil and Environmental Engineering through teaching assistantships. I am grateful for the help that the Department and its faculty offered to me throughout my graduate education.

Development and Verification of an Intelligent Sensor System for Roadway and Bridge Surface Condition Assessments

Introduction

1.1 Background

Formation of surface ice (black ice) on roadways, runways, and bridge decks is a major transportations safety issue. In this work, a novel and low-cost intelligent sensor system is proposed to detect surface ice and other pavement conditions (wet, dry, frozen …). This chapter provides an overview of the safety issue addressed in this thesis, presents the objective and scope of research, and discusses the importance of this work.

1.2 Problem statement

Surface ice, or glazed ice, is a thin layer of frozen water that can form on roadway surface. This ice layer is transparent and allows the roadway surface below to be seen through the ice. This layer is commonly referred to as ‘black ice” because the pavement surface can be seen while the ice may not be visible. Black ice forms when moisture (from rain, fog, etc) meets a surface with a temperature below freezing. Black ice affects vehicular traffic on the road as well as pedestrians and cyclists on sidewalks or walkways. As a layer of ice forms on a surface, the contact friction force decreases significantly. This condition significantly increases the slippage hazard for pedestrians and vehicular traffic.

Surface ice needs two main components to form: moisture and low temperatures. There are many potential sources of moisture for black ice formation including rain, snow, hail, accidental water discharge, sleet, freezing fog, or blowing and drifting snow [(1)]. Black ice can sometimes form when there is a sudden warm-up after a long period of very cold weather. The pavement would stay below freezing, while there is moisture is in the air and on its surface [(1)]. Formation of surface ice occurs more frequently on bridge decks because the decks are exposed to outside temperatures on their bottom surfaces as well.

Drivers can lose control of their vehicles when black ice exists on the roads, especially on highways when speed limits are higher [(2)]. Drivers may realize that ice exists only after they lose control of their vehicles. Some drivers may react by pressing the brake pedal, which could aggravate the situation. Due to the continuity of motion (inertia), once the vehicle tries to brake, tires may become locked [(2)]. A sufficient friction force would need to be developed between tires and the road surface to decelerate and stop the vehicle [(2)]. In case of black ice or other surface ice, the friction factor will be relatively small. The vehicle could slip, rotate, crash into other vehicles, or exit the road altogether. According to www.icyroadsafety.com, black ice annually causes more weather-relevant deaths and injuries than all other severe weather conditions combined [(3)]. Table 1.2-1 shows a 6-state comparison between fatalities caused by tornados and those caused by icy road accidents in 2008-2009 in six states [(3)]. Figure 1.2-1 shows the numbers of fatalities in reported 2009-2010 [(3)]. Figure 1.2-2 shows road ice hazard

varies in different regions of the United States [3]. Such hazards are greatest in the midwestern United States.

Table 1.2-1: Comparison between fatalities due to tornado and icy road conditions in six states [3]

State	Tornado Fatalities	Icy Roads' Fatalities
Oklahoma	7	15
Kansas	2	14
Texas	0	19
Iowa	6	22
Missouri	11	20
Minnesota	1	27

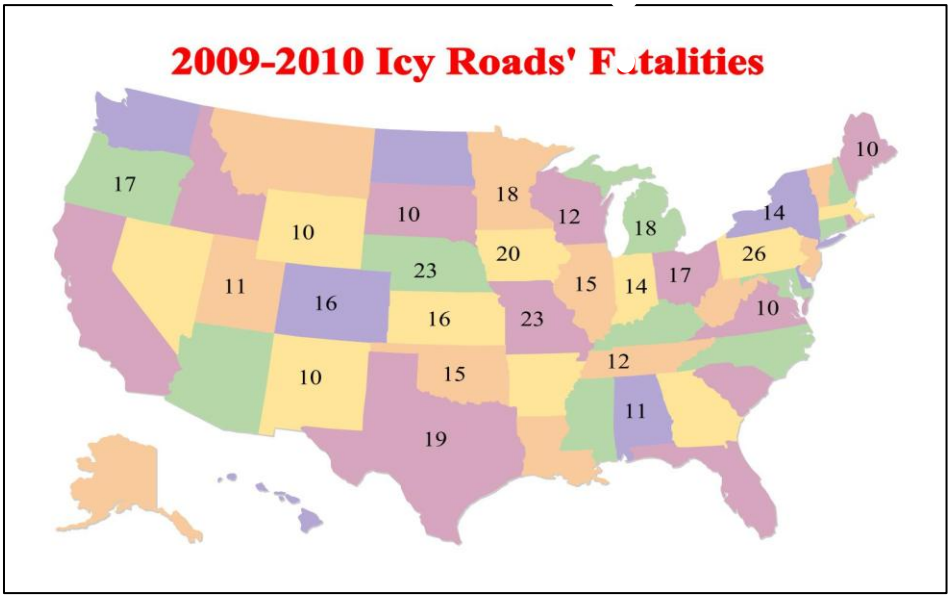

Figure 1.2-1: Icy roads fatalities for 2008-2009[3]

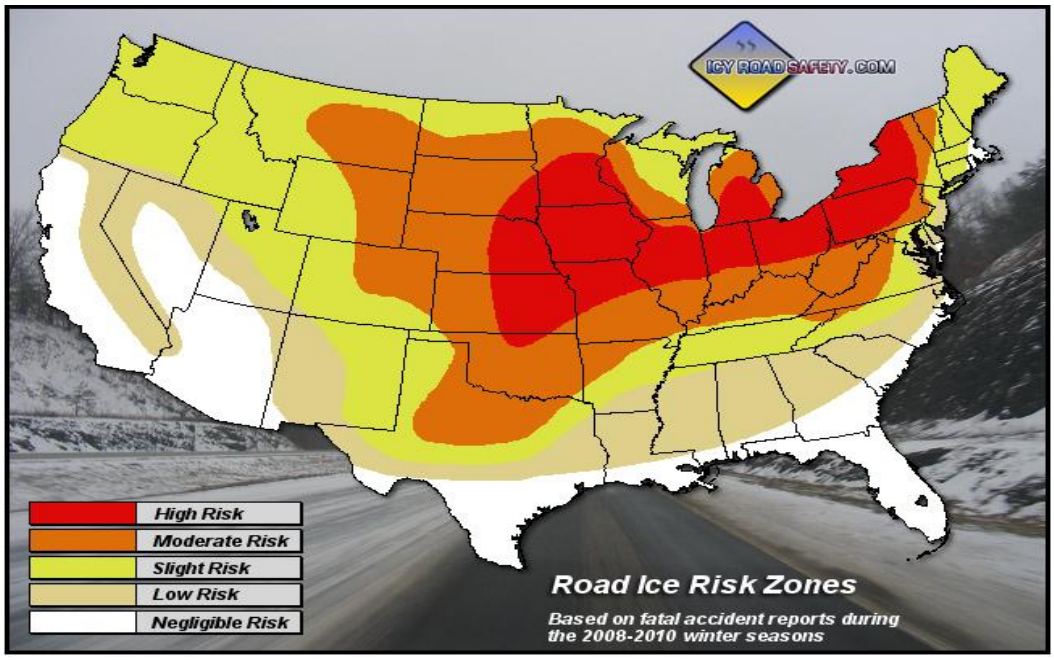

Figure 1.2-2: Variation of risks associated with icy roads in the United States[3]

Ice hazards differ from location to location, and also depend on roadway alignment. For example, if black ice forms on a downhill surface, the potential for slip increases. Vehicles that are approaching the crest of a hill would not be able to see icy condition on the other side of the crest.

Surface ice formation on bridges and overpasses can occur quicker than the approach pavement. Bridges and overpasses are elevated, and are subjected to air circulation both above and below the concrete slab. This causes the temperature of bridge deck to drop more rapidly. Water (from rain, melted snow, fog, or other sources) may then come in contact with the cold surface and result in surface ice.

1.5 Research Objective

The primary objectives of this research program were as follows

- Development of a new intelligent sensor system for detection of surface ice, water, frozen pavement, and dry conditions on roadways, bridges and runways, based on resistance measurements.
- Conducting laboratory tests on the sensor system to verify its effectiveness in detecting varying environmental conditions (in particular surface ice conditions).

1.6 Research Significance

The proposed intelligent sensor system will help address a major transportation safety issues, i.e. the presence of surface ice on roads, bridges, and runways. This low-cost intelligent system can provide timely information to drivers to allow them to take whatever precautions needed to avoid accidents. This development will also help transportation authorities to identify areas that need special services during snow and ice events. More importantly, this will save people's lives by helping them avoid the hazards of icy roads.

This technology could be used to transmit information in the following forms:

a) Local transmission to warning lights/sounds/ messages;
b) Relay of information to transportation monitoring and control centers;
c) Broadcasting through websites, text messages, etc.

The proposed concept could also be used to detect the ice formation in other applications including aircraft wings, bridge stay cables, bridge suspension cables, sign structures, etc.

1.7 Research Scope

A sensor system was developed based on monitoring changes in electrical resistance between poles at the concrete surface. Two different sensors prototypes (I and II) were constructed for testing. These prototypes consisted of 4-in-diameter concrete cylinders with four embedded stainless steel poles embedded at the surface. Two different types of poles were used. Detailed descriptions of the sensor prototypes are given in Chapter 3. Tests on the two prototypes were conducted under various environmental conditions. These environmental conditions included dry, surface ice, wet, and frozen conditions. The frozen condition refers to a situation in which the pores in the concrete all filled with ice, without formation of surface ice. Resistance between sensor poles were measured and recorded. Friction tests were performed to assess concrete surface friction changes under different environmental conditions. All sensor data were analyzed and a decision algorithm was developed to guide the sensor controller on determining the applicable environmental conditions, and to issue warnings when needed (as in surface ice condition).

1.3 A Review of Major Events caused by Roadway Ice:

In recent years, many significant ice conditions have occurred in the United States. Some of the following events are discussed to emphasize the hazards of ice formation in different locations.

Atlanta, GA January 2014 [4]

Atlanta was hit by a snow storm with 1-2 inches of snow. However, highways of Atlanta were turned into parking lots as result of the storm [4]. Surface ice was formed on the roads due to the snow and the sudden drop in temperatures [4]. Some vehicles crashed into each other and scattered all over the road. Drivers did not see any kind of warning on the highway.

Texas, January 2014 [5]

Texas witnessed unusual snow and severe cold weather in 2014. Many accidents occurred on highway bridges and overpasses [5]. Drivers saw no warnings that indicated possible danger. They lost control of their vehicles due to surface ice.

New Jersey, January 2014 [6]

People of New Jersey are familiar with snow and freezing conditions, and the authorities have the manpower and equipments needed to handle snow storms. However, on January 10th, New Jersey experienced freezing rain conditions in which hundreds of vehicles were involved in accidents resulting in many injuries[4]. Authorities tried to warn people by broadcasting alerts on the radio.

However, such warnings were not successful in avoiding major accidents and injuries [6].

Highway 41/45, I-43, and I-94, Wisconsin, December 2013 [7]

Wisconsin is one of the states where severe winter conditions are expected. In one icy area on highway 41/45, many people were injured and three deaths were reported [7]. Vehicles kept spinning out and hitting other vehicles [7]. In this case, it did not matter if the people and the agencies were familiar with snow conditions. The drivers did not receive any kind of warnings on the road.

Twelve states (ND to PA), January 11th-13th 2012 [8]

During three days in January 2012, twelve Midwestern states from North Dakota to Pennsylvania witnessed a total of 20 fatal crashes as well as thousands of other accidents because of icy roads [8]. A thin layer of snow may not appear very dangerous to drivers, who may not adjust their speed to accommodate the hazard[8]. As a result, accidents and loss of control happened at higher speed resulting in fatalities and serious injuries.

Summary of the events

As discussed earlier, many fatalities, injuries, and significant property losses can occur due to the presence of surface ice on roads and bridges. These accidents occurred in small towns and big cities, and in areas that are or are not accustomed to snow storms. Different approaches were used by authorities to avoid crashes, but severe accidents happened nonetheless. It could be concluded that regardless

of the familiarity of authorities and people (drivers), and the general precautions taken by them, accidents can happen due to lack of timely and site-specific warnings of surface ice conditions.

Chapter 2: Literature Review

2.1 Current ice detection methods:

Effective detection methods are needed to minimize the risks associated with ice-related road accidents. Such effective methods should be based on timely and site-specific warning to drivers when icy conditions exist, so that they can slow down and take all precautions needed to avoid accidents. Drivers should be warned early to give them enough time to reduce speed to a safe level and prevent loss of control. In this chapter, a review of existing technologies for ice detection on aircraft wings and on roads is presented. Ice formation is a major problem in multiple areas including pavements, bridge decks, runways, and aircraft wings.

2.1.1 Ice detection on aircrafts:

It is very important for aircraft safety to detect and address ice on aircraft wings. Several methods have been developed over the years to detect ice on aircraft. Some of these methods are described in the following section. The aircraft ice detection systems could be divided into the following major categories: 1) on-ground ice detection systems, 2) in-flight ice detection systems, 3) combination of on-ground and in-flight ice detection systems [9].

A. Microwave ice detector [10]:

This patented system involves transmitting a low-power microwave signal into a dielectric layer [10]. This layer works as a waveguide and includes a termination element. The transmitted and reflected signals are monitored [10].

When ice forms on the surface of the waveguide, the system identifies its presence and location.

B. Ultrasonic detector using flexural waves [11]

This patented system works by monitoring changes in flexural waves transmitted through the outer surface of an aircraft wing [11]. Either a transducer is coupled directly to the airfoil plate, or a waveguide is inserted between the transducer and the plate [11]. Changes in amplitude, phase, or dispersion characteristics of flexural waves indicate ice build-up.

C. Laser ice detector [12]

In this approach, a laser beam is used to detect the formation of ice on aircraft wings. It uses a combination of a light source, light detector and temperature sensors to detect ice formation [12]. The system provides the pilot with a warning in case of ice detection or system failure [12].

D. Fiber optic ice detector [13]

In this patented approach, multiple beams of light are projected onto the semi-transparent ice layer through a window located on the surface below the ice[13]. The light beams are reflected and correlated with the thickness of the layer [13]. When the measured thickness exceeds a certain value, an alarm will be issued to warn the pilot of the presence of ice [13].

2.1.2 Ice detection on roads

In the following sections, a review of current techniques for detection of ice on roadways or bridges surfaces are presented.

A- Infrared Ice Detection System (IRDS) [14]

IRDS, is an active infrared system designed to detect ice, snow, and water on roads. The system is non-contact and does not require sensors embedded in the surface. This sensor has a head pan/tilt capability, but can only cover a limited area in the system's surroundings [14]. This system is typically mounted on an elevated support, and has reportedly experienced some software and hardware issues [14].

B- SensIce [15] **:**

This system is based on infrared spectroscopy [15]. Water and ice absorb most of the infrared light, and the reflected light is sensed by the device [15]. Figure 2.1-1 [15] the "SensIce" system that has been developed in Europe. Some systems include on-site alarms such as blinking lights, while others are used to send raw data to receiving centers that are responsible for issuing warnings. These systems have relatively complicated hardware and software system, and are susceptible to power surges [15]. Maintenance costs are also relatively high.

Figure 2.1-1: SensIce device [15]

C- Automatic Slipperiness Detection System for Cars [16]

This system has been developed by the Technical Research Centre of Finland [16]. It is based on sensors mounted on vehicles travelling on roads [16]. The sensors obtain information regarding the road's slipperiness. The method involves estimating the difference in speed between the drive shaft and the axle [16]. Information is collected from various vehicles and passed on to a monitoring system that issues warnings [16]. Such systems may not be able to warn all drivers ahead of time to avoid accidents.

D- Intelligent Ice Detector System [17]

The "SR-IDS Intelligent Ice Detector" is an integrated system developed in Australia [17]. It is designed to detect the presence of ice on the roads and warn

drivers [17]. The system includes sensors to determine temperature and humidity, and utilizes theses data to issue warnings about presence of ice [17].

E- Vehicle-Mounted infrared ice detection device:

This system perceives and advises drivers about the presence of ice on the roads using an infrared sensor that is attached on the vehicle and is aimed at the road [18]. The system reportedly ignores signals that may be received from sources other than road. A processing unit receives information from the detector [18]. The processing unit also displays the information to the driver and could activate an alarm [18].

F- A light reflection device

This system is another vehicle-mounted system for detecting the presence of surface ice on roads [19]. It generates a light pulse train whose amplitude is changed when ice exists [19].

In general, such systems are reportedly capable of performing their main task, which is detection of surface ice. However, some systems contain complex and hard-to-maintain hardware and software components. High initial and long-term costs, complexity, and accuracy issues have prevented the wide-spread use of such systems on road networks nationwide.

2.2 Concrete resistance and resistivity

As discussed in Chapter 3, this thesis proposes a new sensor system for ice detection based on monitoring changes in resistance of concrete between two sensor poles. In this section, a review of methods for measuring electrical

resistance of concrete is presented. Resistivity is a material property that is indicative of the material's ability to conduct electricity [20]. Resistance and resistivity are two different, but related, terms. Electrical resistance between two points is equal to measured voltage (between the two points) divided by the electrical current. Unlike electrical resistance, resistivity is a material characteristic.

Resistivity (in Ohm-m) can be defined as the voltage (in Ohms) measured across two opposite faces of a cube with dimensions of 1m [20]. The inverse of resistivity is called conductivity. In general, the nature and structure of a material affects its resistivity. For example, porosity and temperature can affect resistivity [20].

Concrete is formed of three main ingredients: Portland cement, aggregates (gravel and sand), and water. Each one of these ingredients has different conductivity and resistivity. The resistivity and conductivity of concrete will therefore depend on the combination of these materials. Resistivity of concrete can also be affected by other factors (e.g. moisture content, temperature, etc.). In general, as concrete becomes drier, its resistivity increases.

Admixtures and supplementary cementitious materials may be added to the concrete mix to improve some of its properties (e.g. strength, durability, workability, etc.) [21][22]. Admixtures may also affect conductivity and resistivity of the concrete.

Monfore et al. [21] noted that the pore water in the hardened concrete mix includes a number of ions. These ions have changing concentration with time. The ion concentration could increase for some ions and decrease for others, which in turn

affects conductivity. Tests by Hammond and Robson [23] showed that the resistivity of a particular concrete increased by drying it using a heat source at 105C˚.

The relationship between resistance and resistivity is shown in the following:

$$R = \rho \frac{L}{A} \quad \text{..... (Eq-1)} \ [21]$$

Where;

R = resistance in Ohms

ρ = resistivity in Ohm-cm

L = length in cm, and

A = cross-sectional area in cm²

Monfore et al. [21] indicated that (L) for composite materials should be replaced by (L_e), the effective path length. In homogenous materials, the current travels along a path of length L through the material, while the length of the path changes to L_e through composite materials. Monfore [21] suggests that L_e is longer that the dimension of the composite material in the direction of the current because of tortuosity.

The water-cement ratio also affects resistivity of concrete [21]. By increasing the water-cement ratio, the resistivity decreases. Resistivity also increases with time. Monfore reported that the resistivity of concrete paste having water-cement ratio of a 0.4 is almost double the resistivity of a paste having water-cement ratio of 0.6 [21]. Dorsch [21] [24] found that the electrical resistivity is inversely related to the lime content of the cement.

Hammond and Robson [23] found that age and humidity affect the resistivity of concrete, and the electrical properties of concrete vary throughout the concrete because:

- Concrete is not a homogeneous material.
- Concrete is placed in layers.
- Differential drying occurs between the outer surface and the inside of the concrete, which causes a "humidity gradient".

Hammond and Robson [23] measured surface and volume resistivities for oven-dried specimens. They found that surface resistivity is much lower than volume resistivity for the same specimen.

2.2.1 Wenner Four-Pole method

This a well-known method that is commonly used to measure resistivity of concrete. It has also been widely used in measuring soil resistivity. This method was developed by Dr. Frank Wenner of the US Bureau of Standards in 1915 [25]. In this approach, four electrodes are used, two for current injection and two for voltage measurement. The four electrodes are embedded into the ground (or connected to the concrete surface) in a straight line. The two outer electrodes serve as current electrodes and the two inner electrodes are used to measure the drop in voltage due to material's resistance. The current passes between the outer electrodes (Figure 2.2-1) [25].

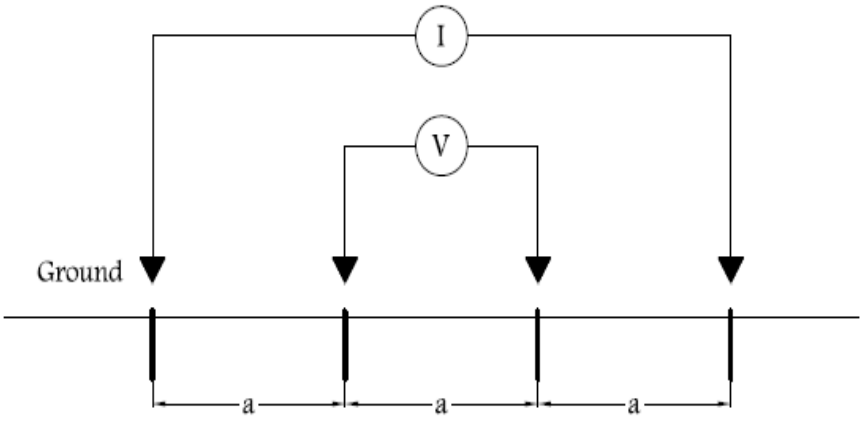

Figure 2.2-1: Wenner four-poles test setup [25]

The resistance can then be quantified (voltage drop divided by the current) and resistivity can be calculated from the following equation:

$$\rho = 2.\pi.a.R \quad \ldots\ldots\ldots\ldots\ldots\ldots\ldots\ldots \text{(Eq-2)}$$

Where:

ρ = Resistivity in Ohm-in

a= Distance between poles, inch

R= Resistance Measurement Ohm

Ramezanianpour et al. [26] used this technique to investigate concrete durability, permeability, and the resistance of concrete to chloride penetration. They used different types of concrete mixtures. However, they used one type of cement (portland cement type I). They also used different types of admixtures. Resistivity measurements were used instead to assess concrete durability. They used 50-mm

diameter concrete cylinders with a height of 100mm. The distance between the embedded electrodes was 1.5mm. The electrodes were connected to resistivity meter. Figure 2.2-2 [26] shows their test setup [26].

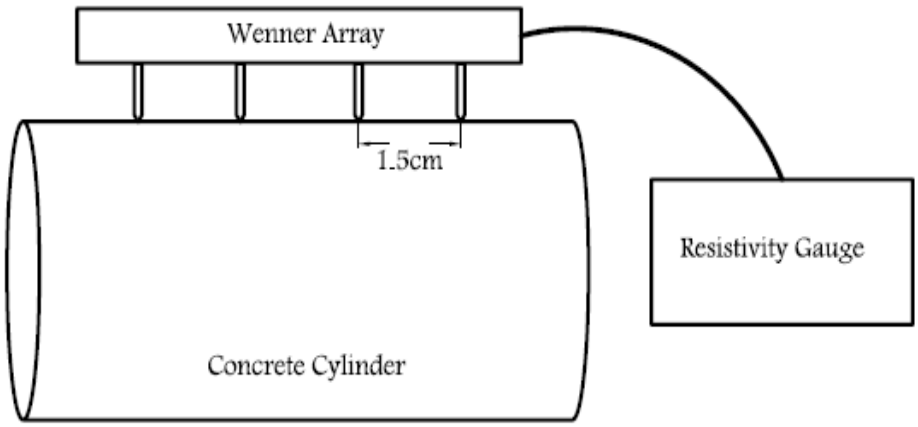

Figure 2.2-2: Wenner Array test setup to measure concrete resistivity [23]

Based on the tests of concrete resistivity as well as Rapid Chloride Penetration tests, a relationship was developed to estimate permeability of concrete from the measured resistivity values [26].The authors concluded that the resistivity test could be used as an indicator of the chloride penetration resistance of concrete [26], but it cannot be an indicator of the concrete compressive strength. The authors, however, did not address variations of concrete resistivity under changing climatic conditions, a topic which is addressed in this thesis.

2.2.2 Wheatstone Bridge:

The Wheatstone bridge is an electrical circuit invented by Samuel Hunter Christie in 1833, and developed by Sir Charles Wheatstone in 1843 [27]. It is widely used

in electrical devices and instruments to measure an unknown electrical resistance or resistance changes. Examples include thermometers, load cells and strain gauges [27]. This type of circuit has four resistors that are arranged as shown in Figure 2.2-3. Three out of four resistors are known and the fourth resistor (R_X) is to be measured.

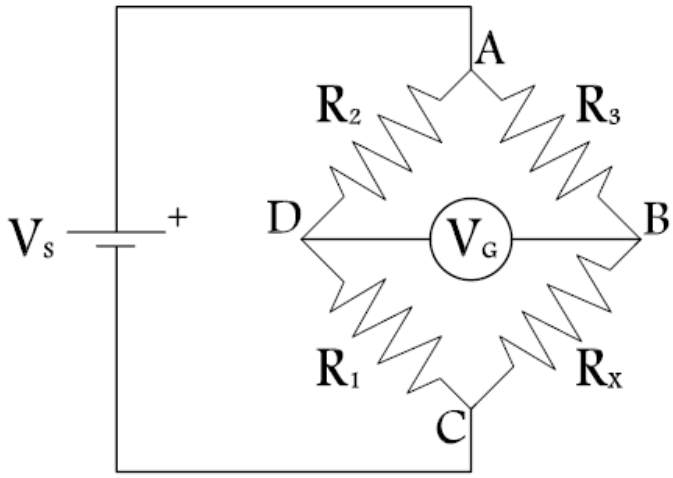

Figure 2.2-3: Wheatstone bridge [27]

A DC power supply provides voltage (V_S) to the circuit through points A and C. The output voltage (V_G), between points (D) and (B), is zero when the ratio of the two resistors on one leg (R_1/R_2) is equal to the ratio in the other leg (R_x/R_3) (Eq.3). The bridge is considered unbalanced when V_G is not zero. To balance a bridge, one of the known resistors can be changed until V_G=0. In a balanced bridge, the unknown resistance R_X can be determined using Eq-4.

$$\frac{R_x}{R_3} = \frac{R_2}{R_1}$$ (for an unbalanced bridge) ..... (Eq-3)

$$R_X = \frac{R_2}{R_1} R_3 \quad \text{..... (Eq.4)}$$

On the other hand, if an unbalanced bridge is used, the value of the unknown R_X can still be determined using an equation that relates V_G to all resistance values in the Wheatstone Bridge. The unbalanced bridge approach is more convenient (measure V_G instead of changing the resistors to balance the bridge). Equation-5 is developed using Kirchhoff's law. In this equation V_S is the excitation voltage [27].

$$V_G = \left(\frac{R_x}{R_3 + R_x} - \frac{R_2}{R_1 + R_2} \right) . V_S \quad \text{..... (Eq.5)}$$

By using the three known resistors, the known excitation (V_s), and the output measured (V_G), the unknown resistor (R_x) could be calculated from Eq.5. The unbalanced Wheatstone Bridge approach is used in this study to measure sensor resistance under different climatic conditions. The concrete between the two sensor poles forms a leg in the circuit (R_x).

A guarded Wheatstone Bridge circuit may be suitable in cases where the resistances are higher, as shown in Figure 2.2-4[28]. However, when guarded Wheatstone Bridge was used, the results did not differ from the basic unguarded circuit. A decision was made to use the conventional Wheatstone Bridge for the testing program described here.

The value of R_1, R_2, and R_3 were selected after several trials to achieve a wide range of circuit output for different environmental conditions. The actual resistance values used are given in Chapter 3.

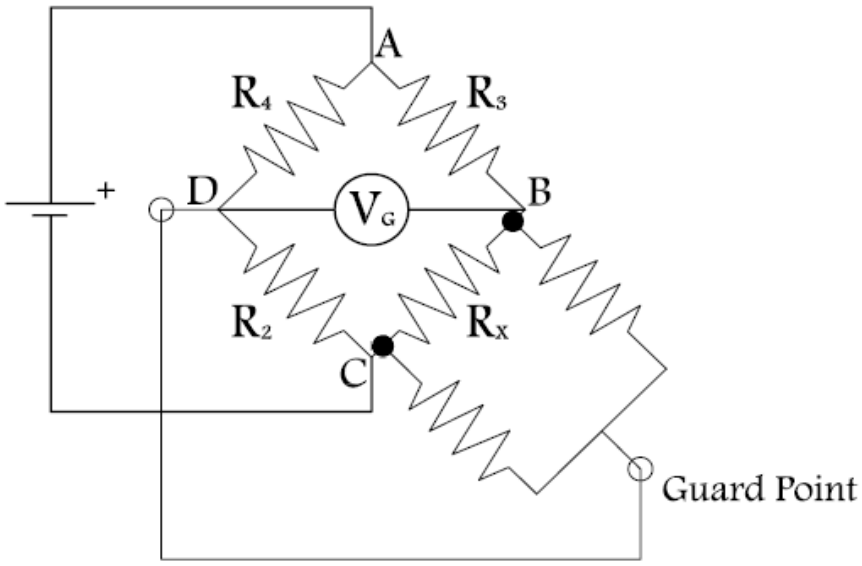

Figure 2.2-4: Guarded Wheatstone bridge [28]

Chapter 3: Proposed Intelligent Sensor System

In this thesis, an intelligent sense system for detection of surface ice on pavement and bridge decks is proposed. The system can identify dry, wet, frozen, or icy conditions, and can transmit the relevant data to either a local warning system or a system-wide information system. The proposed approach takes advantage of the fact that the near-surface resistivity (resistance) of concrete changes when there is an ice layer on the surface, or when there is moisture at the surface (wet surface). The automated sensor system could detect ice as it starts to form, and then transmit wireless signals that could trigger warnings. The local warning can be visible or audible for drivers. Additionally, the sensor will be able to transmit its location, surface temperature, and indications of surface ice, dry surface, or wet conditions.

Advantages of the proposed intelligent sensor system are as follow:

- Relatively low cost.
- Simple technology.
- Can be produced on a mass scale.
- Ability to detect a variety of surface conditions.
- Info can be communicated in multiple ways, as shown in Figure 3-1:-

  1- At the site through warning lights/sounds/messages

  2- Transmission to a transportation control center.

  3- At a web site.

  4- To vehicle information systems / autonomous vehicles.

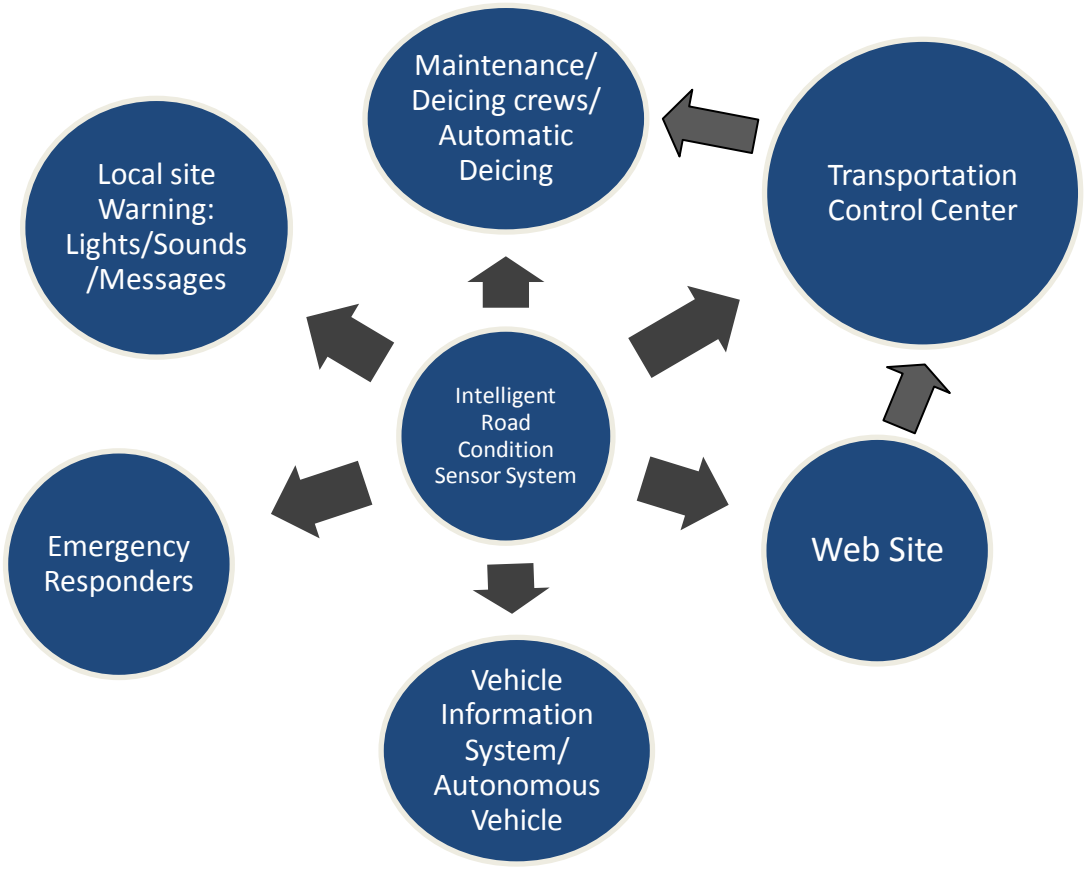

Figure 0-1: Ways of communicating the information

The detection algorithm is based on resistance and surface temperature measurements. In its current form, the sensor is in the shape of concrete cylinder with a mix design that is similar to the surrounding roadway/bridge.

Electrical resistance is measured between two stainless steel poles embedded in concrete. Two sets of poles are used:

- "Look-Up-and-Side" (LUS) poles measure near-surface electrical resistance changes in the concrete between the two poles ("Sides") as well as any material (surface ice) that may exist above the surface ("Up").

- "Look-Up" (LU) poles measure resistance changes above the surface of the concrete between the two poles. Under dry conditions, the resistance between LU poles is near infinity as the space above the surface between LU poles consisting of air only.

The installation of this sensor in existing pavements or bridge decks involves using a 4-in-diameter core drill bit to remove a core, and replacing it with the concrete sensor. A cementitious material is used to bond the sensor to existing pavement.

3.1 Proposed Sensor dimensions:

The proposed cylindrical sensor has a diameter of 4.0 inches, height of 1.5 inch, and includes a 3-in diameter opening at the bottom of the sensor as shown in figures 3.1-1, 3.1-2, 3.1-3 and 3.1-4.

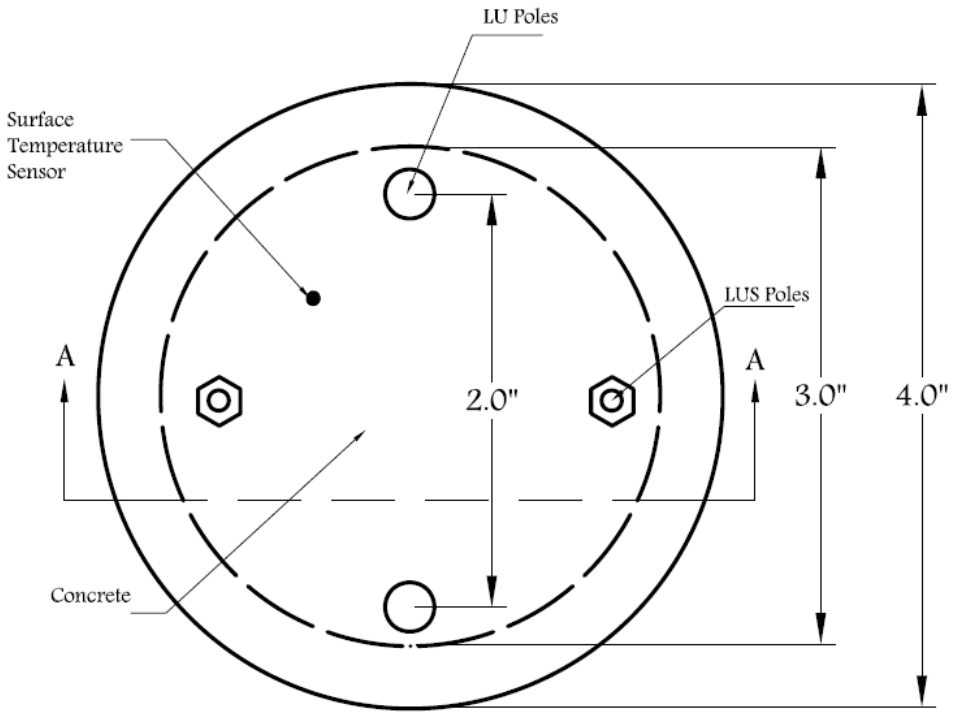

Figure 3.1-1: Dimensions of the proposed sensor

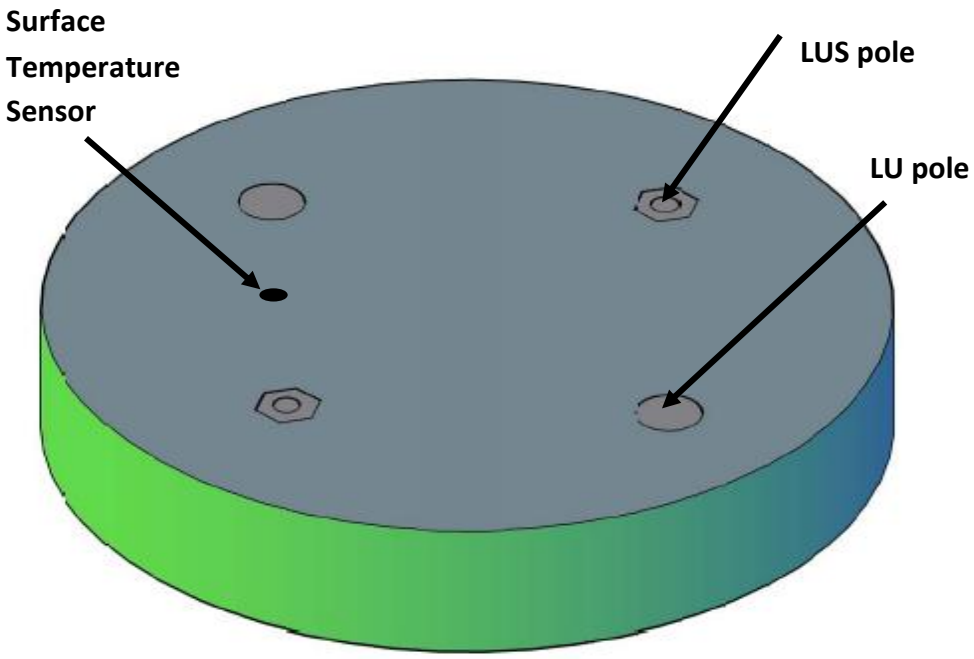

Figure 3.1-2: Top side of the proposed sensor

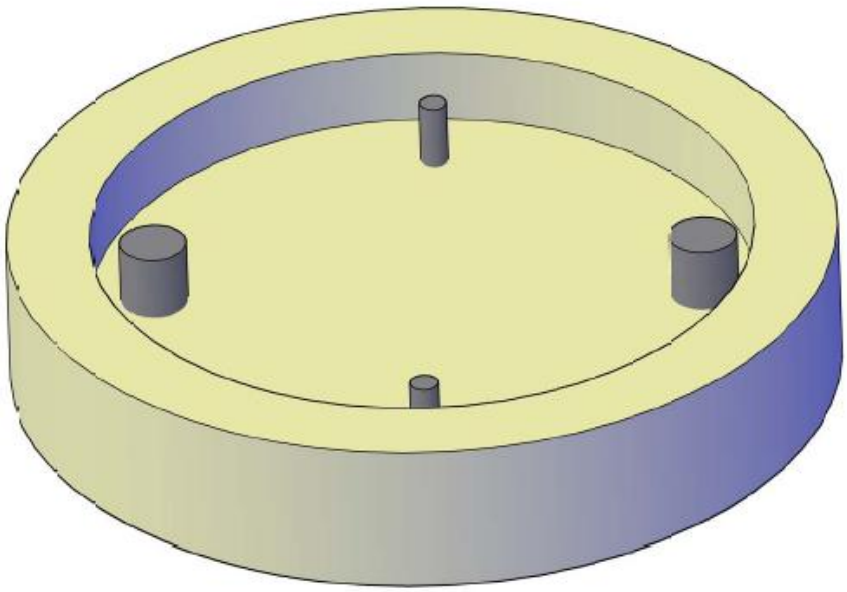

Figure 3.1-3: Bottom side of the proposed sensor

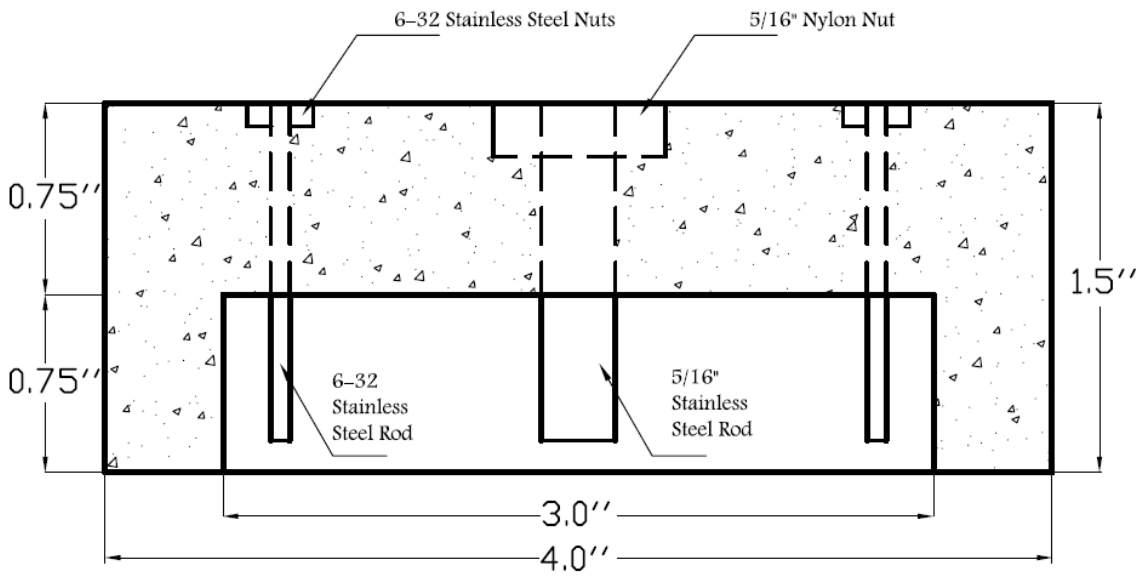

Figure 3.1-4: Section A-A in proposed sensor

Two 6-32 stainless steel threaded rods with 6-32 stainless steel nuts are used as LUS poles, and two 5/16”-in-diameter stainless steel threaded rods used as LU poles. The cross sectional area of the 5/16” pole is equal to that of the 6-32 nut. This assures that both types of poles have the same conductive area projected (facing up) at the surafce. All poles were insulated with a layer of epoxy paint and two layers of electrical shrink tubing, where needed, along the embedded part of their length. The insulated and non-insulated areas of each pole type are shown in Figure 3-3. Also 5/16” plastic nuts were placed at the surface of the speceimen around the 5/16” rods to avoid any electrical contact between the concret and the rods from the sides.

The LU poles are included to address the ice formation on the top of their cross sectional area only, since they are electrically exposed only from the top (i.e. they are sensetive to resistance changes above the surface of the sensor only). On the

other hand, LUS poles are electrically exposed to changes in the concrete resistance as well as changes above the surface as shown in figures 3.1-5, 3.1-6, 3.1-7, and 3.1-8. The use of LU poles alows a conclusive determination of surface ice, when LUS results are not conclusive.

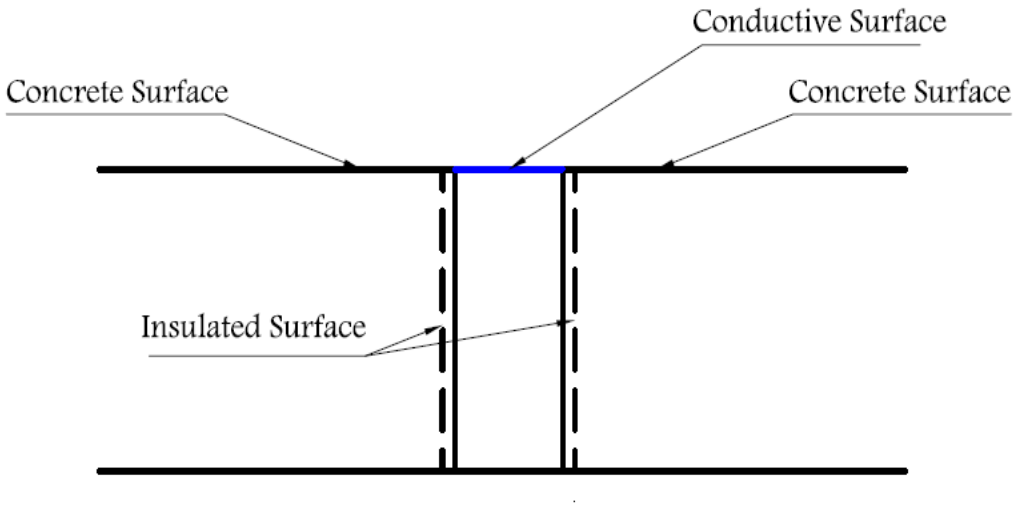

Figure 3.1-5: LU Pole Details

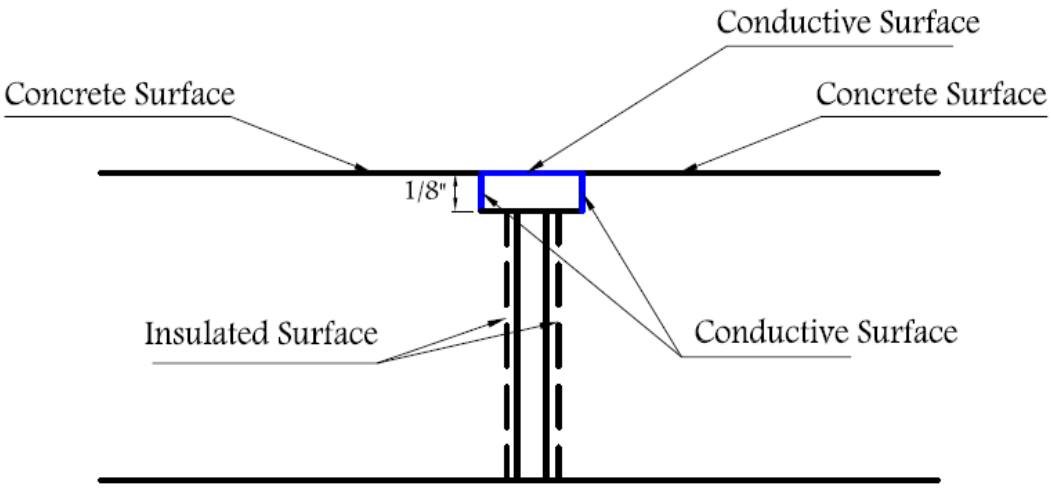

Figure 3.1-6: LUS Pole Details

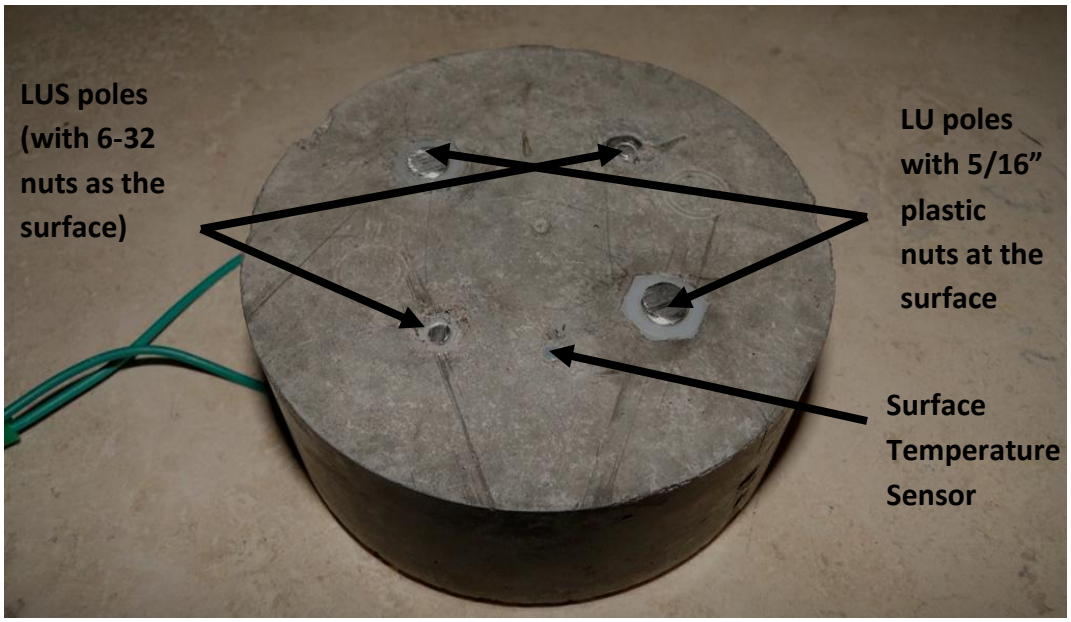

Figure 3.1-7: Top surface of proposed sensor

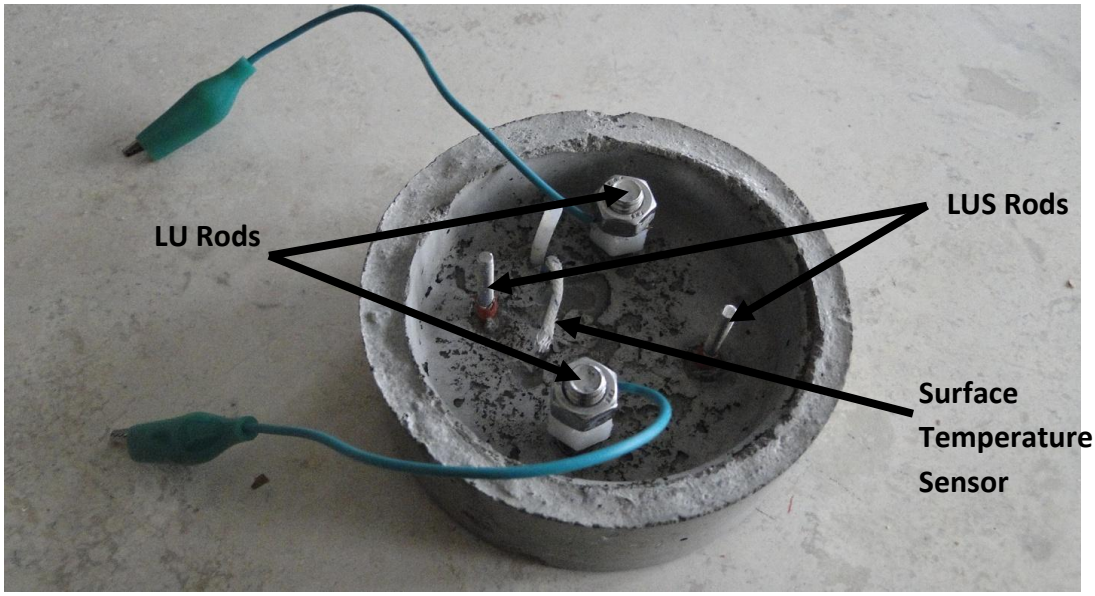

Figure 3.1-8: Bottom side of proposed sensor

In the proposed sensor, stainless steel rods are used as electrical connections to the circuit board (instead of wires). This is done to eliminate the potential for long-term corrosion of conventional wires.

The circuit board is attached within the opening inside the sensor. The circuit board, as indicated in Figures 3.1-9 and 3.1-10 contains two separate Wheatstone Bridges, a power supply unit (battery), a transmission unit, a logic controller, and a temperature sensor. The decision on the conditions is made by the logic controller based on inputs from the two Wheatstone Bridges and the surface temperature, and in accordance with the developed decision algorithm. The decision is then transmitted in the form of a warning, if conditions warrant.

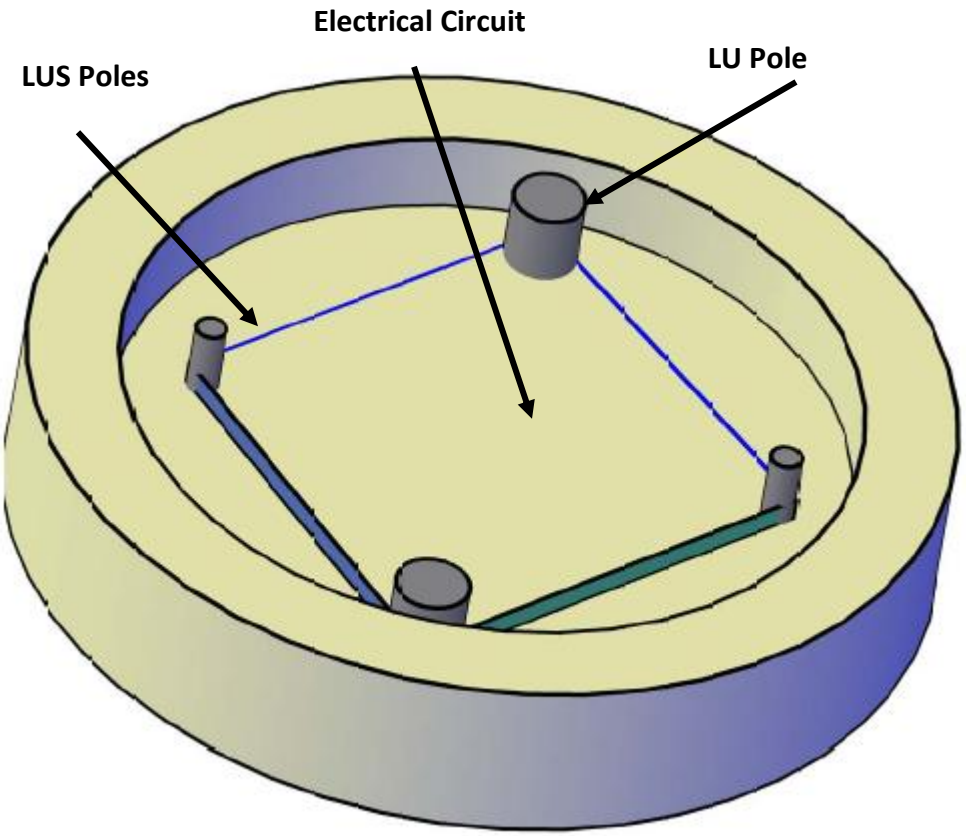

Figure 3.1-9: 3D sketch for proposed sensor showing the conceptual electrical circuit board inside the sensor opening

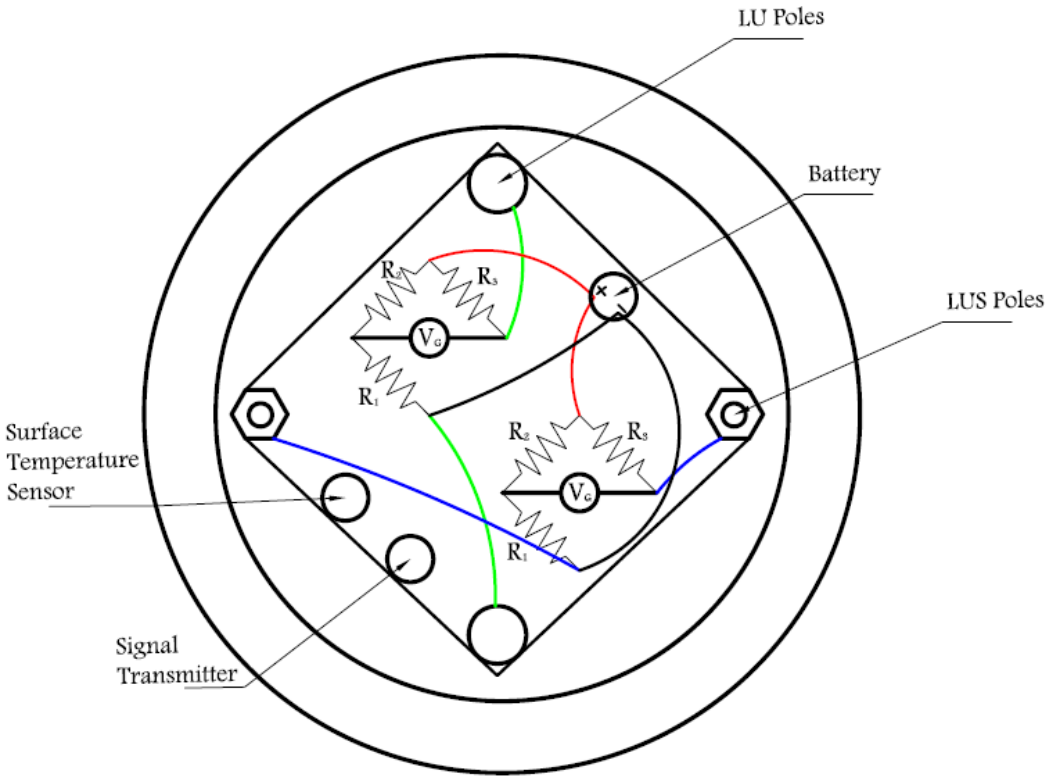

Figure 3.1-10: Schematic of circuit board components

The concrete surface within the opening containing the electrical components should be sealed (painted with epoxy) to avoid moisture penetration into the electrical area. A cover is used to seal the opening and prevent any possible damage to the electrical circuits, as shown in Figure 3.1-11. Information including location sensor and any warning messages can be transmitted to local receivers, as shown in Figure 3.1-12.

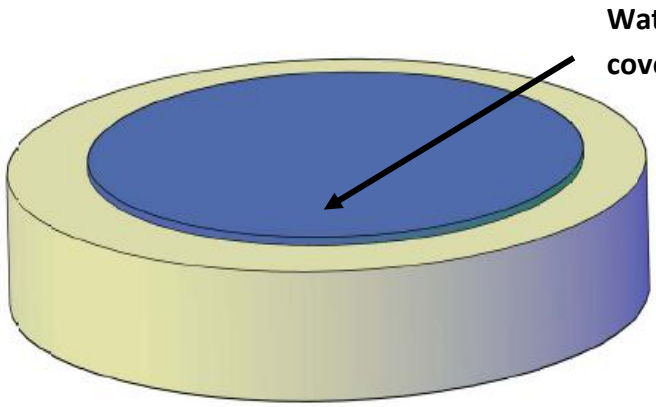

Figure 3.1-11: Sealed bottom of proposed sensor

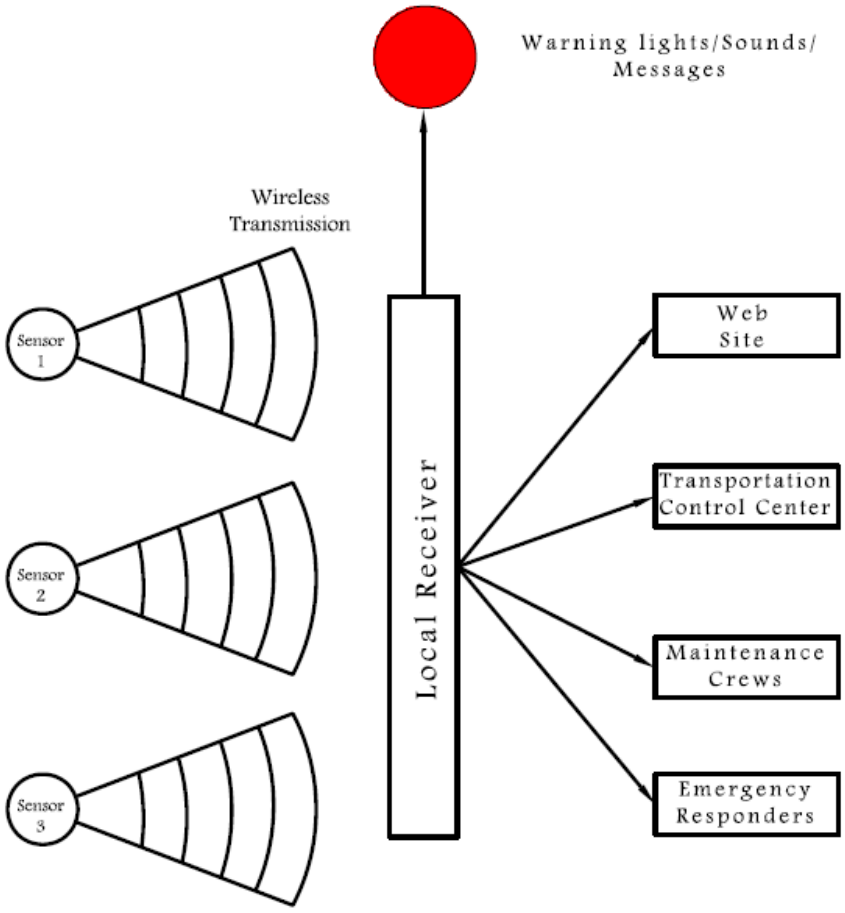

3.1-12: Wireless transmission system

3.2 Usage and installation

A core drill bit with a 4-in-diameter coring bit can be used to drill holes in bridge deck, roadways, and runways. The sensor is then installed and a cementitious mortar is used to fix the sensor in place. A cementitious mortar is proposed to minimize thermal property differences, and to avoid thermally isolating the sensor. Figures 3.2-1, 3.2-2 and 3.2-3 show the installation steps. The sensor's controller performs a self check after installation. The controllers will be designed to preserve power by turning on the system only when needed.

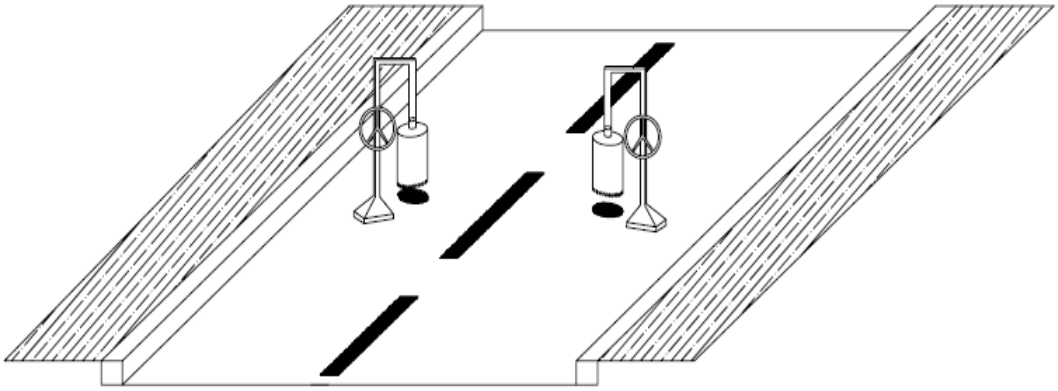

Figure 3.2-1: Drilling 4-in-diameter cores on the road surface

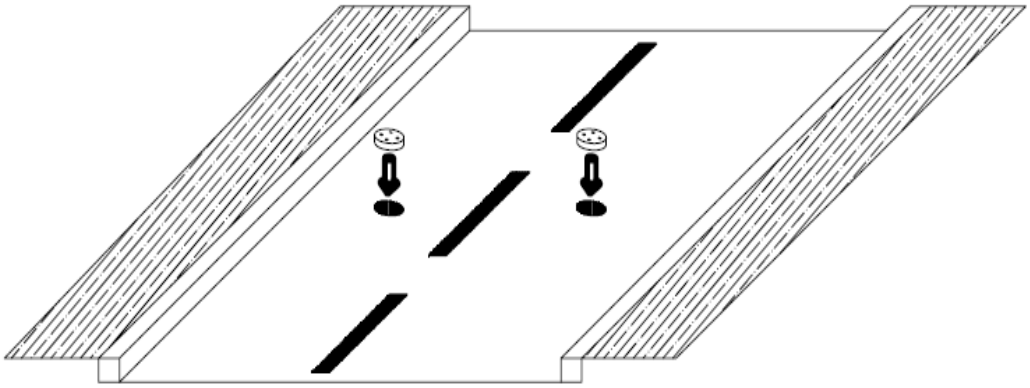

Figure 3.2-2: Sensors are ready to be installed

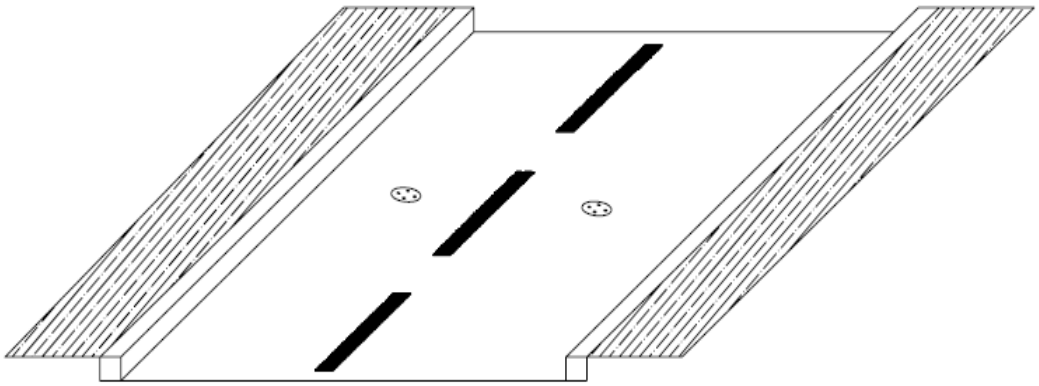

Figure 3.2-3: Sensors are already installed using a Cementitious paste to bond with concrete

Chapter 4: Experimental Development and Verification

The development and verification aspect of this work involved design and building of two sensor prototypes (SP-I and SP-II). These two prototypes were used to generate test data for the development of the decision algorithm, and to establish the feasibility and effectiveness of the proposed sensor concept through laboratory testing.

4.1 Sensor Prototype I (SP-I)

SP-I was the first sensor used in this research. The cylindrical SP-I sensor was made of concrete with a diameter of 4 inches and height of 1.5 inches, as shown in Figure 4-1. SP-I is similar to the proposed sensor described in Chapter 2 except that all the poles in this sensor were LUS poles. Also, the diameter of the opening on the bottom of the sensor is 2.5 inches instead of 3 inches for the proposed sensor.

The bottom opening was 0.75 inches high as shown in Figures 4.1-1, 4.1-2 and 4.1-3. Four stainless steel nuts (poles) were embedded in the sensor mold prior to casting of the concrete. These poles are flush with the top surface of the sensor. Each one of the stainless steel nuts has a nylon threaded rod inside that extended through the thickness of the sensor. Electrical wires were placed in the nuts before tightening the threading rods. These wires were connected to the Wheatstone Bridge circuits. Please note that the proposed concept doe not use wires for protection against long-term corrosion. The measured resistance is between the diagonal placed poles as shown in figure 4.1-4. Figures 4.1-5 and 4.1-6 show detailed sketches for the SP-I sensor.

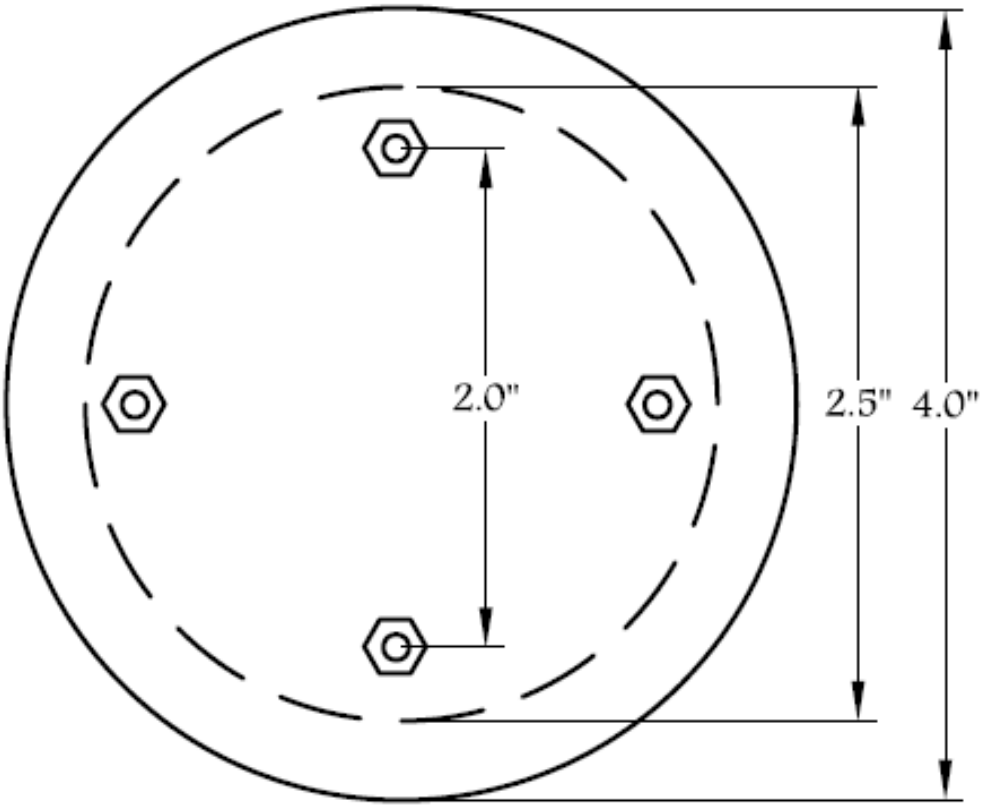

Figure 4.1-1: Sketch of sensor prototype SP-I

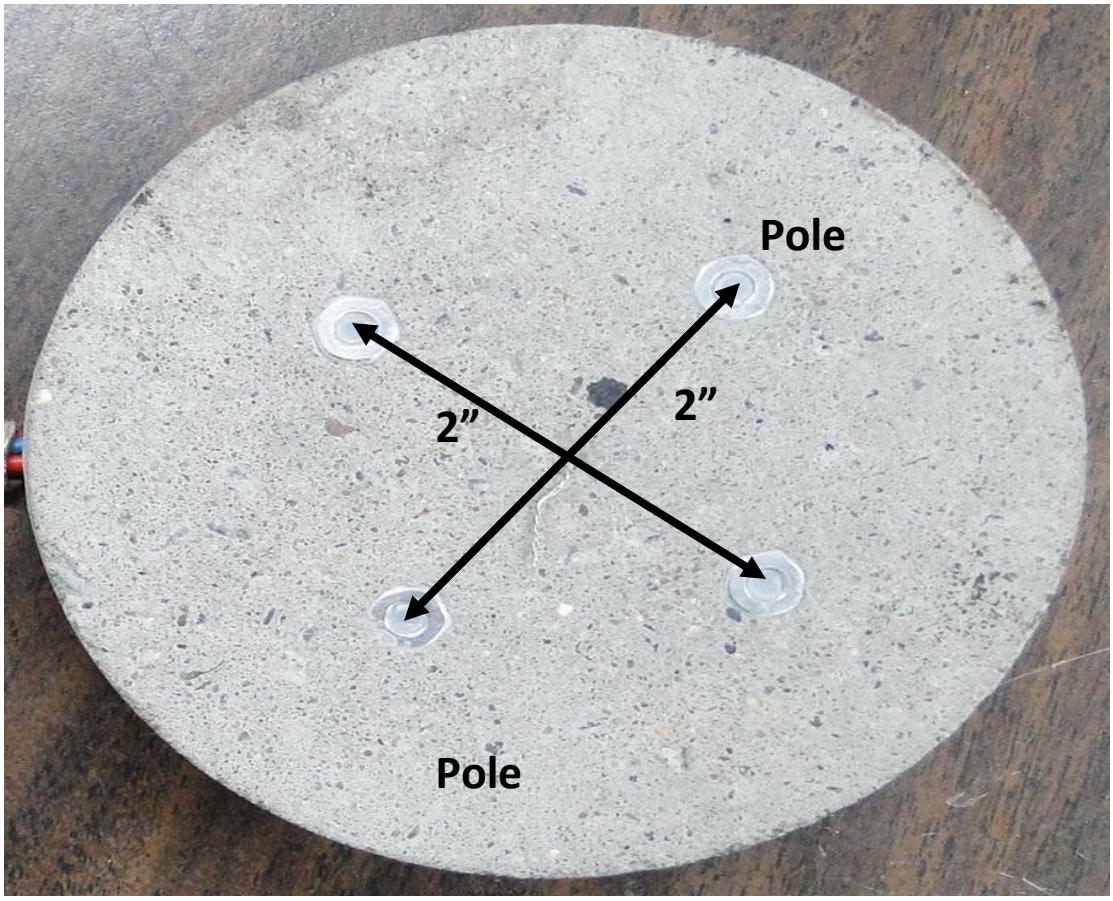

Figure 4.1-2: Details of LUS poles in SP-I

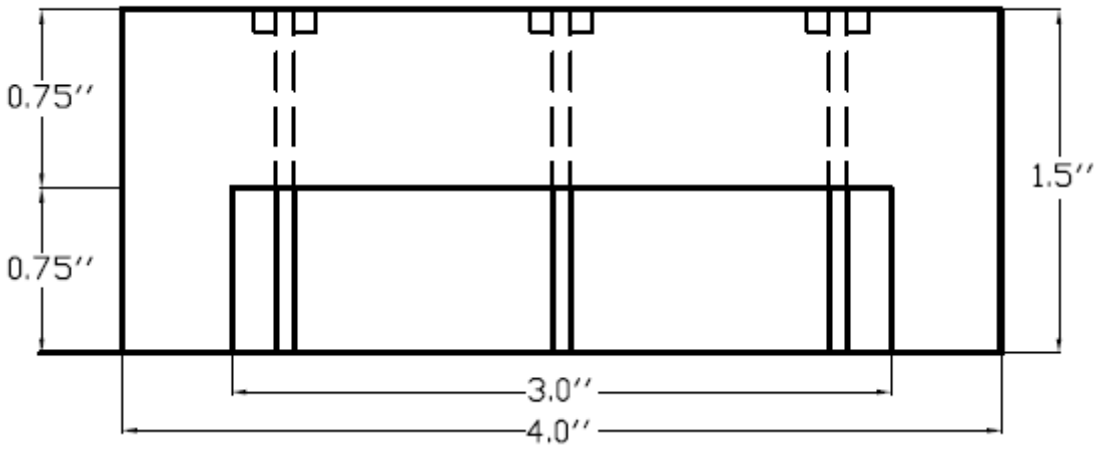

Figure 4.1-3: Cross section of the SP-I sensor

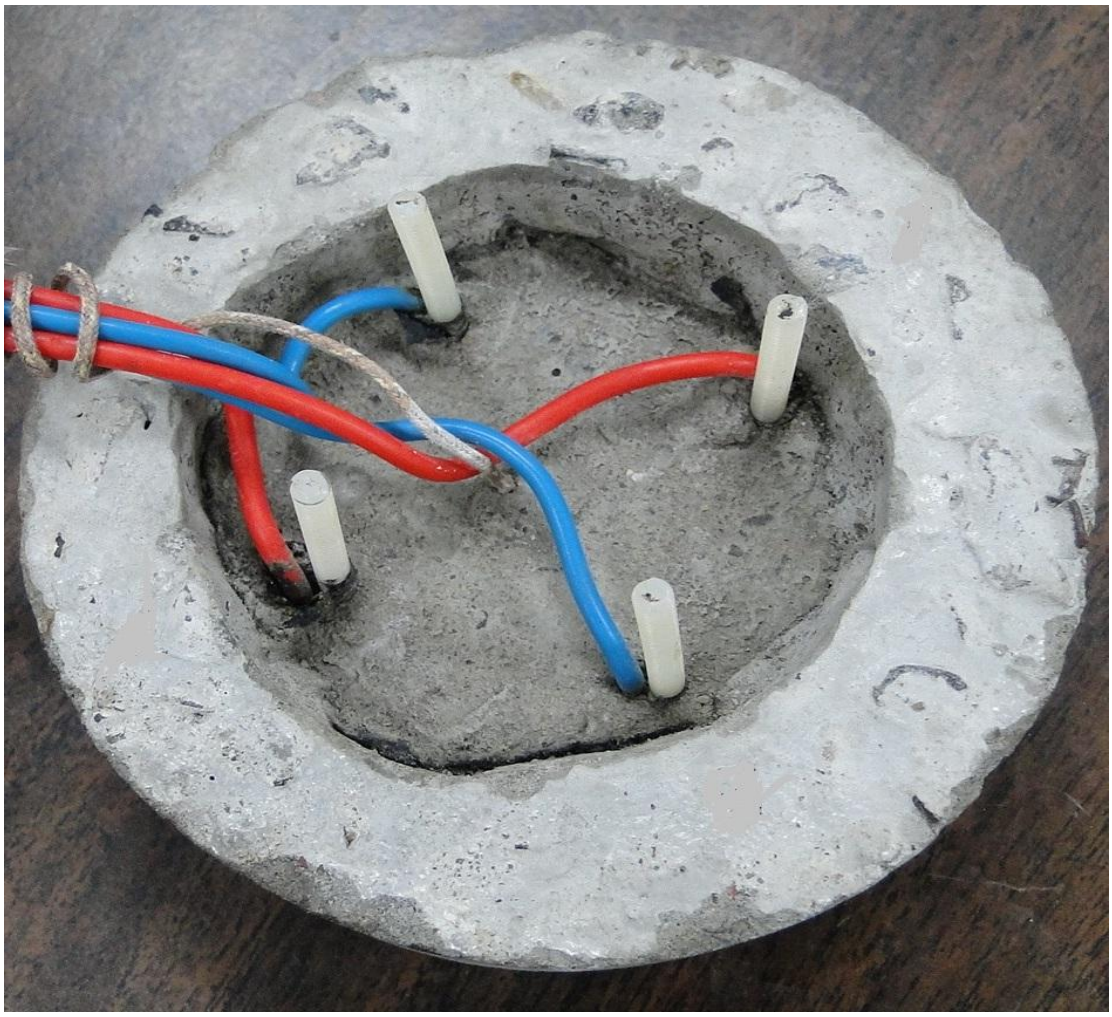

Figure 4.1-4: Bottom side of SP-I

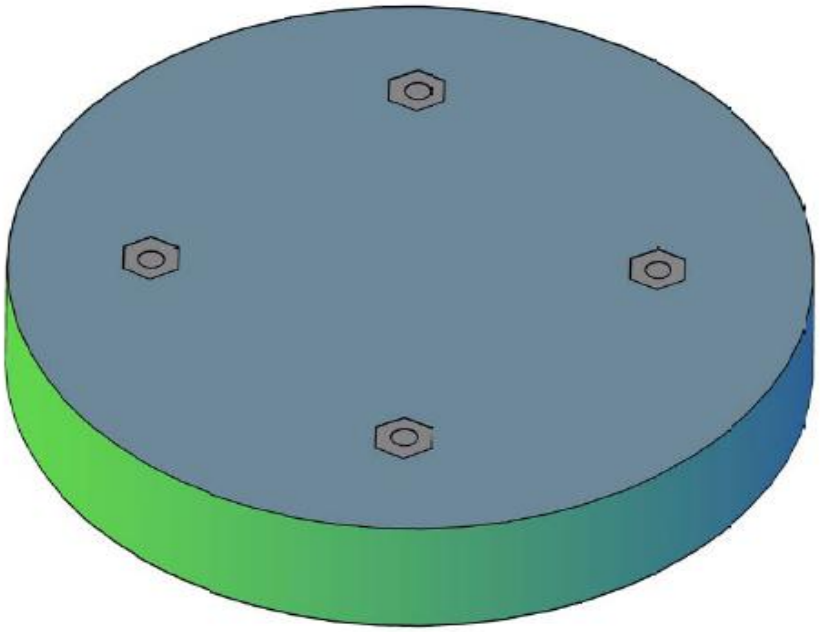

Figure 4.1-5: 3D model for the top surface of the specimen.

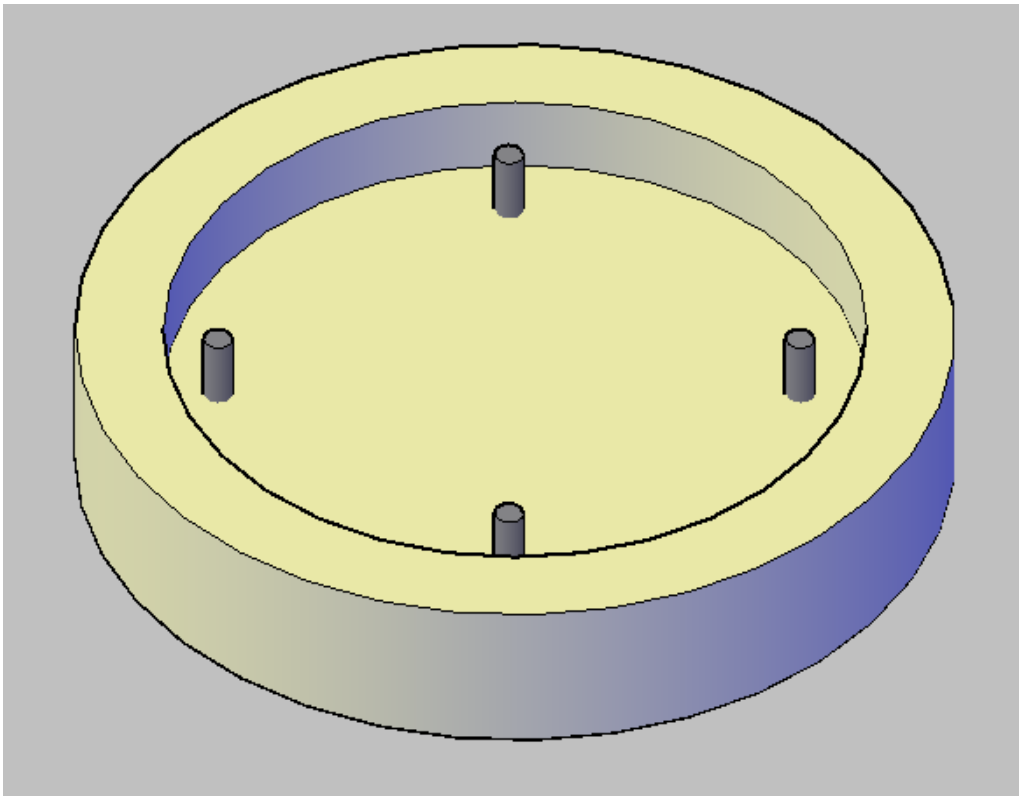

Figure 4.1-6: 3D model for the bottom side of the specimen.

The concrete mix design used consisted of the following: one part (by weight) of portland cement (Type I), two parts of sand, and three parts of pea gravel. The water/cement ratio (W/C) used in this research was 0.4, which is a common value used in pavements and bridge decks. The specimens were stripped from their plastic mold two days after casting of the concrete, and were then wet cured in the laboratory for 7 days.

4.2 Sensor Prototype II (SP-II):

This sensor has the same dimension of SP-I with a diameter of 4.0 inches, height of 1.5 inch, and a 3.0-in-diameter opening at the bottom as shown in Figure 4.2-1, 4.2-2, 4.2-3, and 4.2-4.

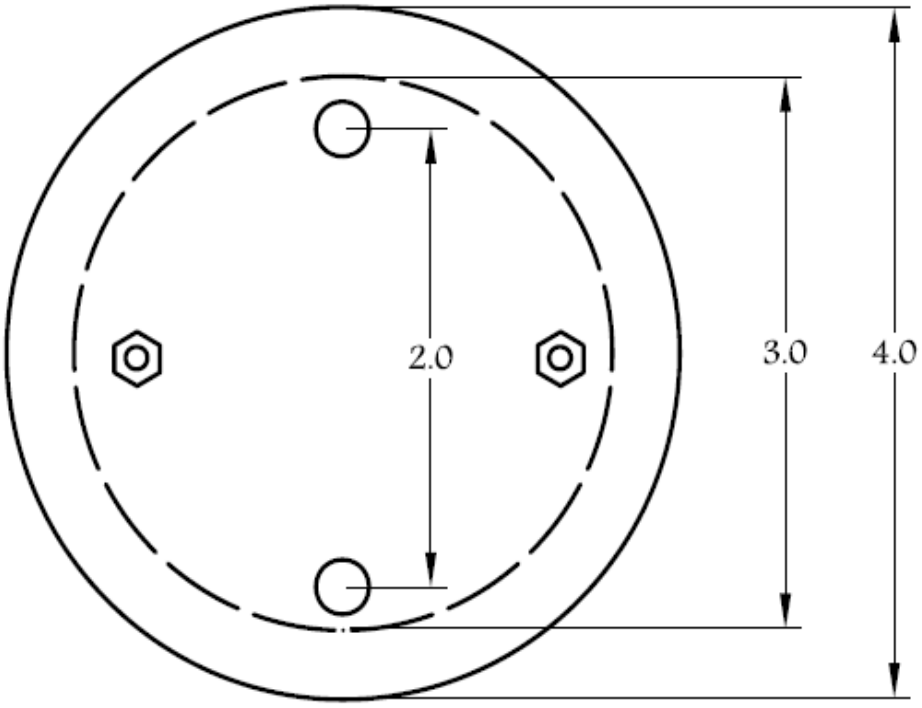

Figure 4.2-1: Sketch of sensor prototype SP-II

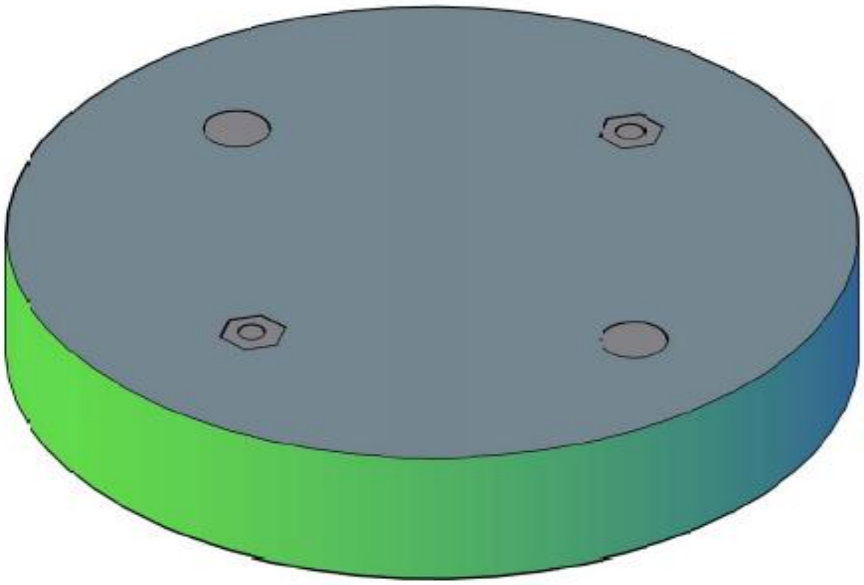

Figure 4.2-2: 3D model for the top surface of SP-II

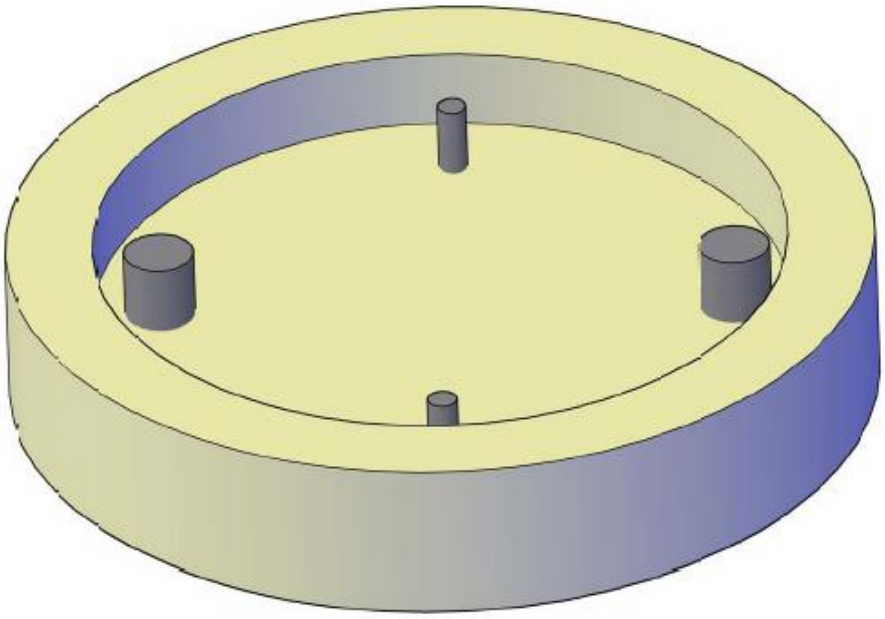

Figure 4.2-3: Sketch for the bottom side of SP-II

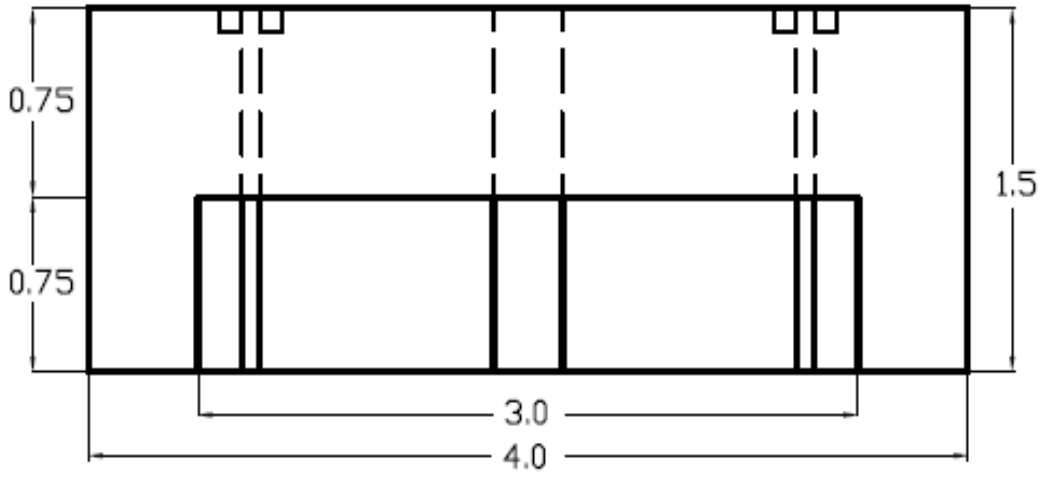

Figure 4.2-4: Cross section of SP-II

Two 6-32 stainless steel threaded rods with 6-32 stainless steel nuts were used as LUS poles similar to those used in SP-I. Two 5/16”-in-diameter stainless steel threaded rods were used as LU poles. The LU (Look-Up) pole was added to distinguish the effect of frozen condition from surface ice. All poles were insulated with a layer of epoxy paint and two layers of electrical shrink tubing throughout the embedded part of their length. This was meant to electrically isolate the LU poles from the concrete throughout the exterior surface of the pole.

In SP-II, stainless steel rods were used as a connection to replace the wires that were used in SP-I. The reason is that wires could corrode overtime which would require maintenance and replacement. Stainless steel rods are chosen solution for addressing the long-term corrosion problem caused by exposure to moisture. The primary reason of using SP-II is to categorically resolve and distinguish surface ice, especially when the surface concrete is contaminated.

4.3 Test setup

As discussed earlier, the output of a Wheatstone Bridge was used in this research as an indicator of resistance changes between two opposite poles in each sensor. The resistance between the two sensor poles was included as a leg of the Wheatstone bridge shown in figure 4.3-1.

The Wheatstone Bridge has been used to measure resistance changes in a variety of different applications. The electrical resistance of near-surface/surface areas between poles was thus measured.

In a Wheatstone Bridge there are four legs, each consisting of a resistance. Three of these resistances were taken to be constant (R_1, R_2, and R_3). R_x is the resistance that is being determined. The value of (R_x) depends on (R_1), (R_2), and (R_3). The output voltage (V_G) of a Wheatstone Bridge is described in Eq.4-1.

$$V_G = \left(\frac{R_x}{R_3 + R_x} - \frac{R_2}{R_1 + R_2}\right).V_S \quad \text{..... (Eq.4-1)}$$

The values of the excitation voltage (Vs) and resistances of the three known legs of the Wheatstone Bridge (R_1 thru R_3) used in the test set up are shown below:

V_s = 6 volts

R_1 = 100 kΩ

R_2 = 150 kΩ

$R_3 = 10\ M\Omega$

Values of R_1, R_2, and R_3 were selected based on trial tests to find a reasonable range of outputs for different environmental conditions

The electrical circuit of the Wheatstone bridge is shown in the Figure (4-13). The output voltage (V_G) is measured across points D and B. Point (A) on the circuit, which is located between R_2 and R_3, is connected to the positive pole of the DC power supply. Point C, which is located between R_1 and R_x, is connected to the negative pole of the DC power supply. Points B and D are connected to the positive and negative poles of the voltmeter, respectively.

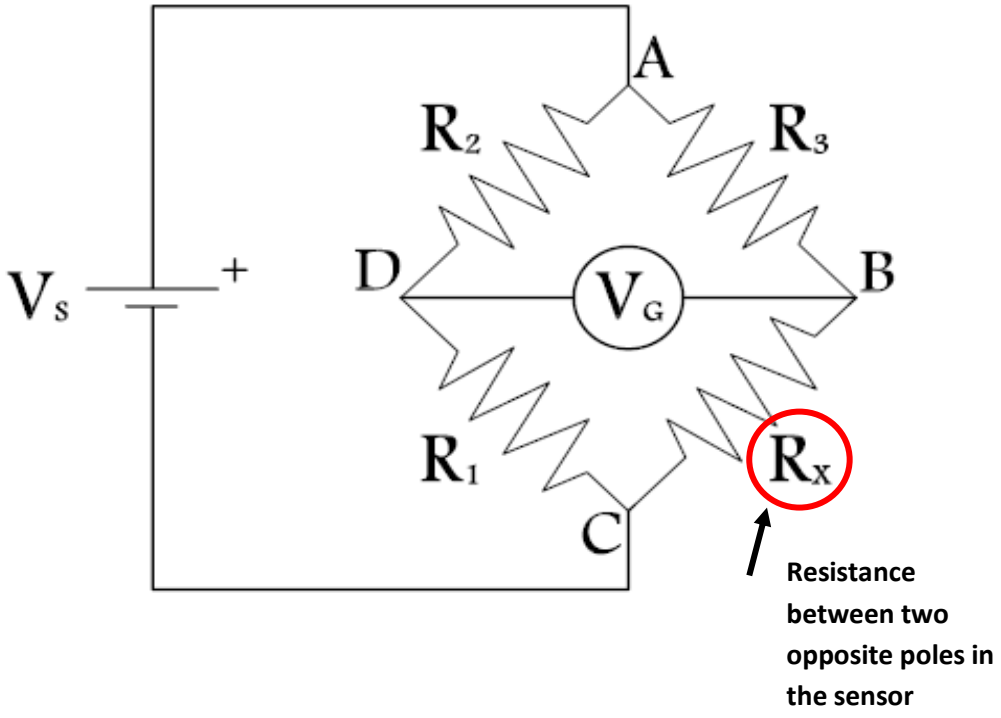

Figure 4.3-1: Wheatstone Bridge

Using Eq. 2-1 and knowing the values of R_1, R_2, R_3, and V_G, the values of (R_x) could be calculated. A circuit built on breadboard as shown in Figure 4.3-2 was assembled to

represent the Wheatstone Bridge circuit for testing purpose. The DC power supply used is shown in Figure 4.3-3.

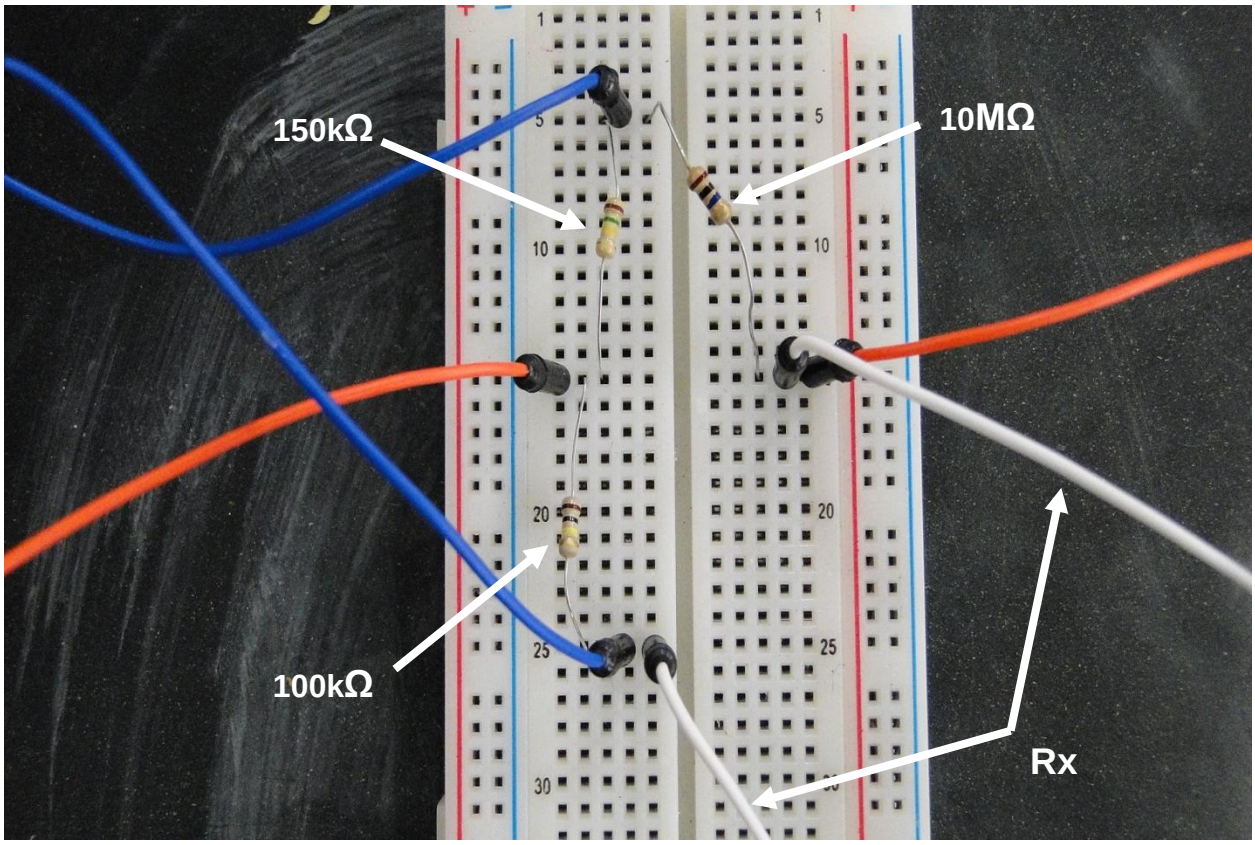

Figure 4.3-2: Wheatstone Bridge circuit assembled on breadboard for testing

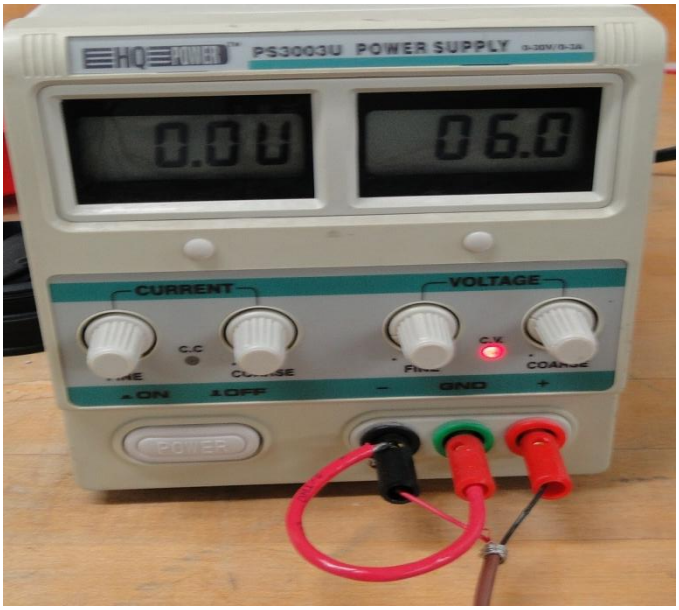

Figure 4.3-3: Power supply used for the Wheatstone Bridge circuit

The temperature at the surface of the sensor was monitored using an infrared non-contact temperature sensor. The temperature was recorded by taking 4 to 6 readings at different spots on the surface of the sensor. The average of the readings was used as surface temperature. The temperature was measured along with the voltage (V_G). Relations between surface temperature and voltage (V_G) were plotted in each test. The following environmental conditions were tested:

1- Surface Ice (Black Ice) (SI)

   The dry sensor was placed in a freezer (temperature of -20C˚ or -4F˚) overnight. Just prior to the beginning of testing, the sensor was removed from the freezer and sprayed with room-temperature water from a spray bottle. The surface ice was then formed (Figure 4.3-4), and measurements were periodically taken as surface temperature increased up to room temperature

Figure 4.3-4: Surface ice formation on cold SP-I sensor

2- Frozen (without surface ice) (FR)

The top of the sensor was immersed in water for a few hours to allow its pores to be filled with water, especially the pores near the surface. Subsequently, the sensor was removed from water and the excess surface water was wiped off. The sensor was then placed in the freezer (temperature of -20C˚ or-4F˚) overnight so that the water in the pores freezes. The sensor was removed from the freezer just before testing. Unlike the SI test, water was not sprayed on the surface. This condition represents the situation in which the pavement is saturated and then frozen without formation of surface ice.

3- Frozen Concrete with Surface ice (FR-SI)

This condition is a combination of the SI and FR conditions described above. The FR procedures were followed but room-temperature water was sprayed onto the top surface to form a surface ice layer on top of the frozen surface.

4- Dry Condition (DR)

The sensor was placed in an oven to be dried for approximately 24 hours at temperature of 48C˚ (118F˚). After that, the sensor was taken out of the oven and allowed to cool down. Then, it was put in the freezer for 24 hours at a temperature of -20C˚ (-4F˚). The sensor was taken out of the freezer and connected to the Wheatstone bridge to monitor the output of the bridge (change in the resistance).

To understand and determine the possible range of concrete resistances, tests are performed under different environmental conditions (described above). The concrete sensor was connected to the electrical circuit as shown in Figure 4.3-5. In all tests described above, the sensor was monitored periodically as the surface temperature increased up to room temperature.

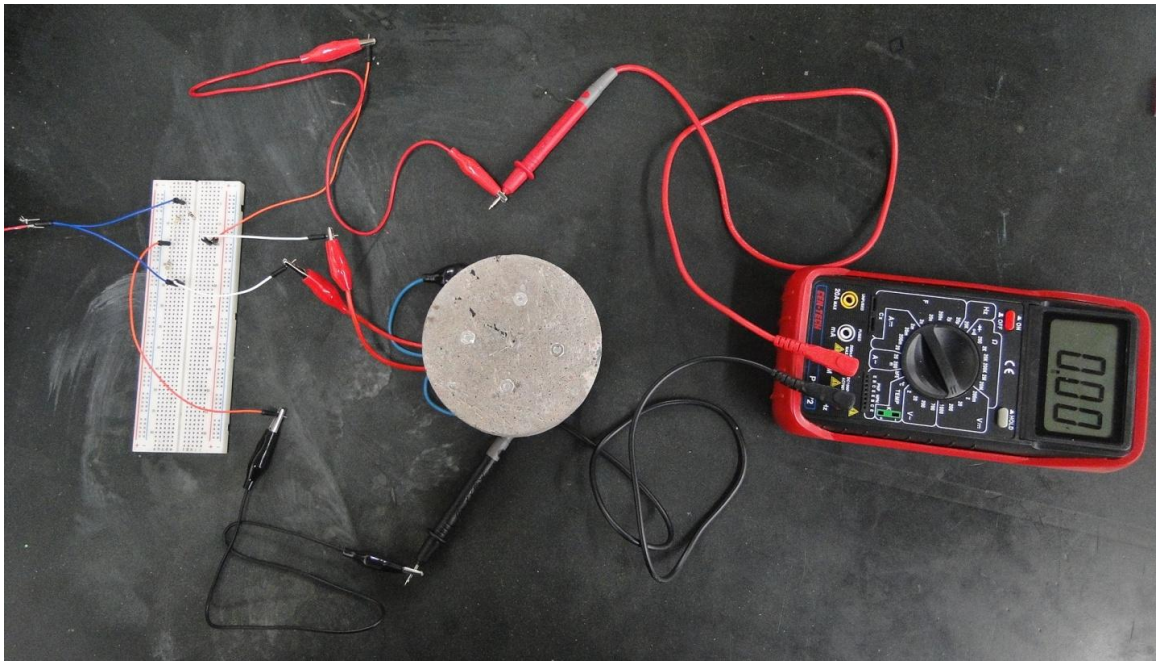

Figure 4.3-5: Test connections

4.4 Resistance calculations

The measure output voltage V_G, the known resistors R_1, R_2, and R_3 were used to calculate R_X using Eq. 4-2. Calculations could also be performed to predict the resistance value (between poles) under different surface conditions using simple equations for parallel or series resistors. Assume that the concrete resistance between the sensor poles is equal to measured dry resistance from the tests with LUS poles. This resistance is in parallel with the resistance associated with whatever material (e.g. ice) that may exist on the sensor's top surface in a LUS poles setup. The following equation for parallel resistors could be used:

$$\frac{1}{R} = \frac{1}{Rs} + \frac{1}{Rc} \quad \ldots\ldots\ldots\ldots\ldots\ldots\ldots \text{(Eq. 4-2)}$$

Where; R = Effective resistance (MΩ) of two parallel R_S and R_C resistors.

R_S= Surface Resistance (MΩ)

R_C= Dry Concrete Resistance (MΩ)

4.5 Test results

4.5.1 Tests on SP-I sensor

Dry test (DR)

Three DR tests were performed on the SP-I sensor (DRI-1, 2, and3). The sensor was dried in the oven for 24 hours prior to test DRI-1. In tests DRI-2 and DRI-3, the sensor was not dried in the oven before testing. The sensor was then put in the freezer for 24 hours. Figure 4.5-1 and 4.5-2 show voltage and resistance changes with temperature for the (DR) tests in SP-I. As the surface temperature approached 0C˚ (32F˚), condensation formed on the surface, which caused a dip in the output voltage and resistance. However aside from the condensation effects, the output voltage (for V_S=6volts) is on the order of 1.75v (resistance of 22-23 MΩ).

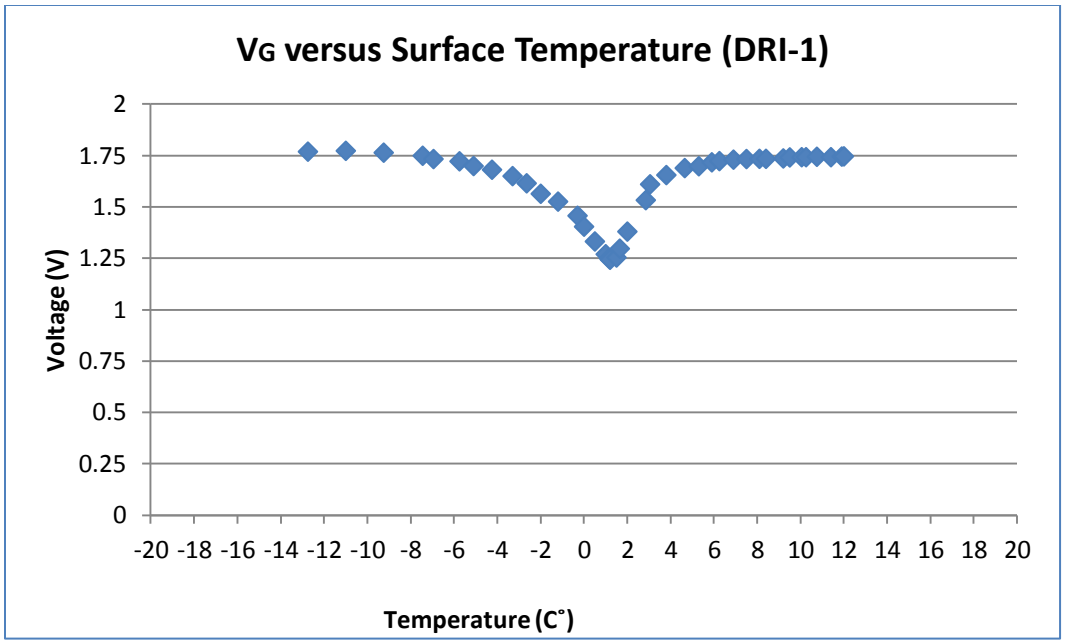

Figure 4.5-1: Output voltage versus surface temperature for SP-I under dry condition (test1)

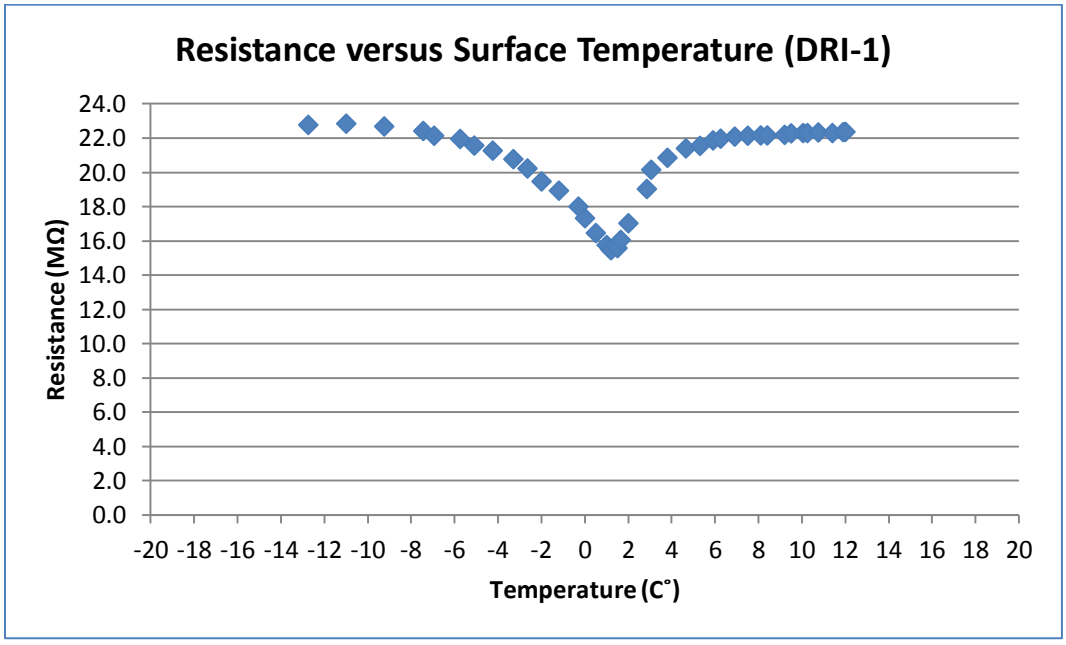

Figure 4.5-2: Resistance versus surface temperature for SP-I under dry condition (test1).

The results of DRI-2 test are shown in figures 4.5-3 and 4.5-4. In this test, the condensation affect was larger (condensation is related to the humidity of the

laboratory). The dry resistance is again on the order of 22-23 MΩ. Test DRI-3 did not differ significantly from test DRI-2, except to show more pronounced indication of moisture development in the concrete pores due to condensation. Figures 4.5-5 and 4.5-6 show plots of results of Test DRI-3. Figures 4.5-7 and 4.5-8 show all three tests of the DR test for SP-I.

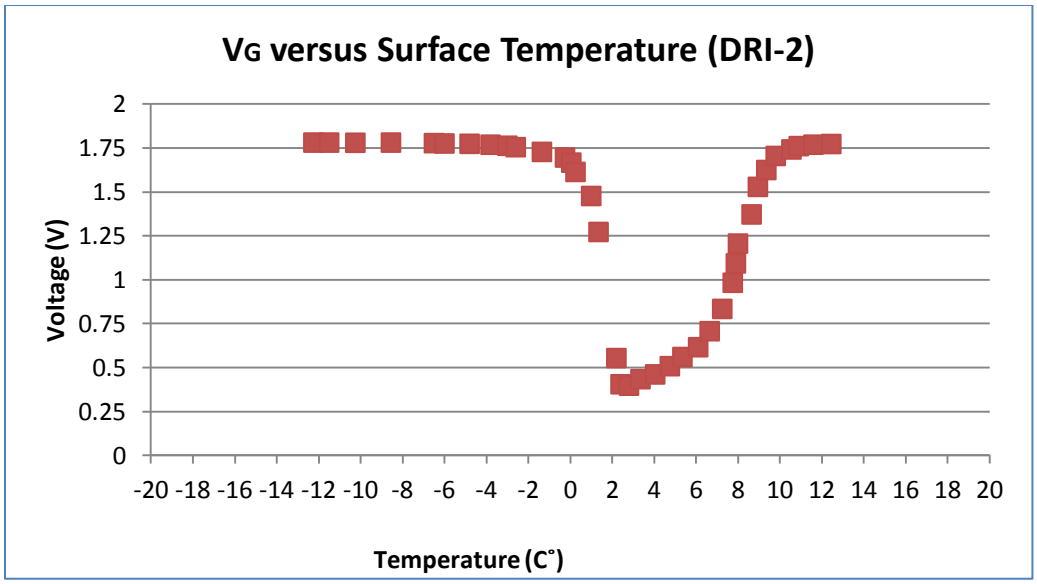

Figure 4.5-3: Output voltage versus surface temperature for SP-I under dry condition (test2).

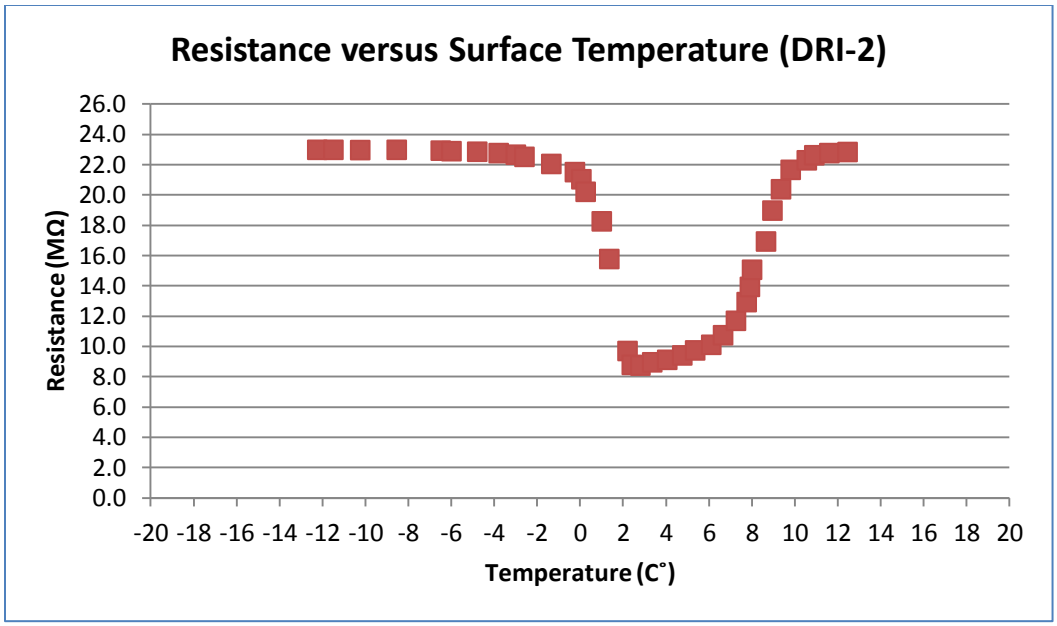

Figure 4.5-4: Resistance versus surface temperature for SP-I under dry condition (test2).

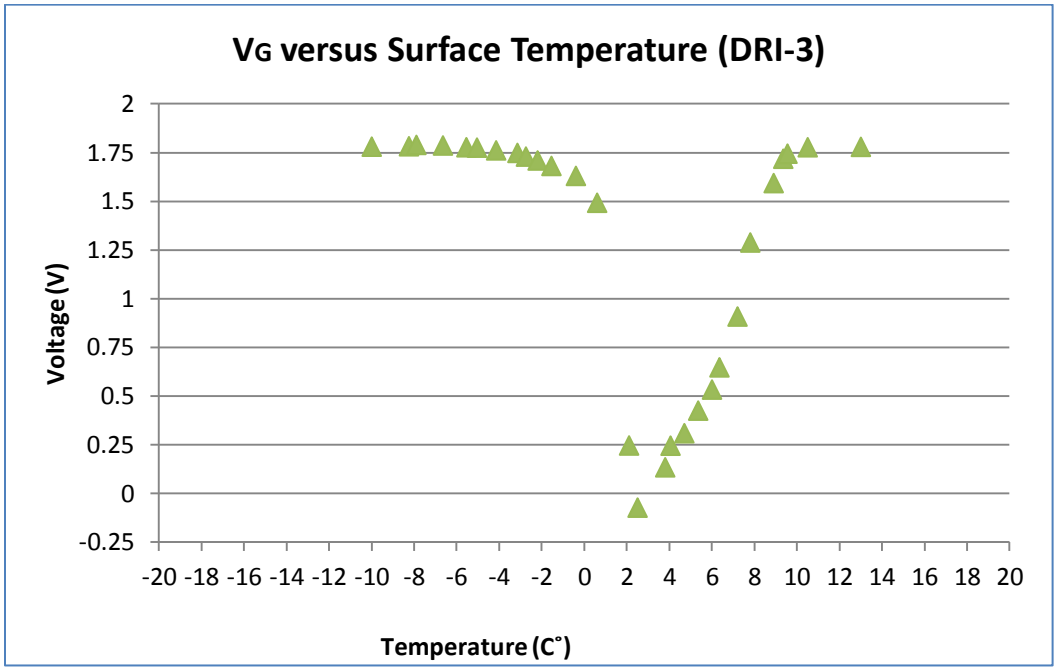

Figure 4.5-5: Output voltage versus surface temperature for SP-I under dry condition (test3).

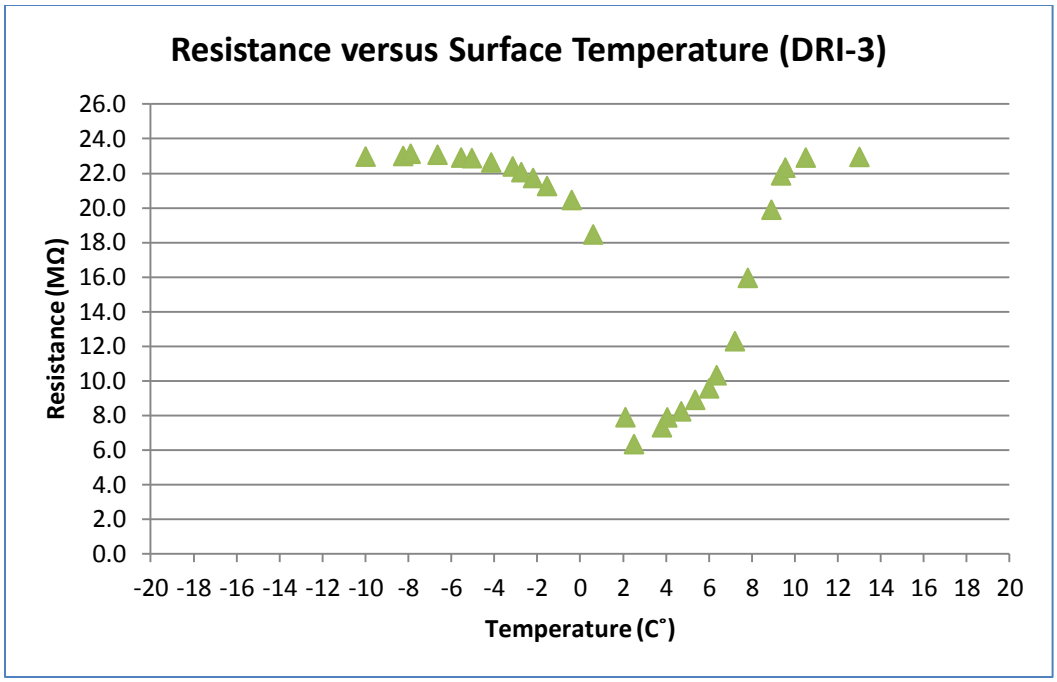

Figure 4.5-6: Resistance versus surface temperature for SP-I under dry condition (test3).

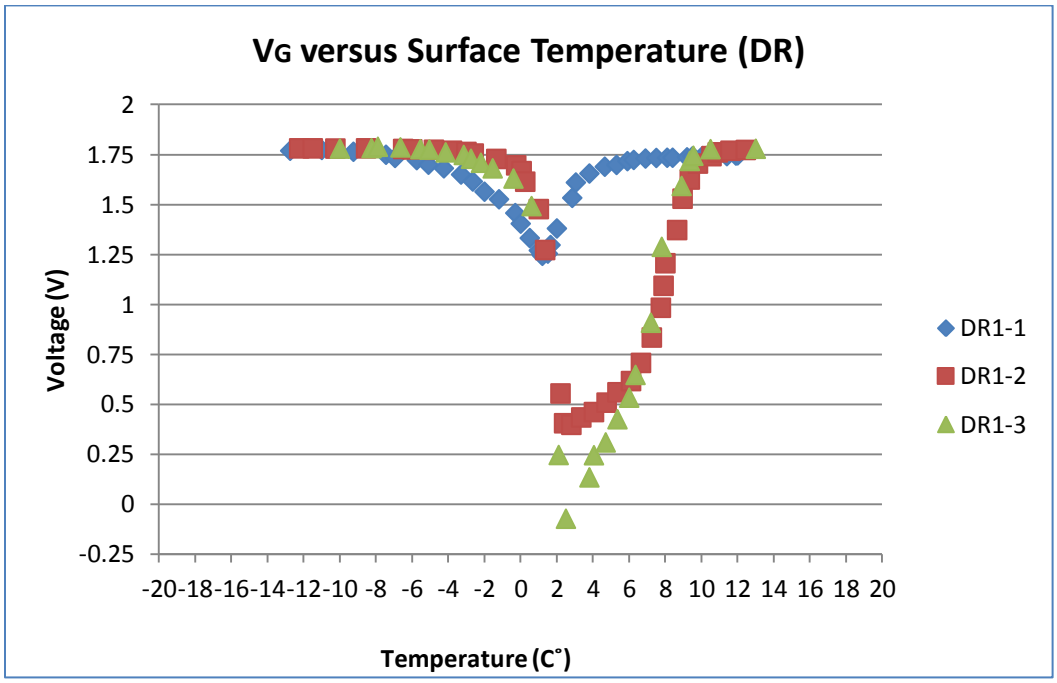

Figure 4.5-7: Output voltage versus surface temperature for SP-I under dry condition (all three tests).

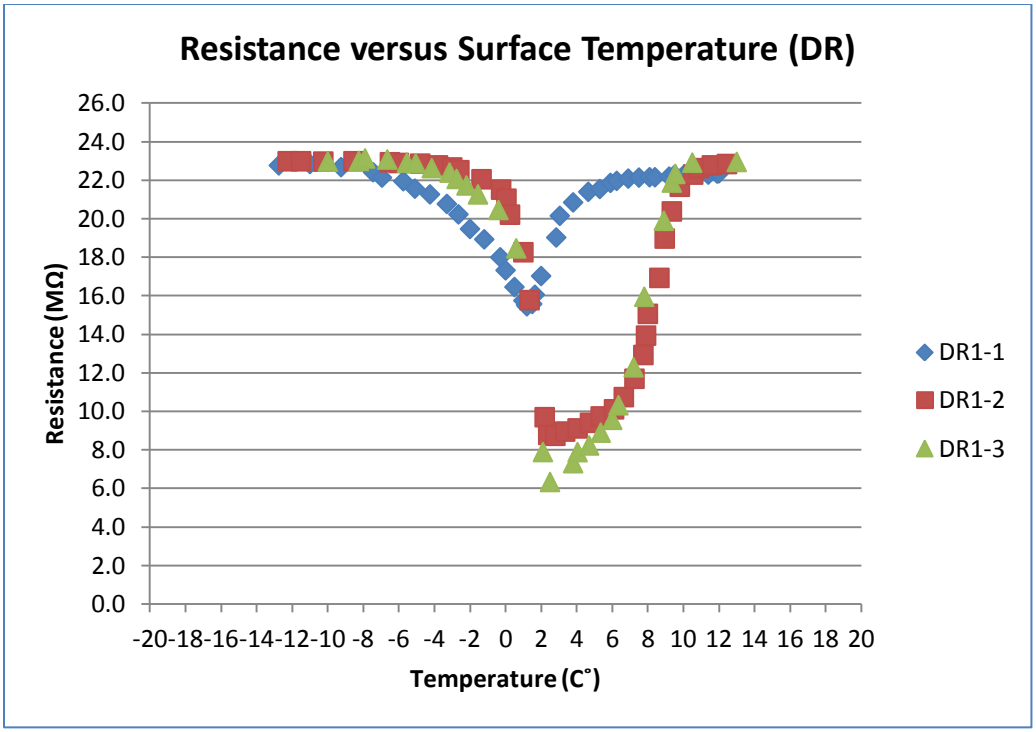

Figure 4.5-8: Resistance versus surface temperature for SP-I under dry condition (all three tests).

It could be noticed that at extreme cold temperatures below -8C˚ (18F˚) and at warmer temperatures above +8C˚ (46F˚), the resistance and voltage for the three tests are similar and approximately equal to 1.75v. Test DRI-1 started to differ from test DRI-2 and test DRI-3 within the temperature range of -6C˚ to +10C˚. The presence of moisture due to condensation drives the output voltage and resistance low. As the moisture disappears at higher temperature, the output voltage and resistance values for both tests (DRI-2 and DRI-3) are similar to those values for (DRI-1).

Frozen test (FR)

The top surface of the SP-I was immersed in water for 2-3 hours as shown in figure 4.5-9. It was then removed and placed in the freezer for 24 hours. The sensor was subsequently taken out of the freezer before testing.

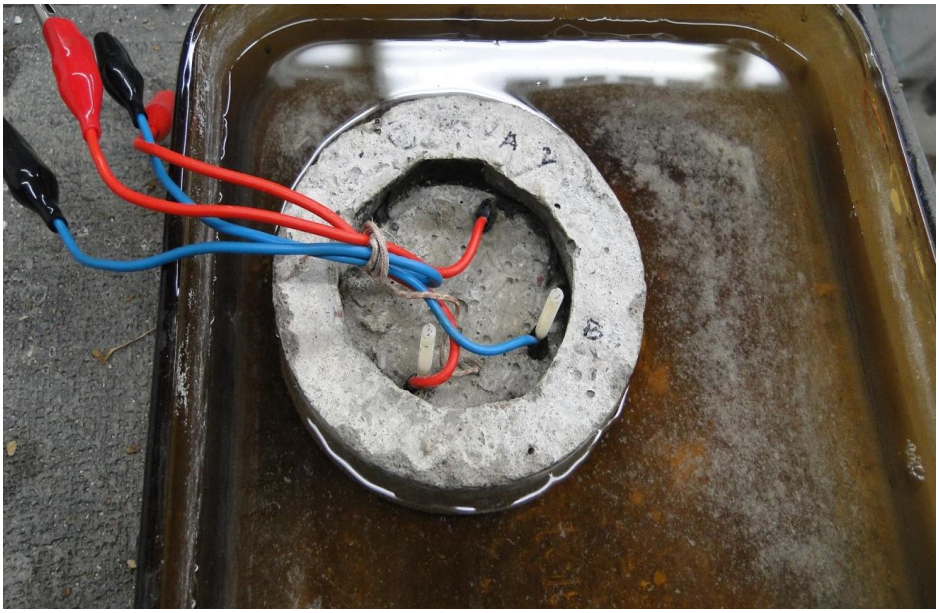

Figure 4.5-9: SP-I is placed in water tray

The output data and the surface temperature were periodically monitored while the sensor's temperature changed. Plots for resistance and output voltage versus temperature were generated. This test was done to understand the effect of the presence of frozen water in the concrete pores, and to see how the change from pore ice to pore water would affect the concrete electrical resistance. The voltage and resistance results are shown in Figures 4.5-10 and 4.5-11, respectively. It could be seen that, for the temperature range -11C˚ (12F˚) to 2C˚ (36F˚), the voltage (and resistance) decreased as the temperature increased. The output dropped rapidly as ice in concrete pores began to melt. There is a nearly linear relationship between voltage (resistance) and temperature at temperatures below zero. The voltage levels under FR condition are much lower than the in DR tests described earlier. For temperatures above 2C˚ (36F˚), voltage and resistance values stayed nearly constant. This can be explained by the fact that the ice in the

concrete pores has been converted from solid (ice) into liquid form, and the output is associated with a moist concrete condition.

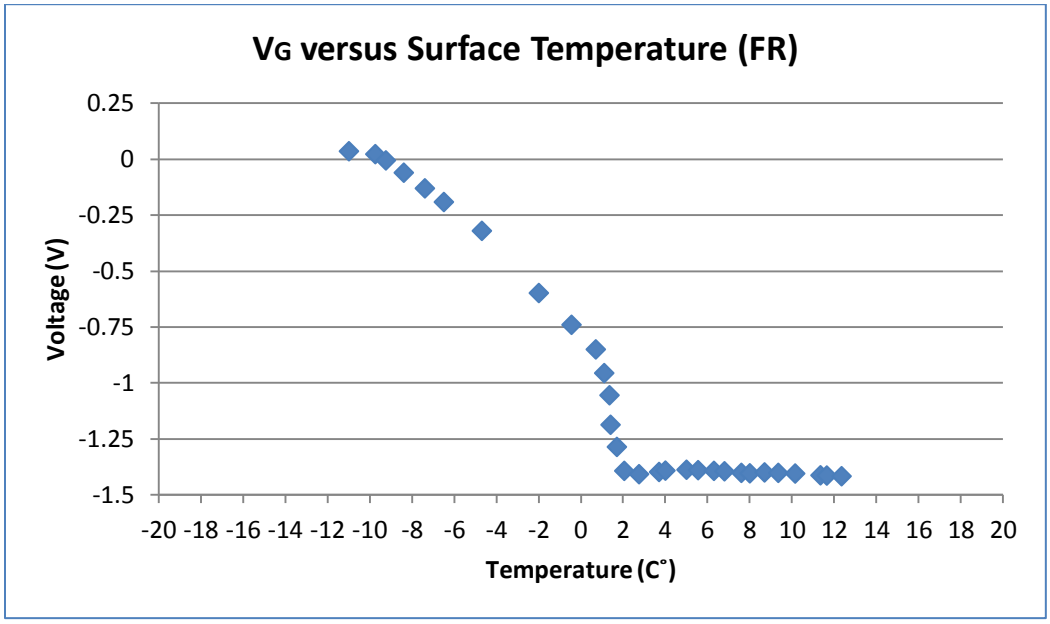

Figure 4.5-10: Output voltage versus surface temperature for SP-I under frozen condition

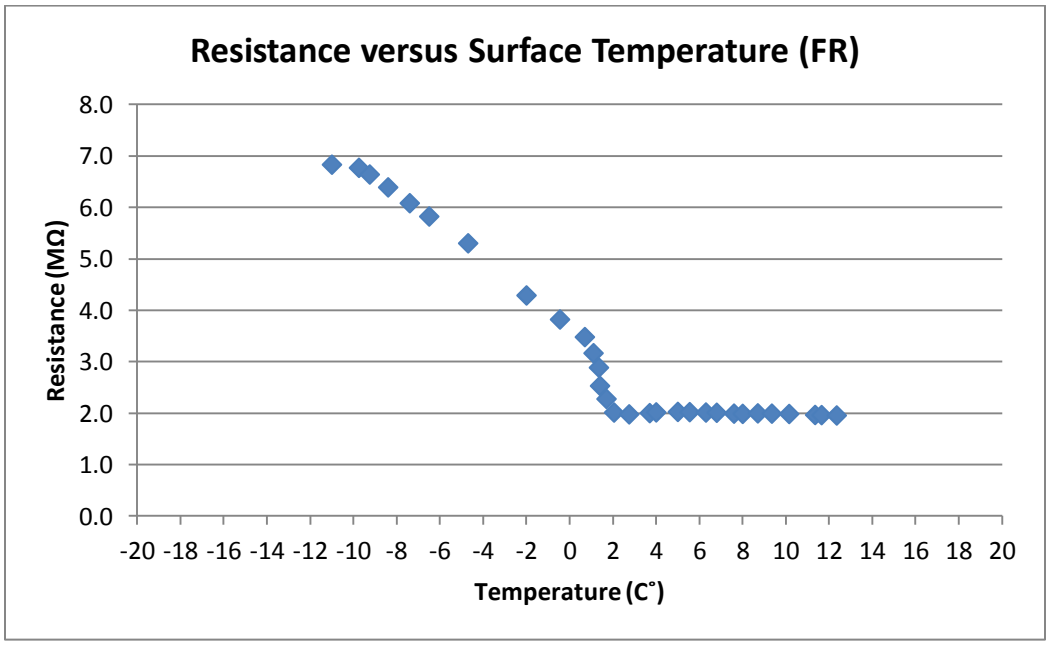

Figure 4.5-11 Resistance versus surface temperature for SP-I under frozen condition

The resistance of concrete is related to the presence of moisture in the pores structure. Therefore, the measured resistance and voltage both decrease as water content increases. Voltage output for frozen concrete ranged between +0.1v and -0.8v (7.0MΩ to 3.5 MΩ), while moist concrete output voltage were on the order of -1.4v (2.0MΩ).

Surface ice test (SI)

Surface ice is the most dangerous pavement condition. The main area of interest in this research, therefore, was on proper detection of such conditions. In this test, the SP-I (with all LUS poles) was put in a freezer for about 24 hours at a temperature of -20C˚ (-4F˚). Then it was moved to the lab to be tested by connecting the sensor's poles to the Wheatstone Bridge circuit. Water (which was at room-temperature) was sprayed on the cold surface of the sensor to simulate surface ice formation. Once the surface ice formed, the process of monitoring output voltage and surface temperature began. Figure 4.5-12 shows the sensor with black ice formed on its surface. The black ice layer is relatively thin (about 1/16").

Figure 4.5-12 Surface ice formation on SP-I

The relationship between voltage (resistance) and surface temperature for the first test (SI-I-1) are shown in Figures 4.5-13 and 4.5-14. There is a linear relationship between output voltage and surface temperature when there is surface ice present. The output voltage is in on the order of 0v to +0.25v. As the ice melts, the output voltage drops to -0.75v. The output voltage under moist condition is in the range of -0.75v to -1.0v.

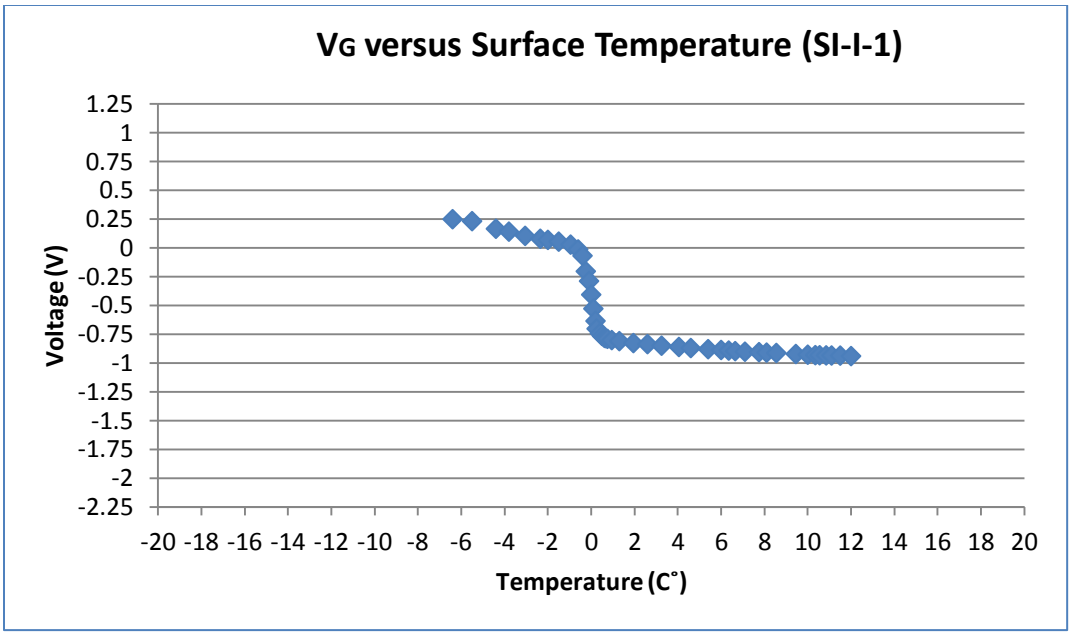

Figure 4.5-13 Output voltage versus surface temperature for SP-I under surface ice condition (test1)

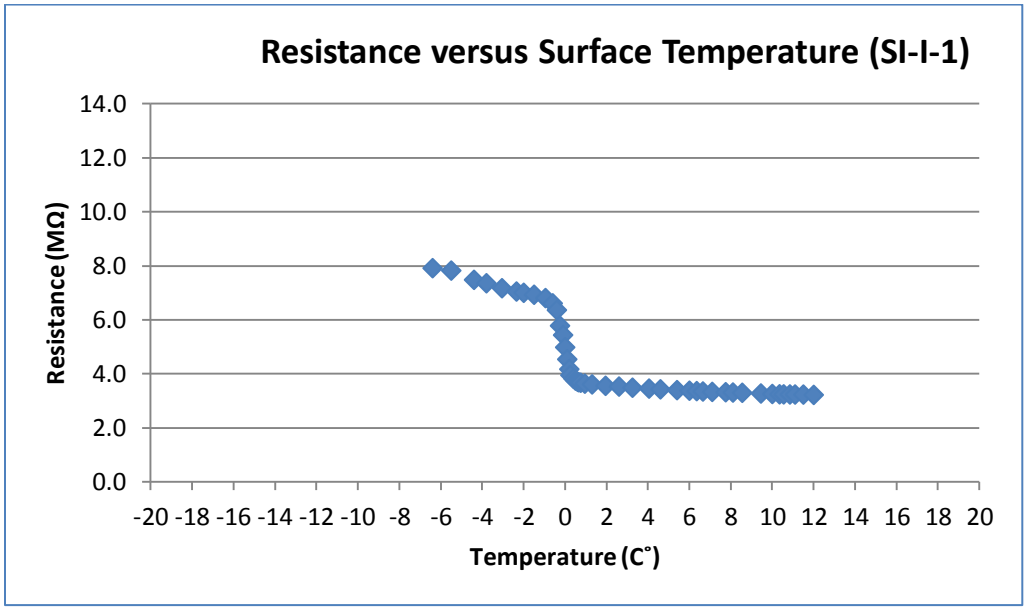

Figure 4.5-14 Resistance versus surface temperature for SP-I under surface ice condition (test1)

In Test SI-I-2, Results showed a similar pattern as in the first test, as shown figures 4.5-15 and 4.5-16. The linear output voltage-temperature behavior under SI condition in evident. The output voltage ranges from 0v to +0.9v. The output

voltage drops to -1.1v when the ice melts. The moist surface condition has a voltage output of -0.8v to -1.1v.

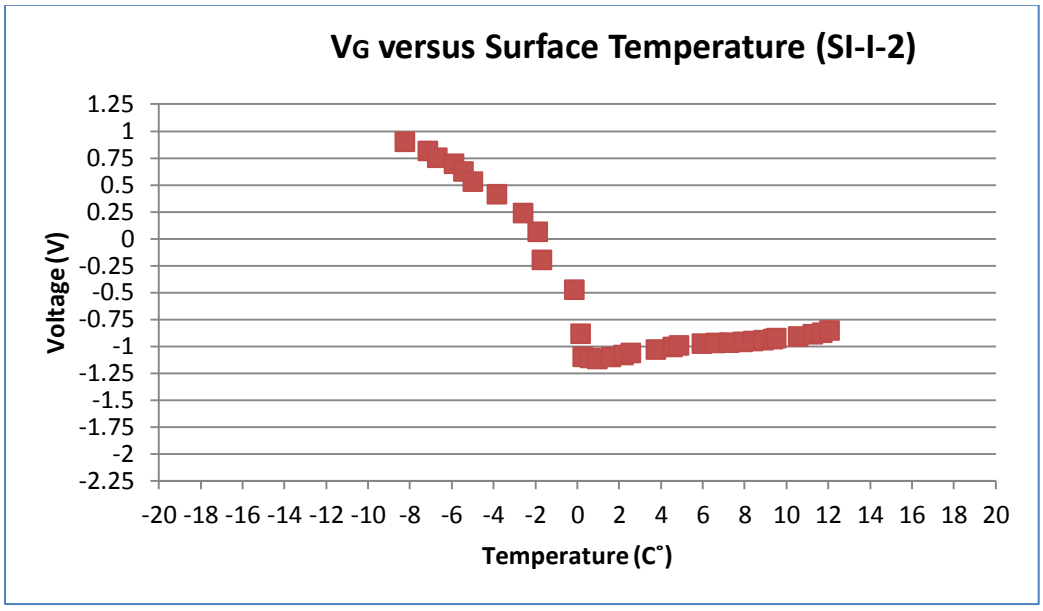

Figure 4.5-15 Output voltage versus surface temperature for SP-I under surface ice condition (test2)

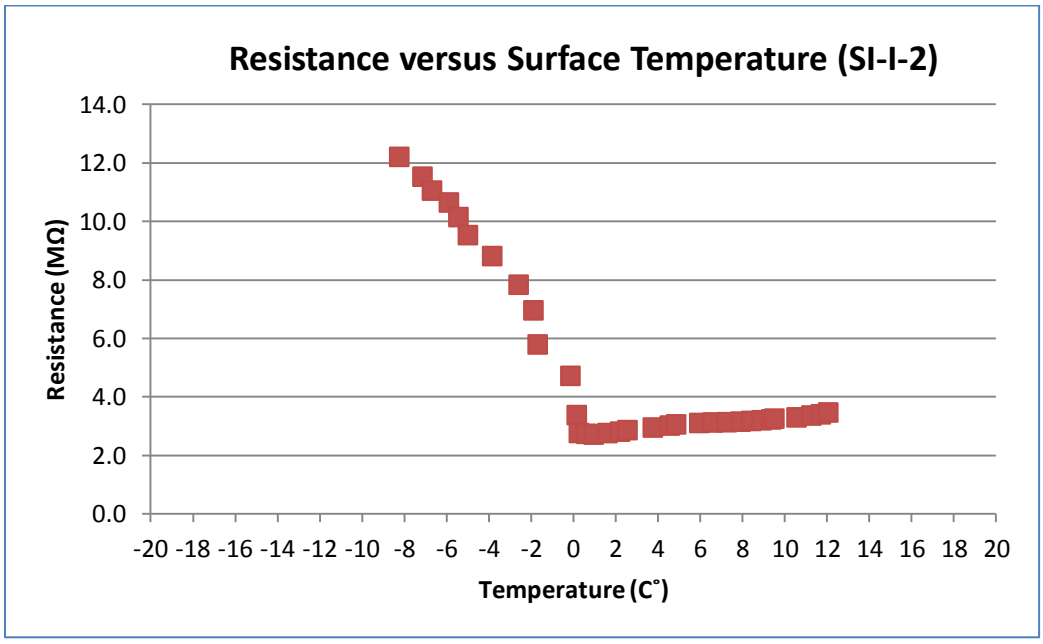

Figure 4.5-16: Resistance versus surface temperature for SP-I under surface ice condition (test2)

Results show that there are some differences between the two tests. Figures 4.5-17 and 4.5-18 show plots for the two tests together. A difference could be clearly

seen when temperature was in range of -10C˚ (14F˚) to -3.5C˚ (26F˚). Variation in the thickness of the ice can change the resistance of the ice-concrete combination in LUS poles. This may be the primary facts in the observed difference. For the range of temperature between -3.5C˚ (26F˚) to 0C˚ (32F˚), both tests tend to perform in a similar manner. The general conclusion drawn is that resistance is decreased as the temperature is increased when surface ice exists. Plots for both tests tend to stabilize within a reasonably close range once the ice totally melts and as the temperature increase above 0C˚ (32F˚).

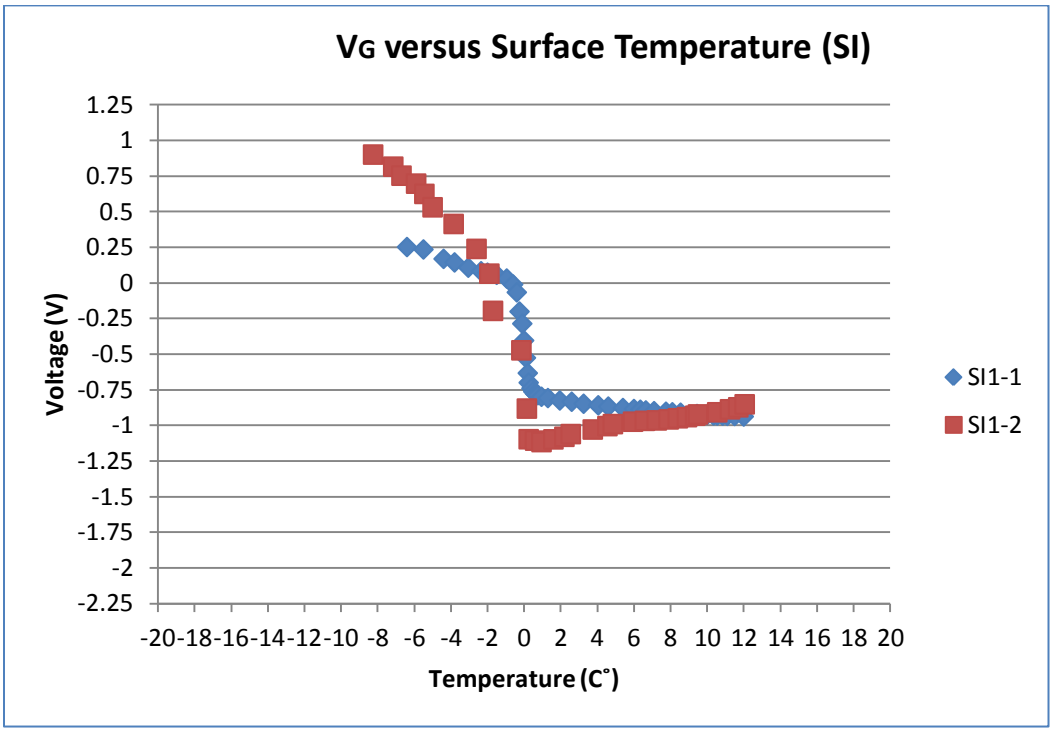

Figure 4.5-17: Output voltage versus surface temperature for SP-I under surface ice condition (both tests)

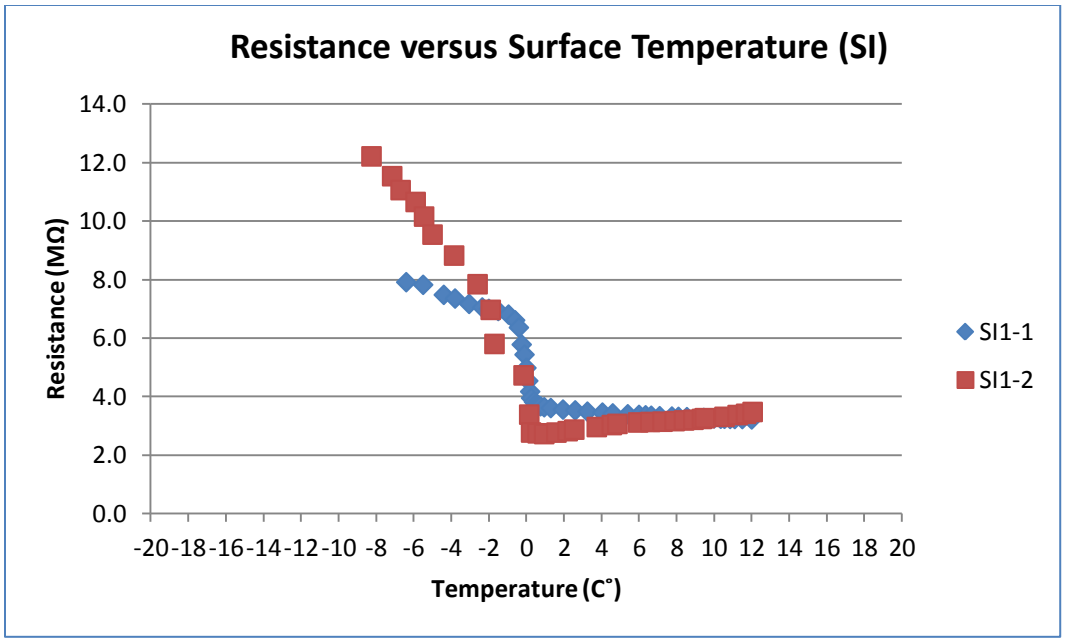

Figure 4.5-18: Resistance versus surface temperature for SP-I under surface ice condition (both tests)

Frozen-Surface Ice test (FR-SI)

In this test, performed on SP-I (with LUS poles) water was present in the concrete pores (was saturated with water) before placing the sensor in the freezer. This condition could be happening on a bridge overpass or pavement where rain or fog deposits moisture on a cold and frozen surface. The sensor was submerged in water for 2-3 hours, was placed in the freezer for approximately (24) hours, and then moved to the laboratory for testing. The sensor was connected to Wheatstone Bridge and water was sprayed on its surface to simulate the surface ice formation. The output voltage was monitored as temperature increased. The relationships between output voltage and resistance versus change temperature as shown in figures 4.5-19 and 4.5-20 for Test FR-SI I-1.

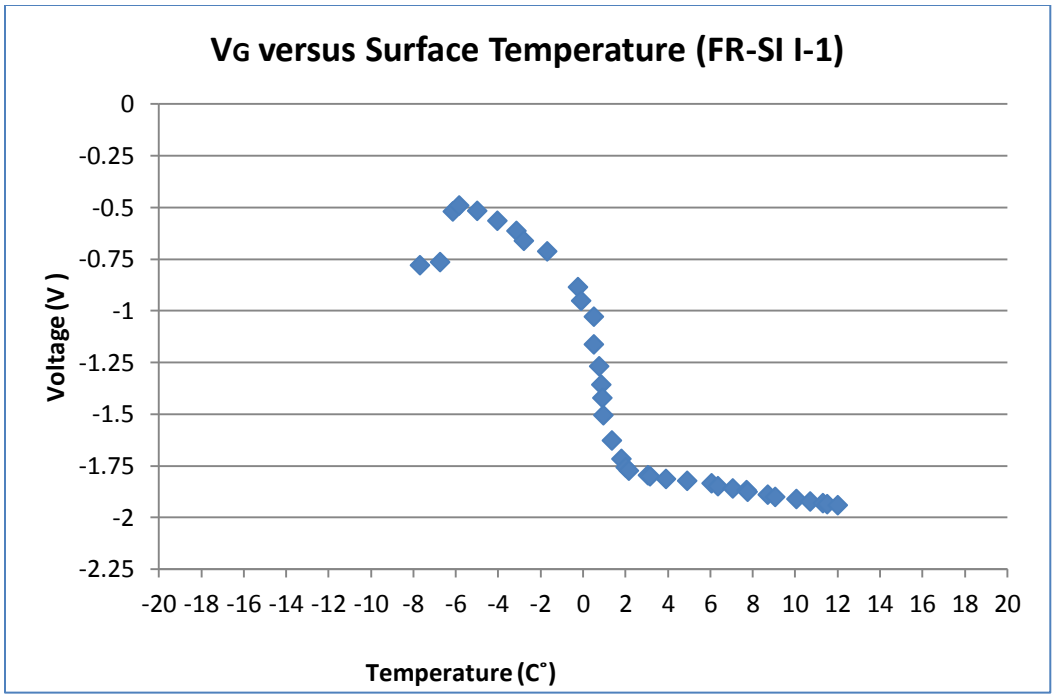

Figure 4.5-19: Output voltage versus surface temperature for SP-I under FR-SI condition (test1)

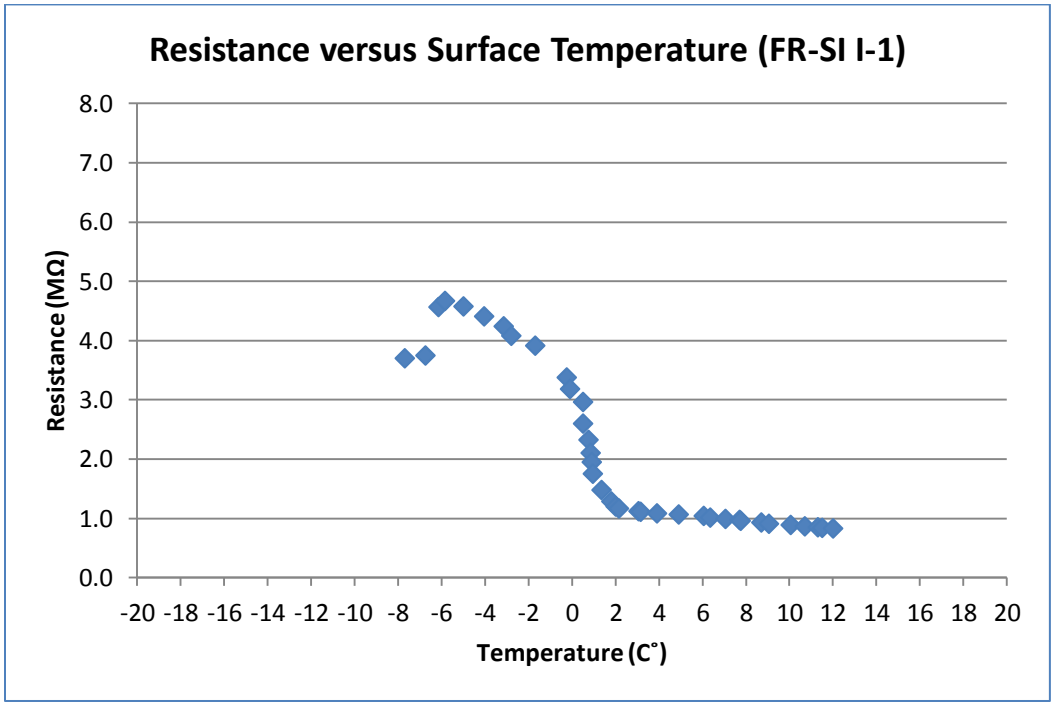

Figure 4.5-20: Resistance versus surface temperature for SP-I under FR-SI condition (test1)

Procedure for the second test (FR-SI I-2) was the same as the first test. Output voltage and resistance are plotted versus temperature change as in figures 4.5-21 and 4.5-22, respectively.

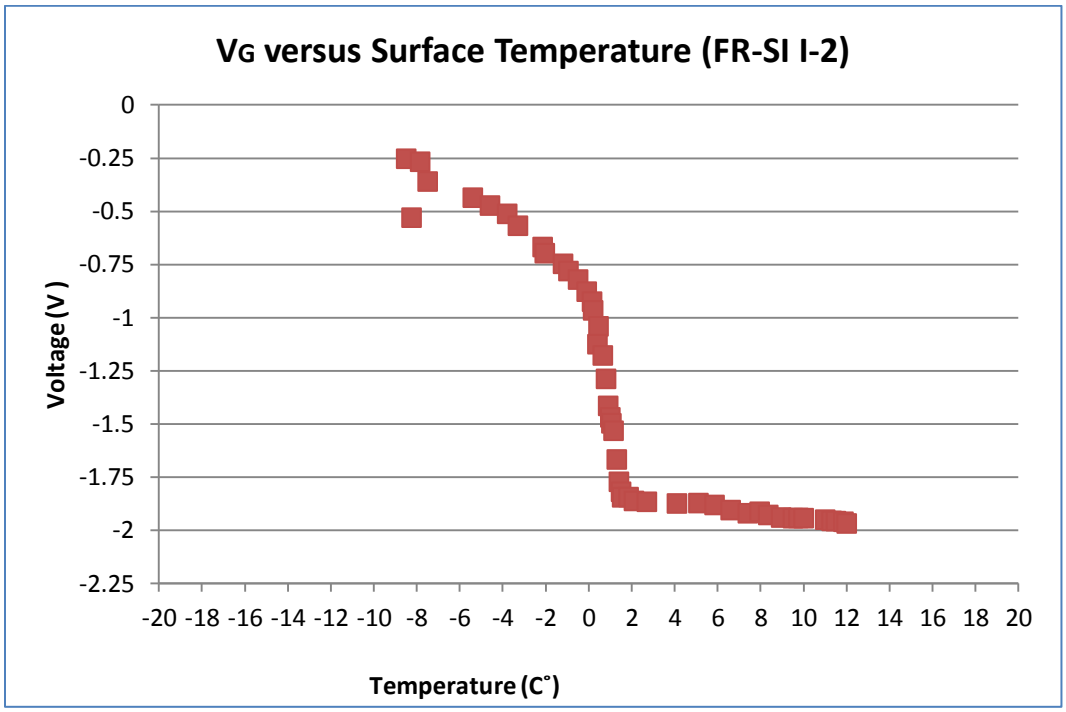

Figure 4.5-21: Output voltage versus surface temperature for SP-I under FR-SI condition (test 2)

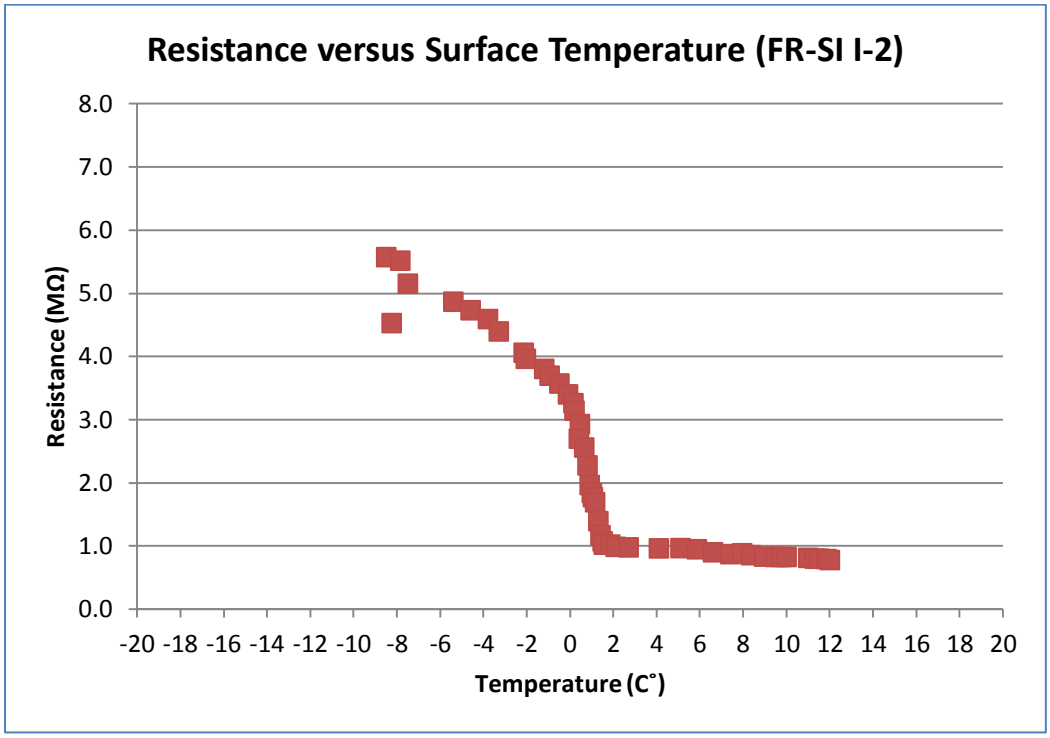

Figure 4.5-22: Resistance versus surface temperature for SP-I under FR-SI condition (test2)

Both FR-SI tests had similar outcomes and patterns. Both tests had a slight initial increase in output. As water was sprayed on the sensor, output voltage initially decreased, and as ice started forming, output voltage increased. Under icy conditions, there is a linear relationship between output voltage and temperature. The presence of ice in the sensor's concrete pores caused the output voltage (and resistance) to have lower value compared to when the sensor did not have ice in its pores. As the temperature increased, further water melted, and the resistance decreased for the range of temperature between -8C˚ (18F˚) to 2C˚ (36F˚). Figures 4.5-23 and 4.5-24 show both test results combined together. As the ice on the top of the sensor melts with time, a steep drop in bridge output (and resistance) occurs. When the temperature reaches above 2C˚ (36F˚) (wet

condition), the output voltage (and resistance) values reach a range of -1.75v to -2v and resistance ≈1 MΩ, respectively.

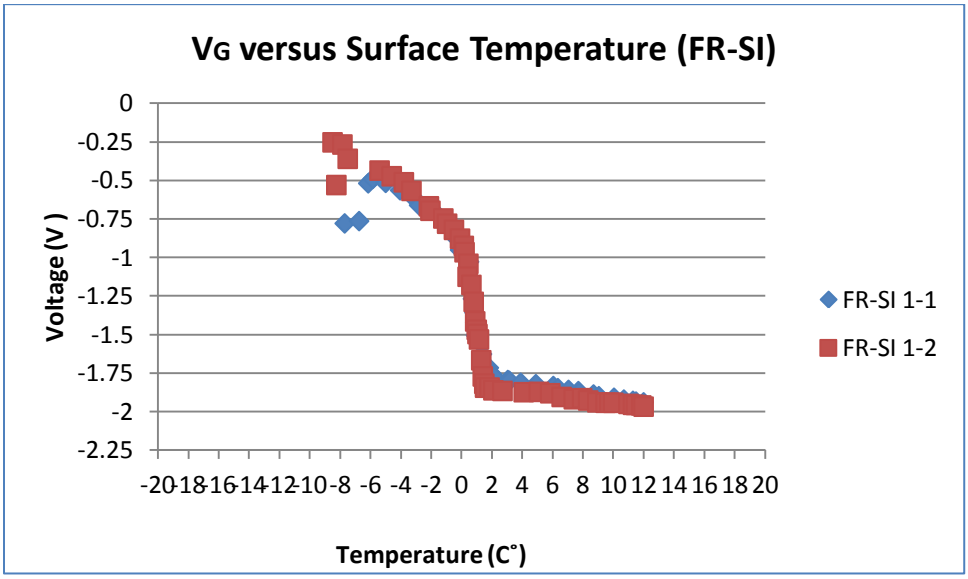

Figure 4.5-23: Output voltage versus surface temperature for SP-I under FR-SI condition (both test)

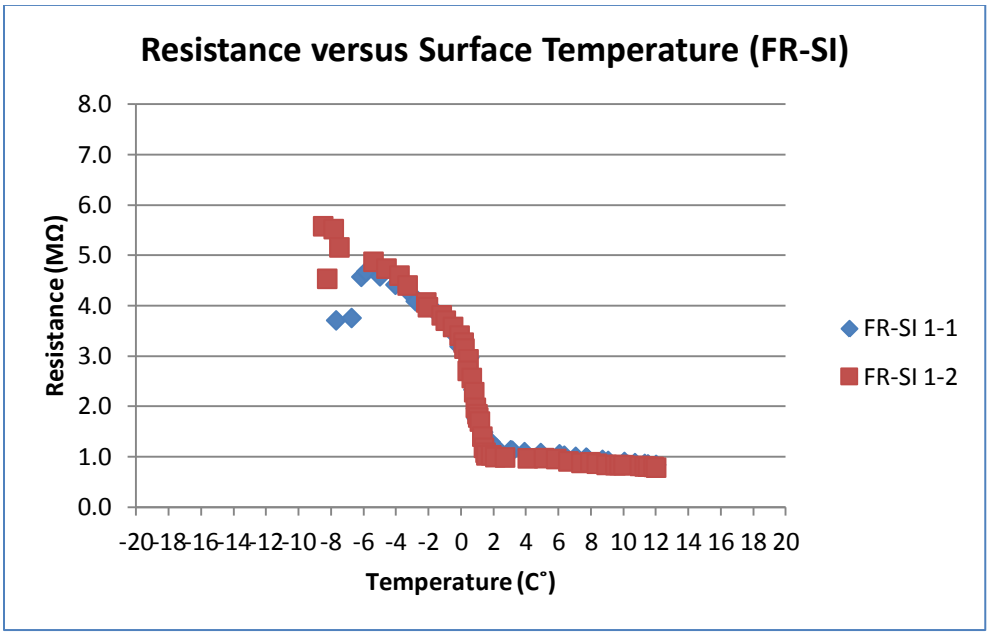

Figure 4.5-24: Resistance versus surface temperature for SP-I under FR-SI condition (both tests)

Surface ice with saltwater (SI-SW):

Icy roads are commonly treated with deicing salt during winter. Therefore, icing may not occur in presence of deicing salts at temperature below 0C˚ (32F˚). This test tries to simulate such conditions. The sensor was put in the freezer for about 24 hour. Subsequently, it was moved to the laboratory and its surface was sprayed with water to form surface ice. The test was started and readings were taking until the temperature increased up to -4C˚ (25F˚), then saltwater (SW) was sprayed on the sensor, and readings were taken as the temperature increased. The saltwater was a 6% NaCl solution at room temperature. Figures 4.5-25 and 4.5-26 show changes in output voltage and resistance with temperature, respectively for test SI-SW I-1.

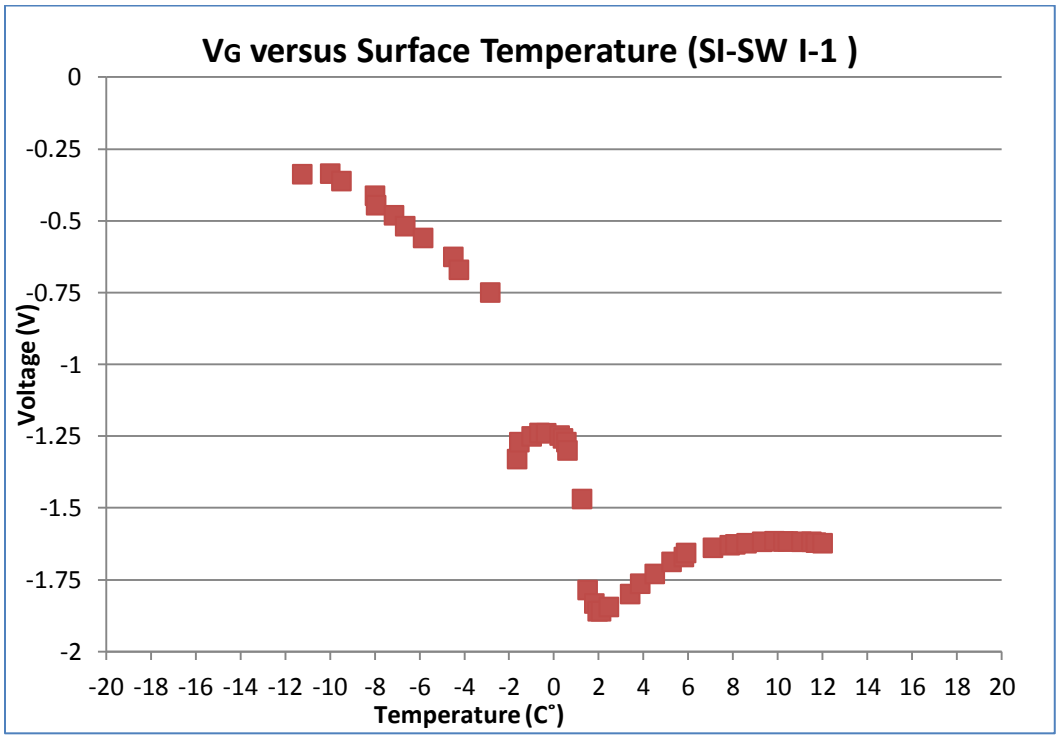

Figure 4.5-25: Output voltage versus surface temperature for SP-I under SI-SW (test1)

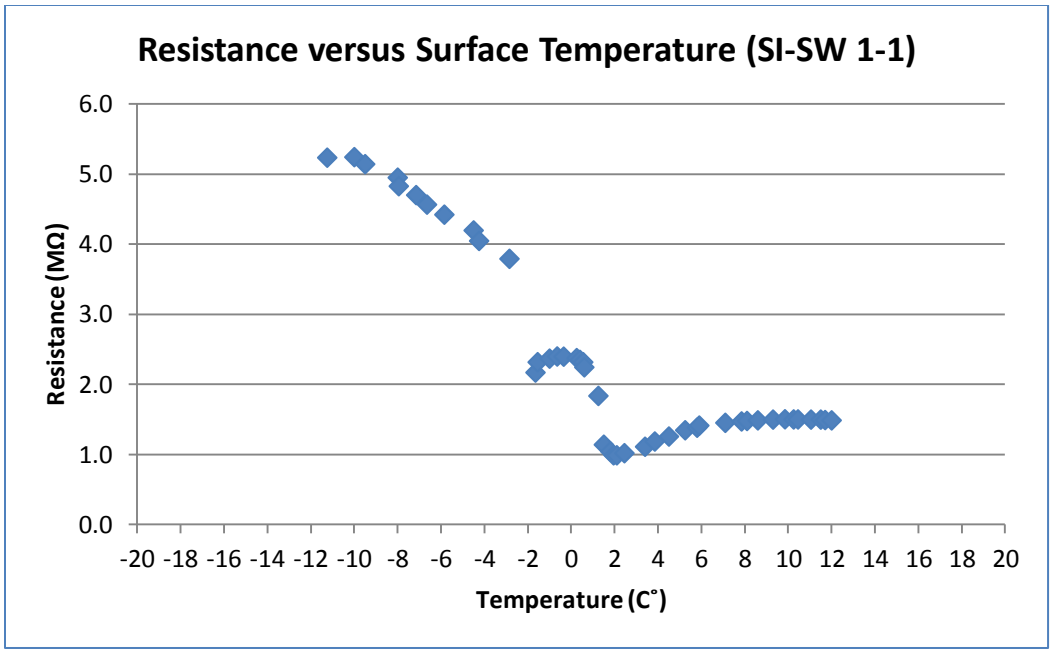

Figure 4.5-26: Resistance versus surface temperature for SP-I under SI-SW condition (test2)

Similar procedures were repeated in test SI-SW I-2, Figures 4.5-27 and 4.5-28 show changes in output voltage and resistance versus temperature for test SI-SW I-2, respectively.

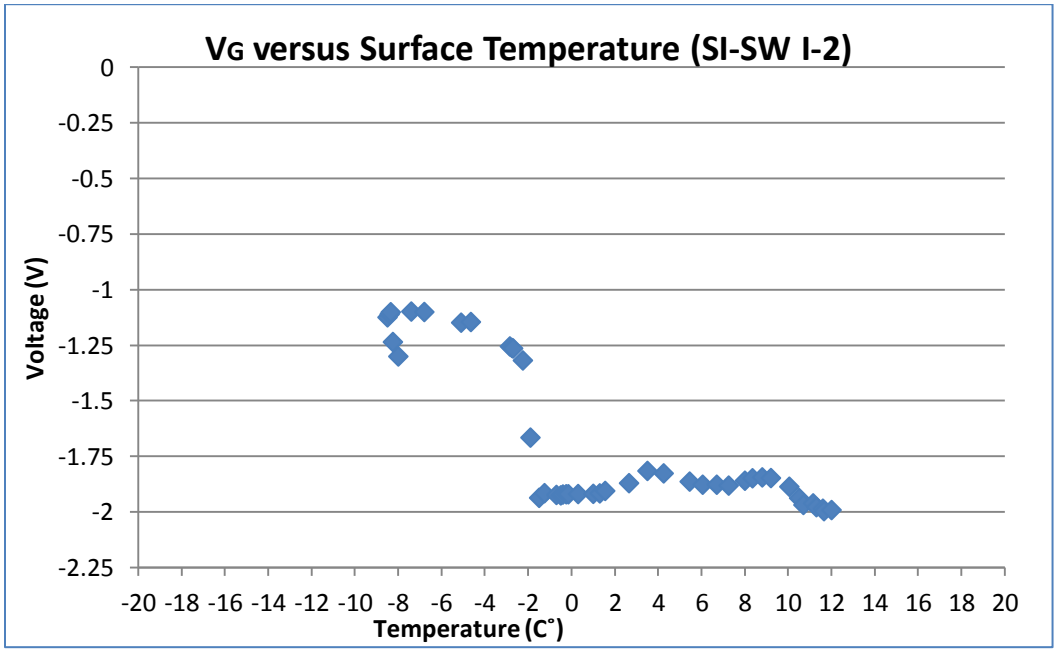

Figure 4.5-27: Output voltage versus surface temperature for SP-I under SI-SW condition (test2)

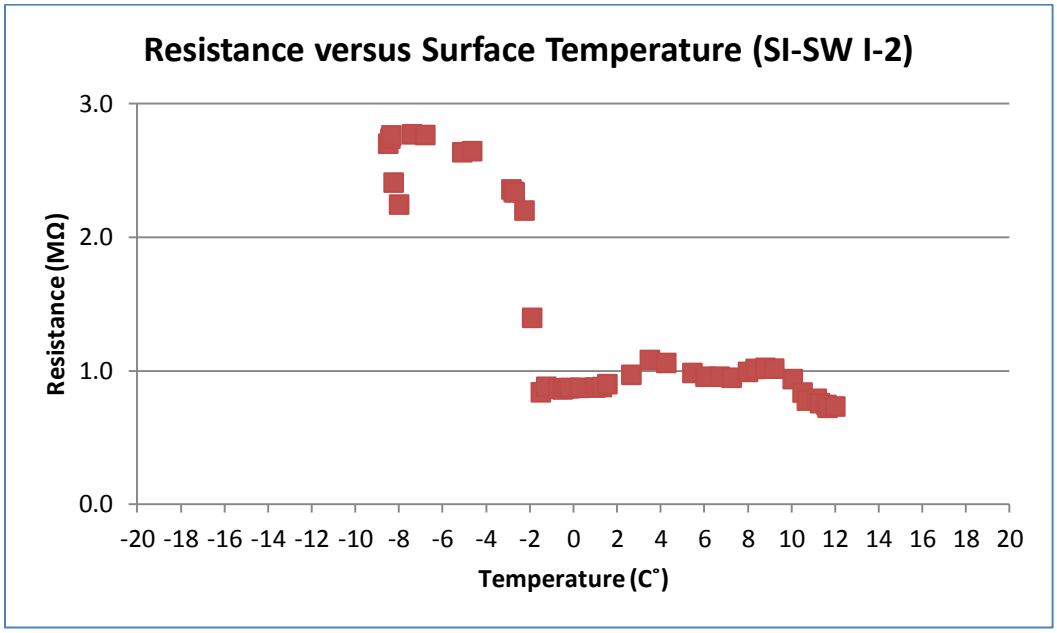

Figure 4.5-28: Resistance versus surface temperature for SP-I under SI-SW condition (test2)

For the range of temperature between -12C˚ (10F˚) to -4C˚ (25F˚), the plot for SI-SW I-1 shows an expected trend for surface ice. The initial increase in voltage is due to the icing of water as it is sprayed on the surface. After saltwater was sprayed, temperature increased rapidly, and output voltage and resistance decreased. The presence of salt reduced the electrical resistance of concrete. For the temperature between -2C˚ (28F˚) to 2C˚ (36F˚), test SI-SW I-1 shows a gradual reduction in output voltage and resistance.

Test SI-SW I-2 was performed on the same sensor following conclusion of test SI-SW I-1. Therefore, it is thought that the deicing salt used in the first test was absorbed by the concrete and stayed in its pores. This caused the sensor to be contaminated with salt, which caused a difference between results of SI-SW I-1 and SI-SW I-2. Figures 4.5-29 and 4.5-30 show combined plots for both tests. For

temperature above 2C˚ (36F˚), test SI-SW I-1showed the normal trend of concrete having melted ice on its surface. Test SI-SW I-2 however, shows the effect of salt contamination within the concrete pores and on the surface where voltage and resistance are lower prior to saltwater spraying.

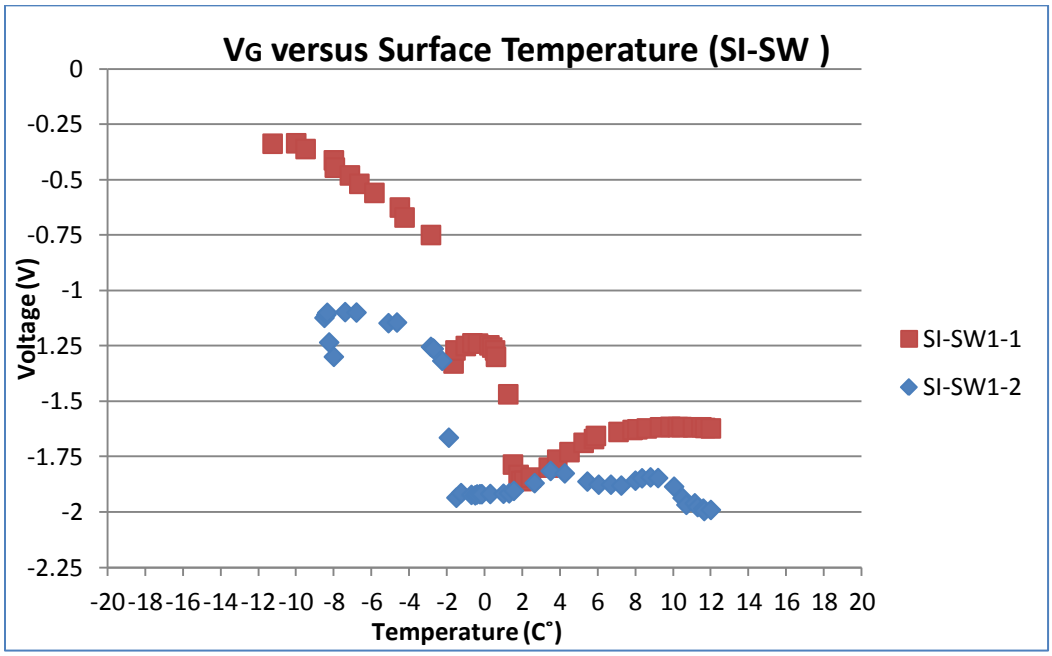

Figure 4.5-29: Output voltage versus surface temperature for SP-I under SI-SW condition (both tests)

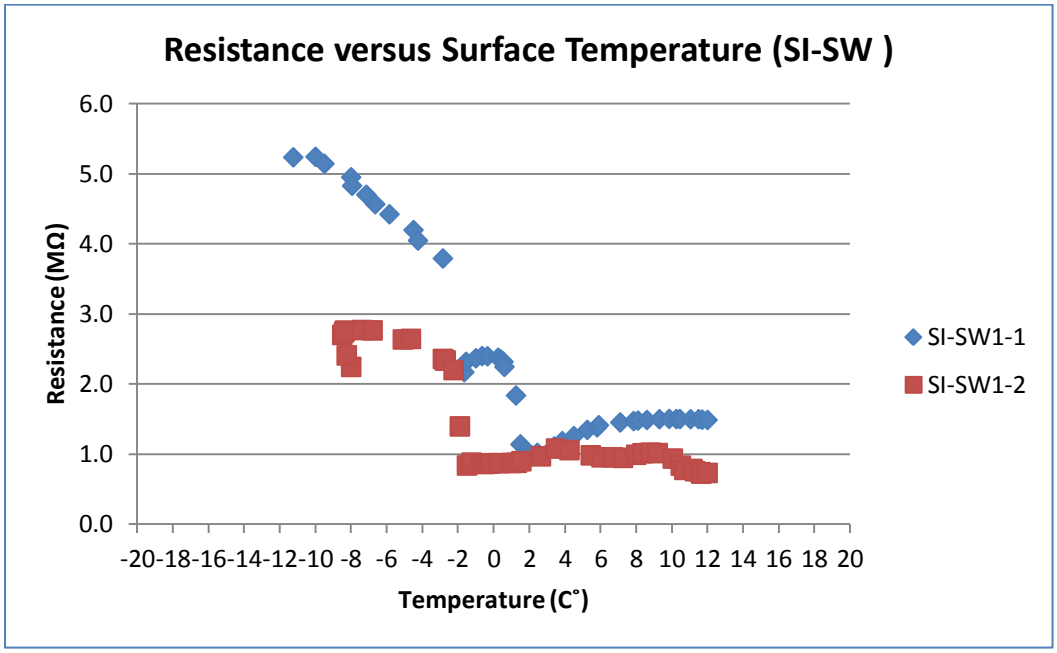

Figure 4.5-30: Resistance versus surface temperature for SP-I under SI-SW condition (both tests)

Frozen with Chloride Contaminated Concrete (FR-CC)

In this test, SP- I sensor was submerged in water for about 2-3 hours, and then placed in the freezer for 24 hours. The sensor was already contaminated with salt due to the previous tests. Readings were taken after the sensor was removed from the freezer and connected to the Wheatstone Bridge. Readings were taken as the temperature increased from -15C˚ (5F˚) to -10.5C˚ (13F˚), after which saltwater was sprayed on the surface. There was a rapid increase in temperature and a rapid decrease in output voltage as a result of the addition of saltwater. At temperatures above 0C˚ (32F˚), the output voltage was on the order of -2.0v, and the resistance on the order of less than 1.0 MΩ. The lower resistance under wet conditions is due to chloride contamination. Figures 4.5-31 and 4.5-32 show relationships between the output voltage and resistance versus surface temperature,

respectively. The presence of salt affects the conductivity of concrete and the overall resistance decreases when salt in present. However, there is still a significant difference in output voltage between surface ice and wet condition under chloride contamination. This allows the sensor to work even in chloride-contaminated environments. Nevertheless, the presence of salt affects the output, and this is considered in the decision algorithm proposed for the sensor in Chapter 5.

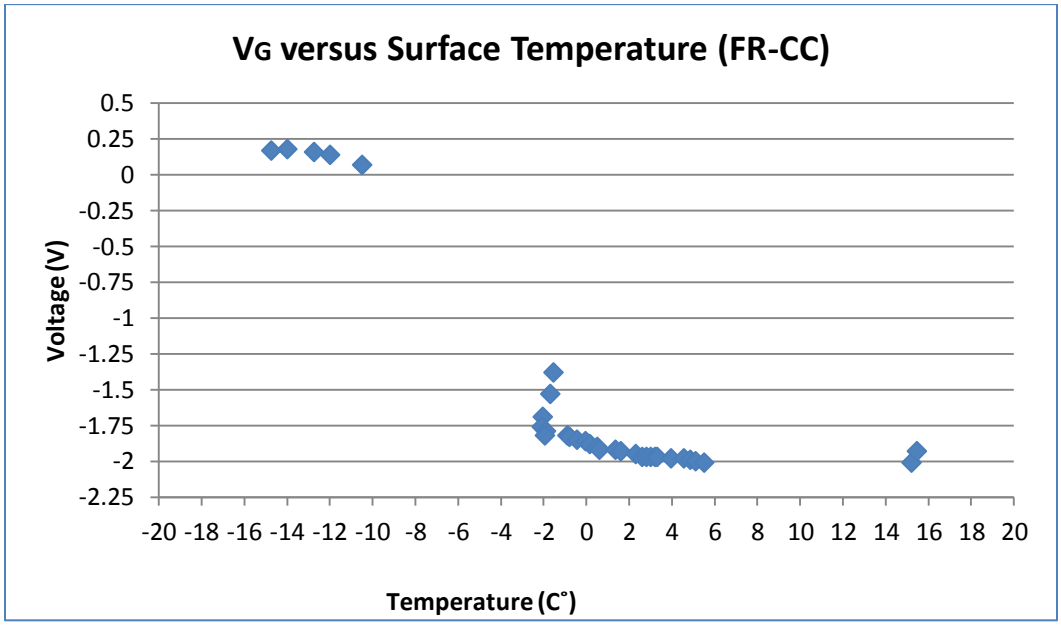

Figure 4.5-31: Output Voltage versus surface temperature for SP-I under FR-CC condition

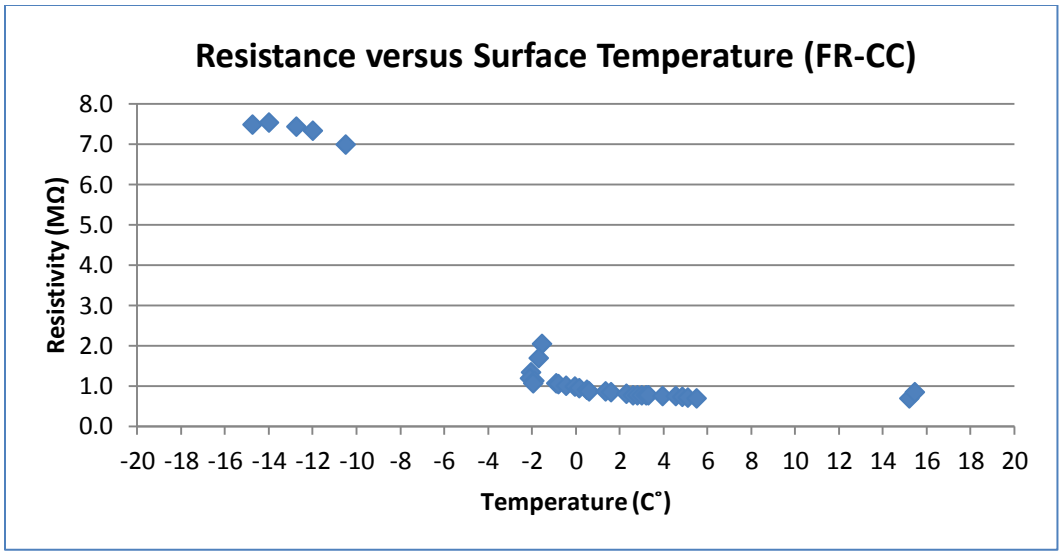

Figure 4.5-32: Resistance versus surface temperature for SP-I under FR-CC condition

Surface Ice on Chloride Contaminated Sensor (SI-CC)

In the previous test, saltwater was sprayed onto the sensor, and that caused the sensor to be contaminated with chlorides. Salt (sodium chloride) penetrates into the concrete pores, and that drives down the voltage and resistance. In this test, a condition when the sensor is previously contaminated with chlorides (or any other material that causes a reduction in the resistance of concrete) was simulated. The dry sensor was placed for 24 hours in the freezer with a temperature of -20C˚ (-4F˚). The sensor was then moved to the laboratory and was connected to the Wheatstone bridge circuit. Water was sprayed on its surface to create an icy surface. Two tests were done using this same approach. Figures 4.5-33 and 4.5-34 show the surface temperature change versus output voltage and resistance plots respectively for test SI-CC I-1.

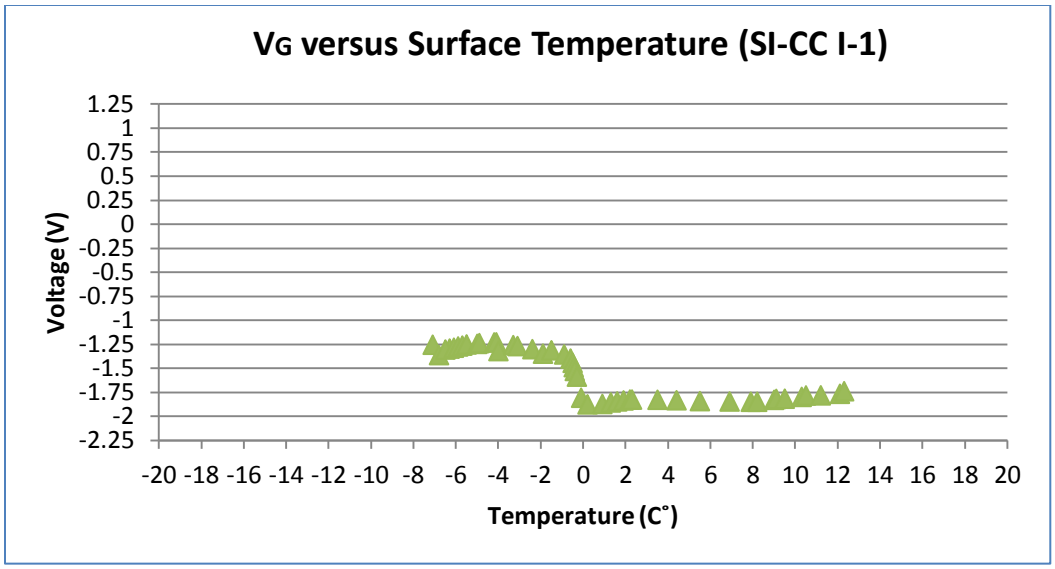

Figure 4.5-33: Output voltage versus surface temperature for SP-I under SI-CC condition (test1)

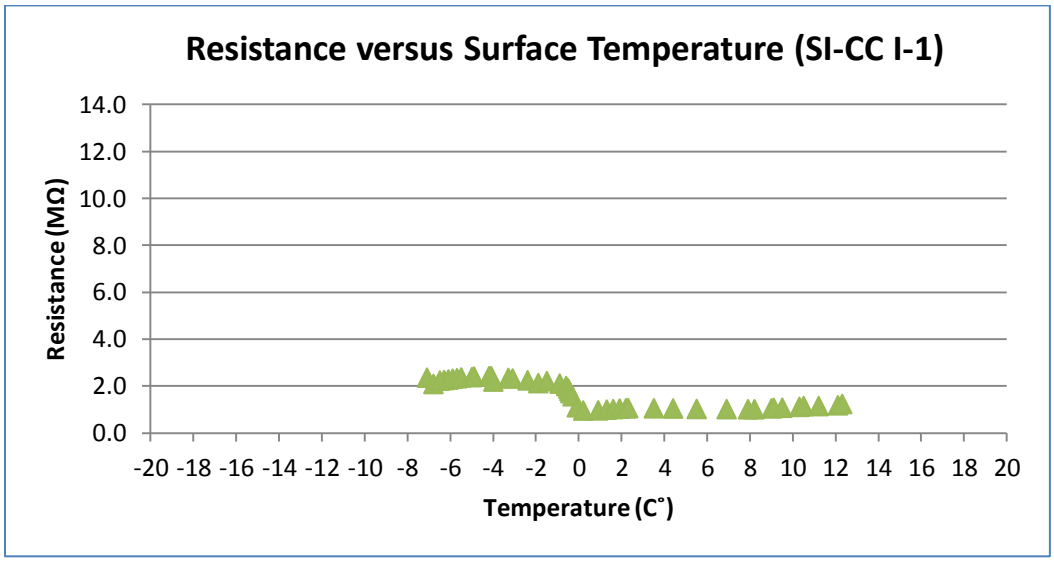

Figure 4.5-34: Resistance versus surface temperature for SP-I under SI-CC condition (test1)

Figures 4.5-35 and 4.5-36 show relationships between output voltage and resistance versus surface temperature for test SI-CC I-2.

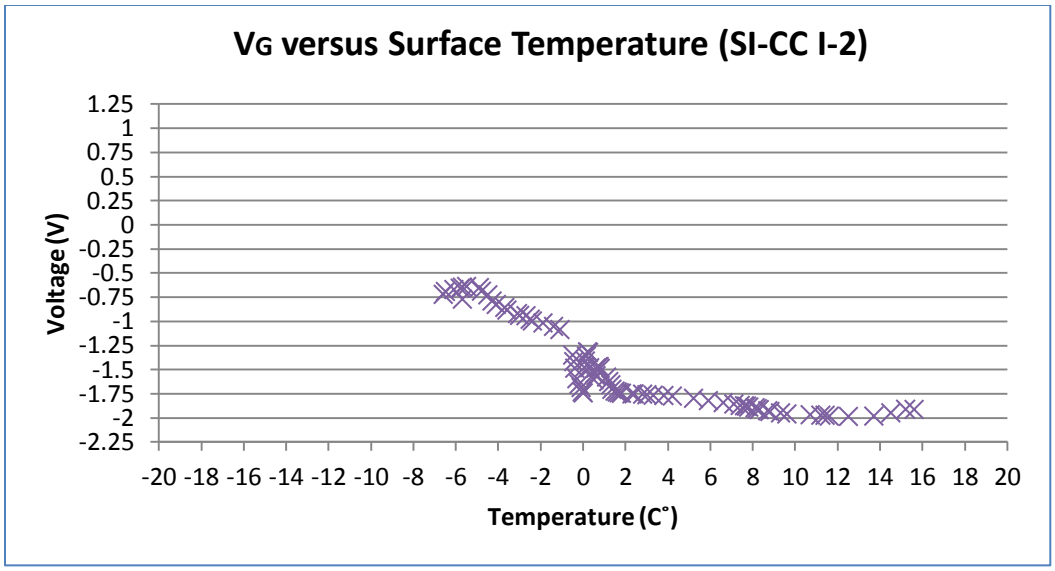

Figure 4.5-35: Output voltage versus surface temperature for SP-I under SI-CC condition (test2)

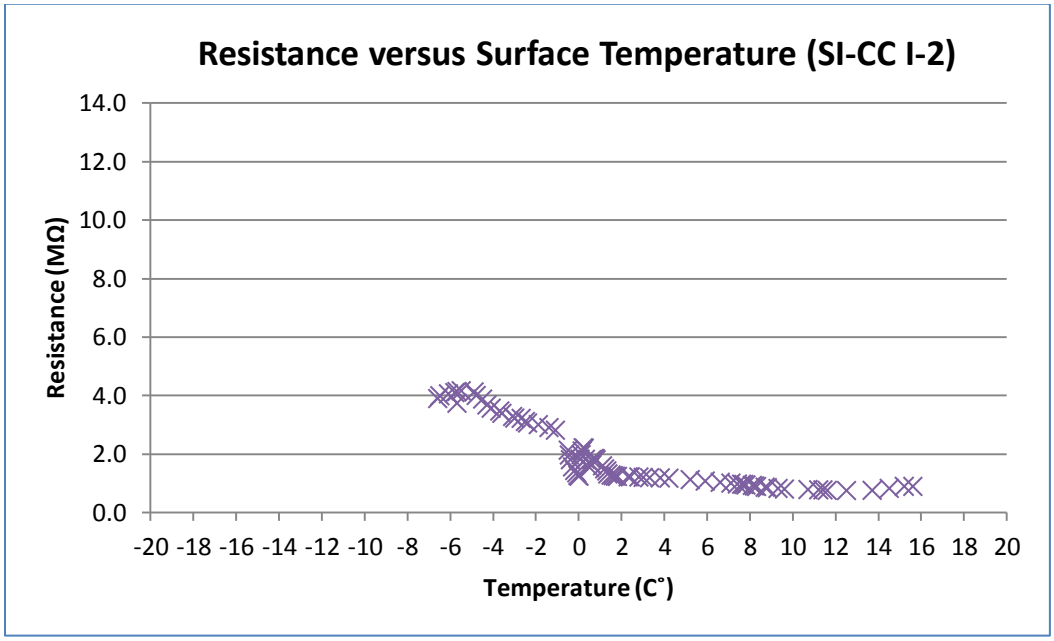

Figure 4.5-36: Resistance versus surface temperature for SP-I under SI-CC condition (test2)

During the process of surface ice formation, right after spraying water, there were some voltage fluctuations observed that reflect the icing and melting that occurs in the presence of salt. The presence of ice on the surface of both tests could be

observed with its characteristic response. Figures 4.5-37 and 4.5-38 show combined plots for both tests.

It is thought that the difference in the results of the two tests may be due to the amount of chloride contamination of the sensor in the two tests. As the ice melts completely, and temperature increases up to the room temperature, resistance and voltage results for both tests (SI-CC I-1 and SI-CC I-2) fall within a range of -1.75v to -2.0v (≈1MΩ)

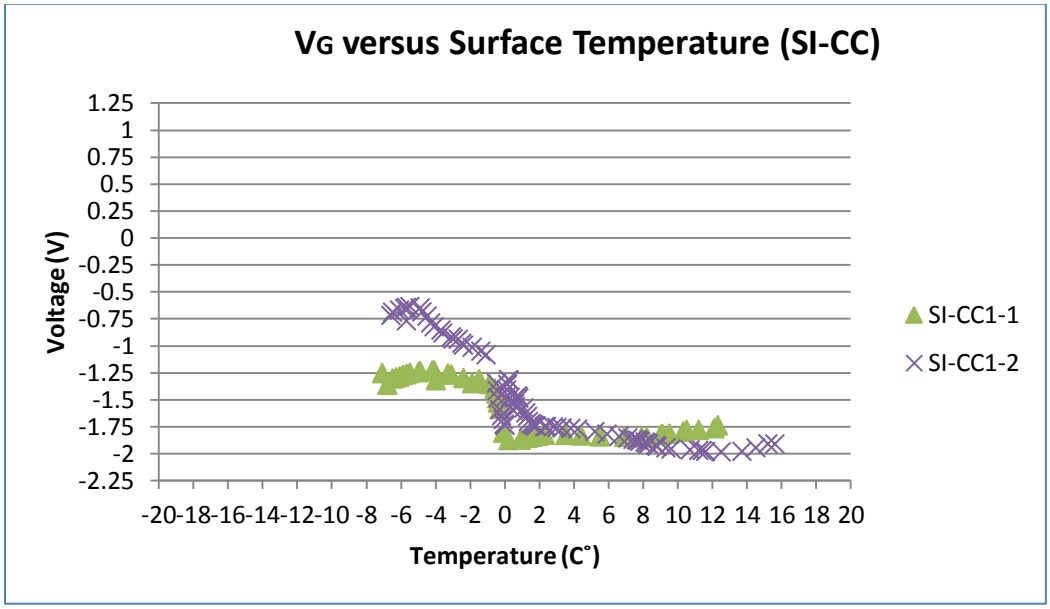

Figure 4.5-37: Output voltage versus surface temperature for SP-I under SI-CC condition (both tests)

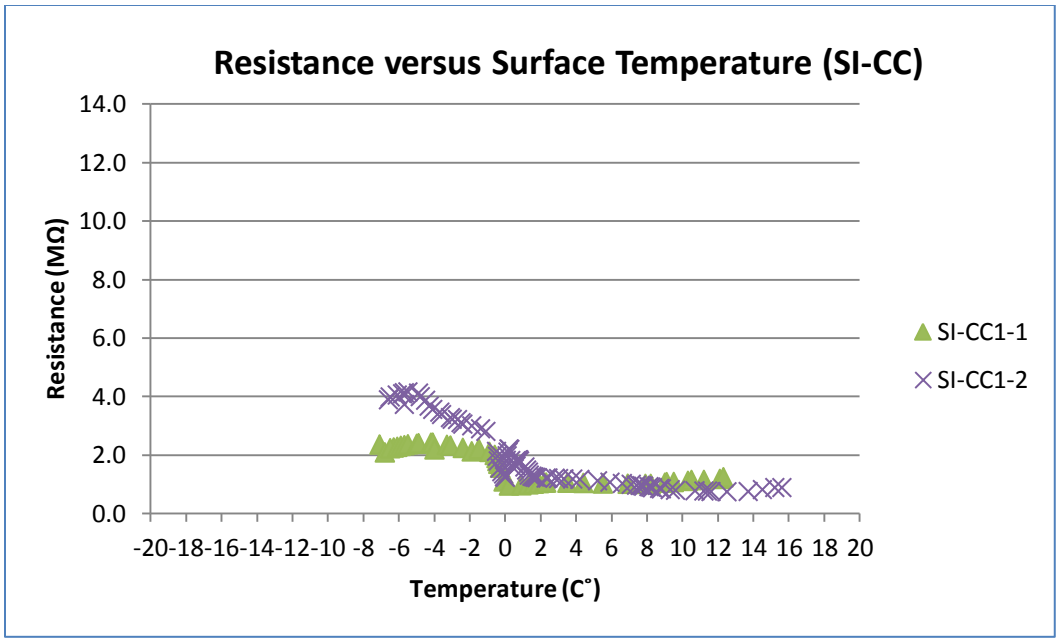

Figure 4.5-38: Resistance versus surface temperature for SP-I under SI-CC condition (both tests)

Surface Ice on Rubber Contaminated Sensor (SI-RC)

Tires are worn out with usage due to friction, as a result, rubber shavings can be present on pavement surface. In this test, an attempt was made to simulate the condition when there is combination due to rubber shavings on the surface of the sensor. Powdered rubber (from a tire wear test on concrete specimen) was rubbed on the surface of the sensor prior to this test. Figures 4.5-39 and 4.5-40 show the results. Since the sensor was already contaminated with salt from previous test, the response was similar to chloride contaminated tests described earlier. Overall, the rubber shavings on the sensor surface did not appear to change the results drastically. Outputs stayed within the range of icy surface results in clean or chloride contaminated tests.

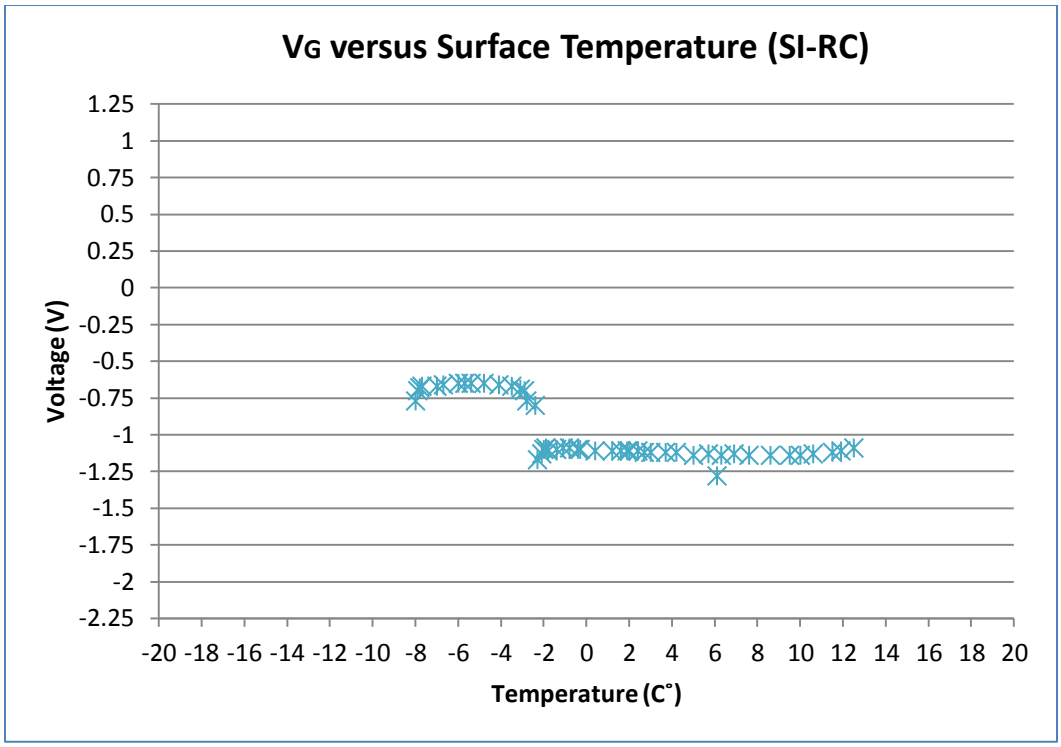

Figure 4.5-39: Output voltage versus surface temperature for SP-I under SI-RC condition

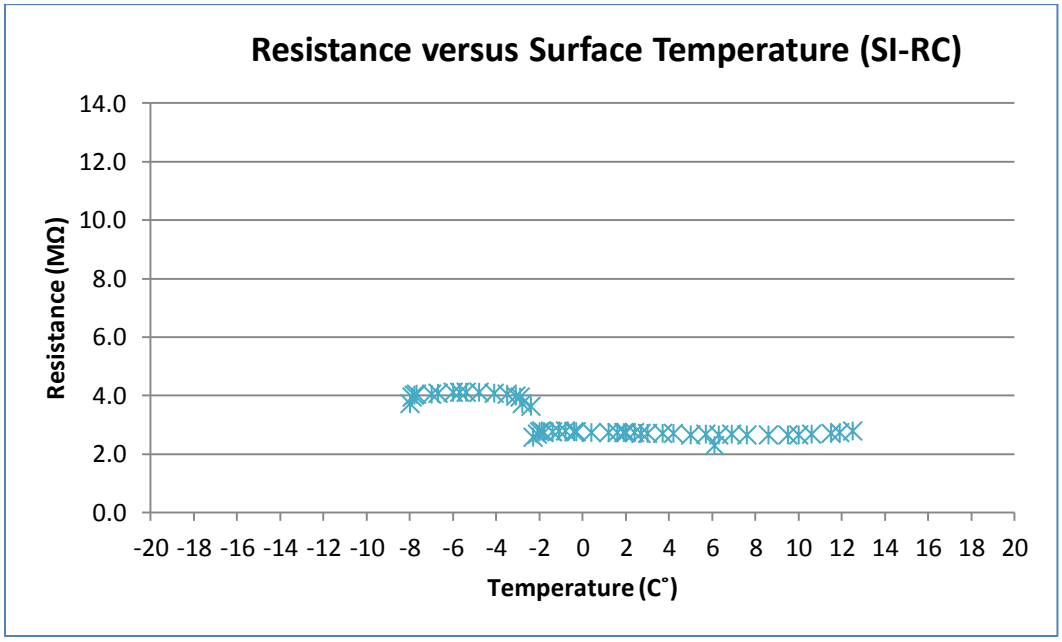

Figure 4.5-40: Resistance versus surface temperature for SP-I under SI-RC condition

Crushed Ice on SP-I Surface (CI-LUS)

SP- I sensor was placed inside in the freezer (-20C°) for 24 hours. While it was in the freezer, crushed ice was placed on the top surface of the sensor, as shown in figure 4.5-41. This test was designed to assess the sensor under snow condition. The sensor then was moved to the laboratory inside an insulation box to slow the temperature increase. The sensor output voltage was monitored as the temperature increased and ice melted. Figures 4.5-42 and 4.5-43 show changes in output voltage and resistance versus surface temperature, respectively.

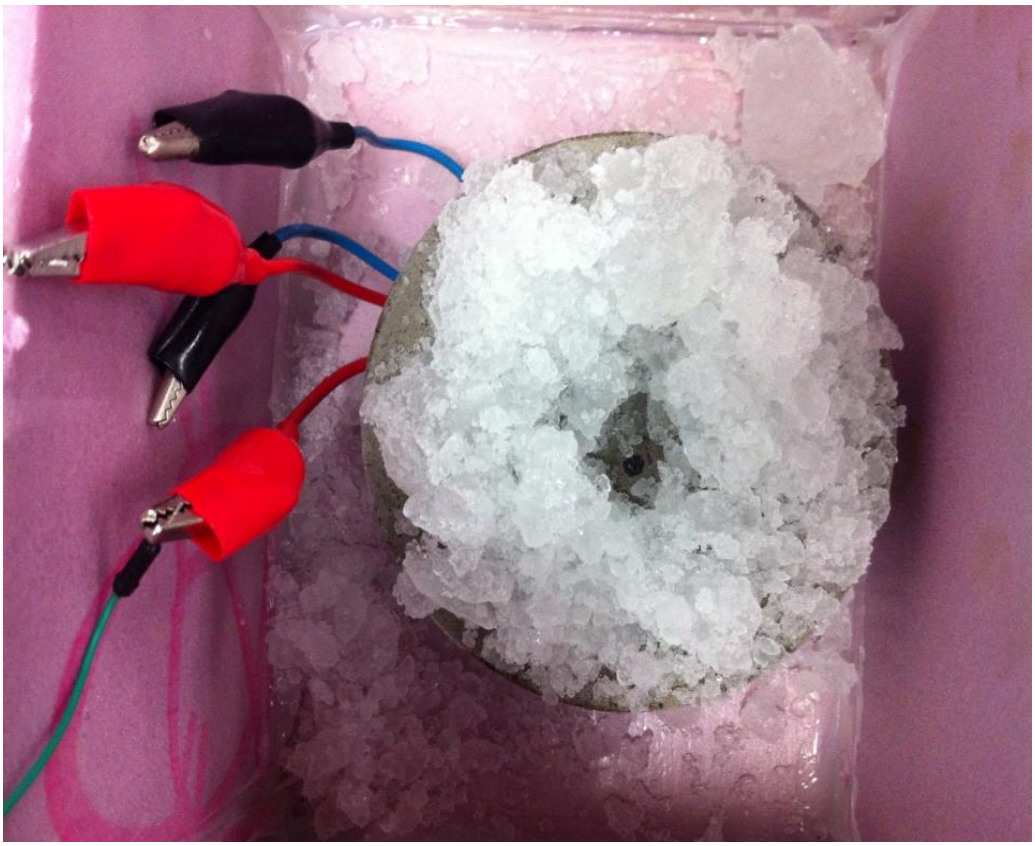

Figure 4.5-41: Crashed ice on SP-1 test

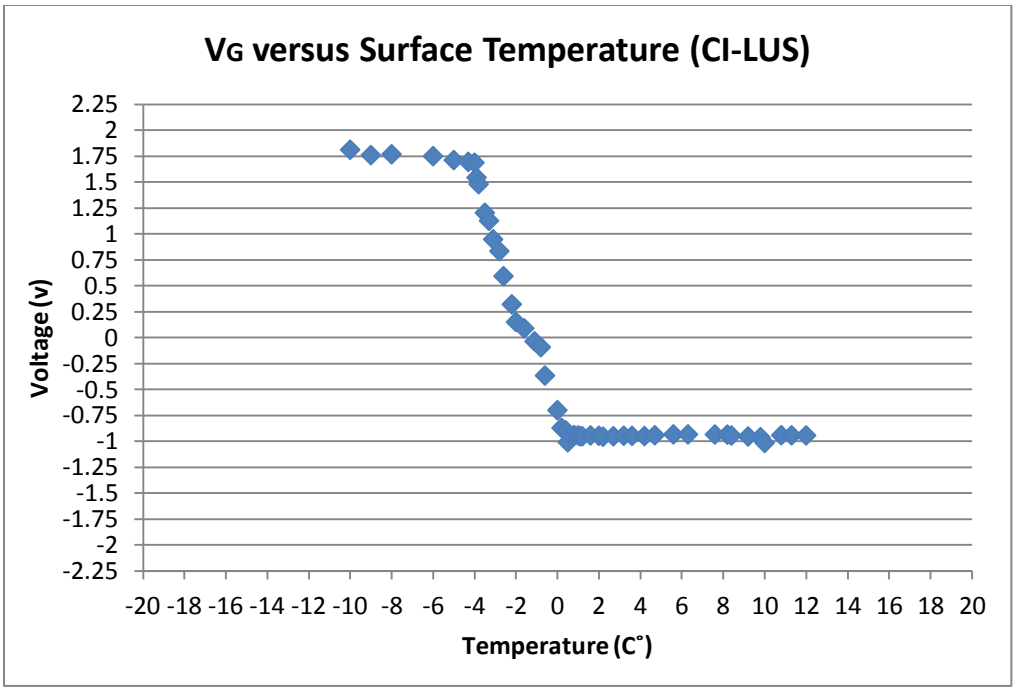

Figure 4.5-42: Output voltage versus surface temperature for crushed ice condition

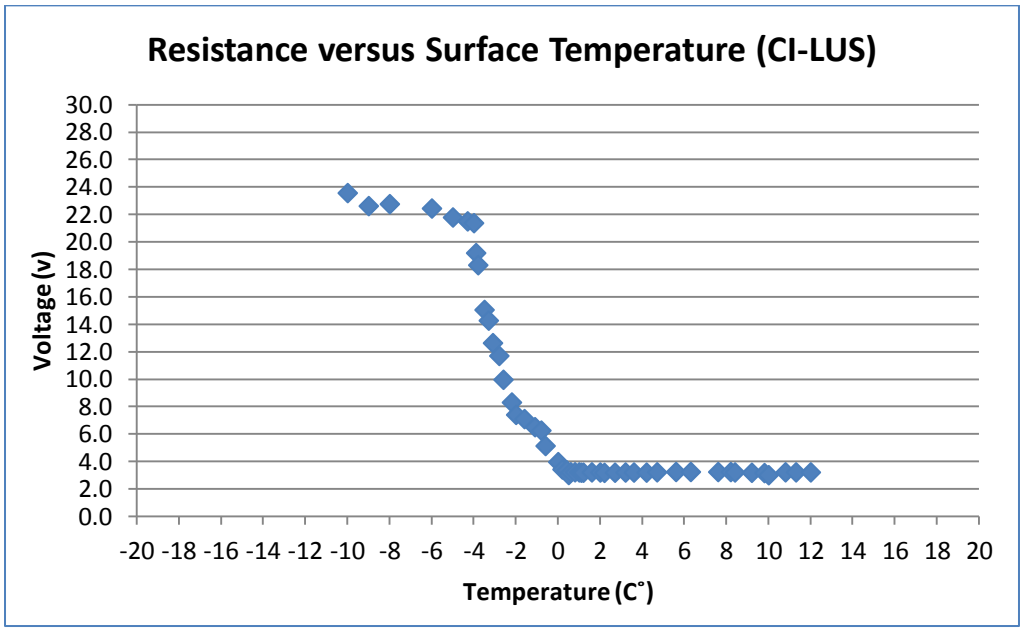

Figure 4.5-43: Resistance versus surface temperature for crushed ice condition

As surface temperature increased (crushed ice melted), the output voltage and resistance decreased. At lower temperature, the output voltage level was similar to the dry condition even though there was crushed ice on the surface. It

is believed that, due to the voids between the crushed ice/snow particles, the electrical resistance is not similar to the surface ice condition. In fact, the output voltage is close to the dry condition when the crushed ice has not melted. This pattern could be seen for the temperature range of -10C˚ to -3C˚ (14F˚ to 27F˚). As temperature increases and ice converts to liquid form, some water becomes ice again with the cold sensor values of output voltage and resistance drops. Output voltage reaches -0.94v (resistance ≈3.0MΩ) for temperatures above +1˚C.

4.5.2 Tests on SP-II sensor

Two main tests have been conducted, on the sensor prototype II, which are surface ice and frozen condition, since the purpose of it was to clearly distinguish between the two cases. An excitation voltage of 6 volts (two 3 volts batteries) was used as power supply, while the other conditions used were similar to those used in sensor prototype I tests, as shown in Figure 4.5-44.

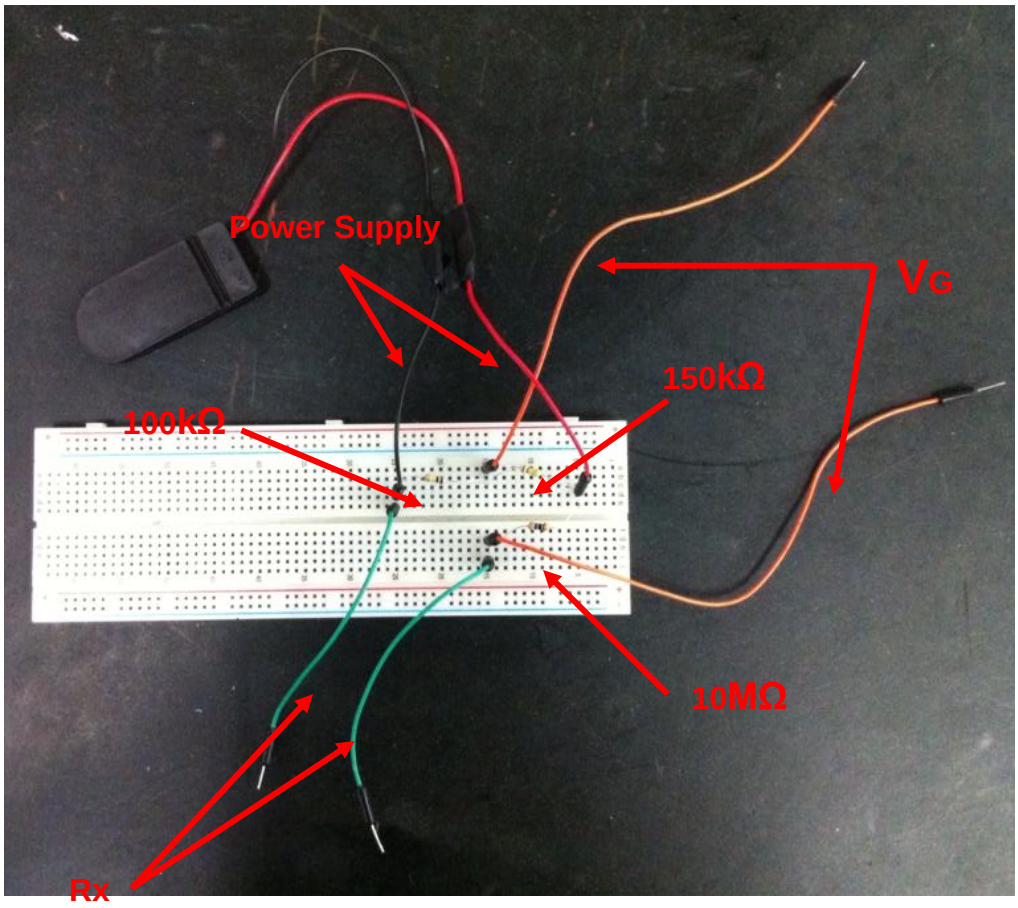

Figure 4.5-44: Wheatstone connections for SP-II

Surface Ice test (SI-LU)

The sensor was dried out by placing it in the oven with temperature of 35 C° (95F°) for 24 hours. The sensor was then put in the freezer for another 24 hours. While still cold, water was sprayed on its surface to form surface ice. The LU poles were connected to the electrical circuit to monitor the changes in the resistance associated with the changes in the temperature. In the first test LU-SI-1, the output voltage and resistance was monitored as the surface temperature of the sensor increased from -11.5C° (11F°) to 14C° (57F°). The first four readings were taking while the sensor was cold and dry without moisture on its surface. Water

was sprayed on the surface and surface ice started to form. It is noticed that the temperature dropped rapidly from -9C˚ (16F˚) to -2C˚ (28F˚), as shown in figures 4.5-45 and 4.5-46. Ice formation on the surface caused a rapid decreasing in the output voltage and resistance values. The change continued as the ice is being melted for the temperature between -2C˚ (28F˚) to 0C˚ (32F˚). Voltage and resistance almost stabilized for the temperature change from 0C˚ (F˚) to 12C˚ (54F˚).

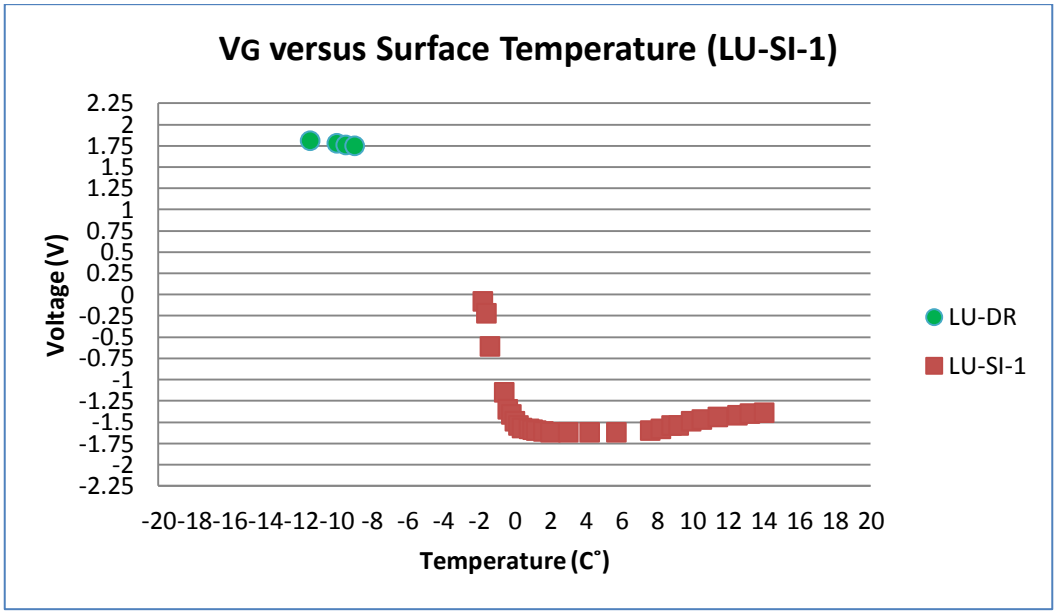

Figure 4.5-45: Output voltage versus surface temperature for SP-II under surface ice condition (test1)

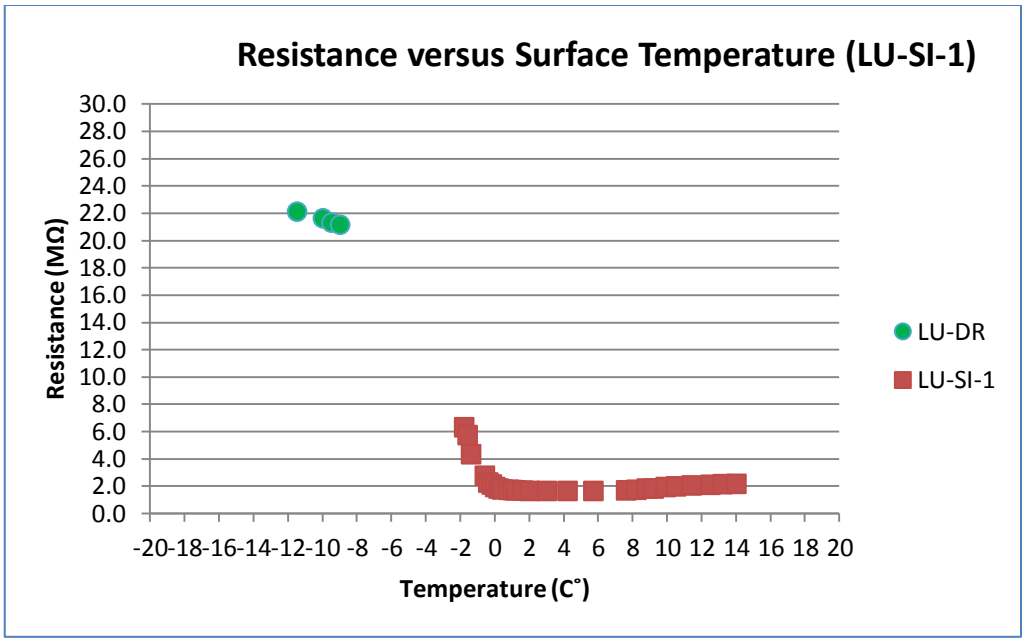

Figure 4.5-46: Resistance versus surface temperature for SP-II under surface ice condition (test1)

The previous test was repeated in test LU-SI-2 except that readings were not taken for the cold dry. Monitoring began after spraying the sensor with water and the formation of surface ice. The output voltage was reduced as the temperature increased from -3C˚ (27F˚) to 13C˚ (55F˚). The temperature change between -3C˚ (27F˚) to 0C˚ (32F˚) was associated with drop in the resistance and output voltage, which agrees with the previous findings of LUS poles. As the ice melts and is converted to liquid, the resistance and voltage tend to stabilize at -1.4v to -1.7v for the temperature change from 0C˚ (32F˚) to 13C˚ (55F˚), as shown in figures 4.5-47 and 4.5-48.

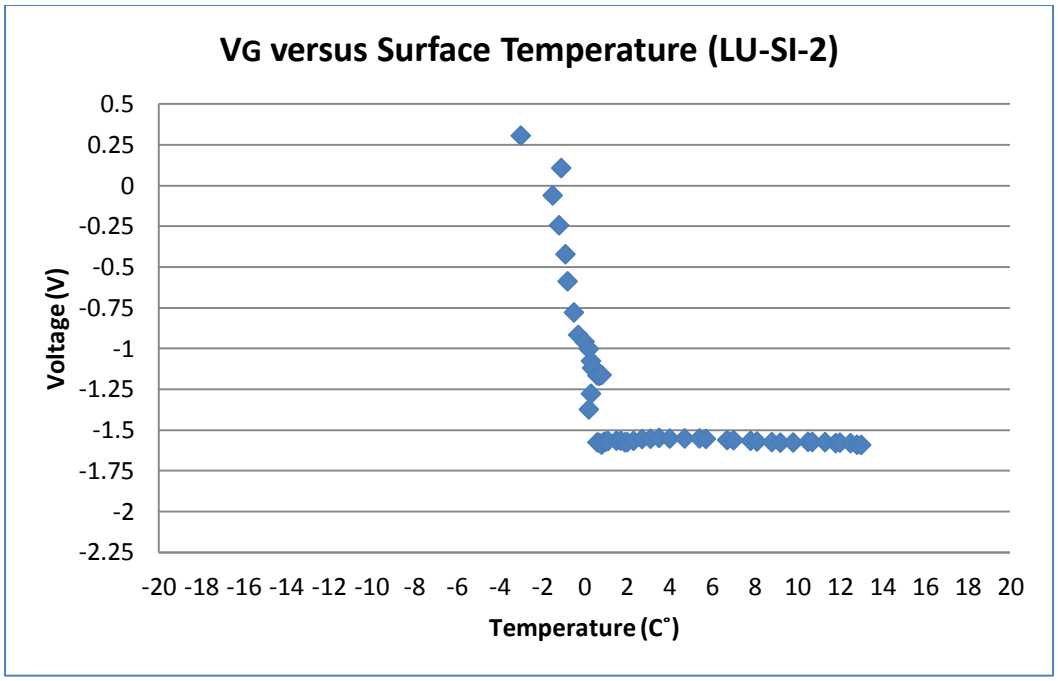

Figure 4.5-47: Output voltage versus surface temperature for SP-II under surface ice condition (test2)

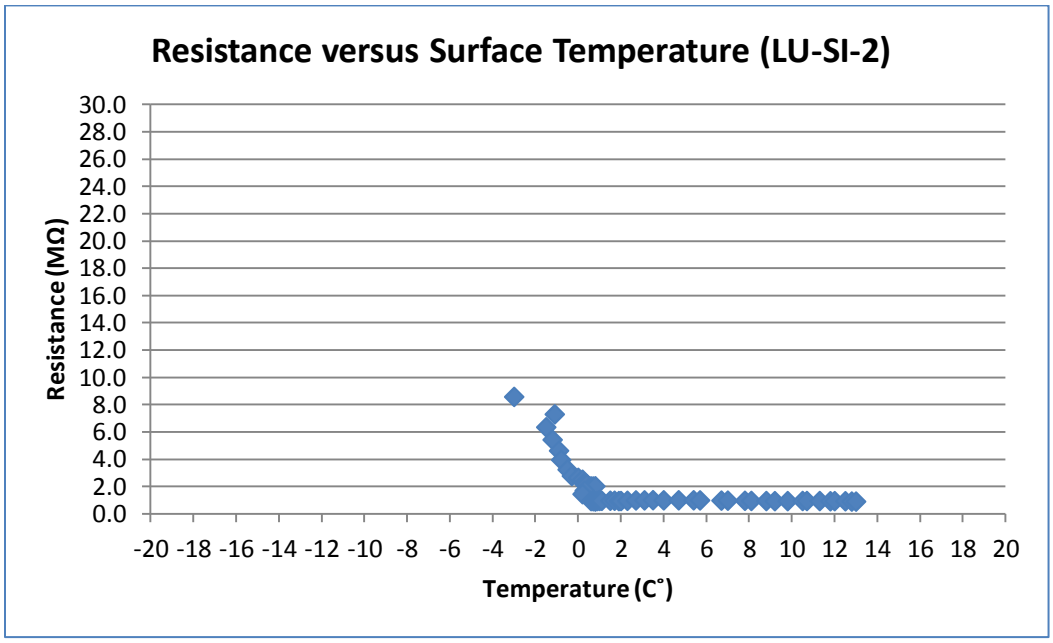

Figure 4.5-48: Resistance versus surface temperature for SP-II under surface ice condition (test2)

A third test, LU-SI-3, was performed on the same sensor using same procedure of test LU-SI-2. Results were somewhat similar to second test LU-SI-2, as shown in Figures 4.5-49 and 4.5-50.

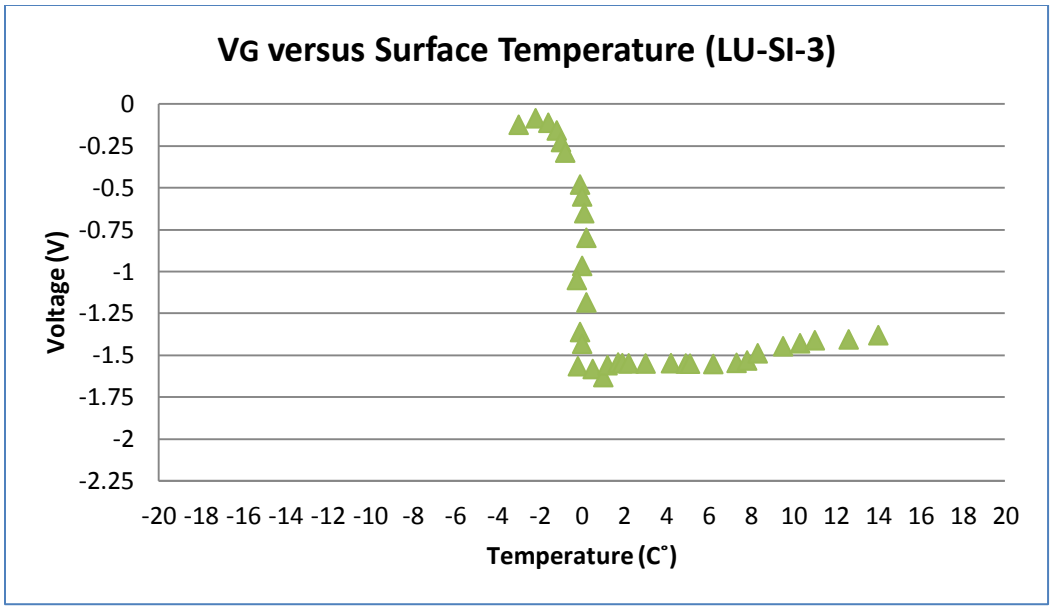

Figure 4.5-49: Output voltage versus surface temperature for SP-II under surface ice condition (test2)

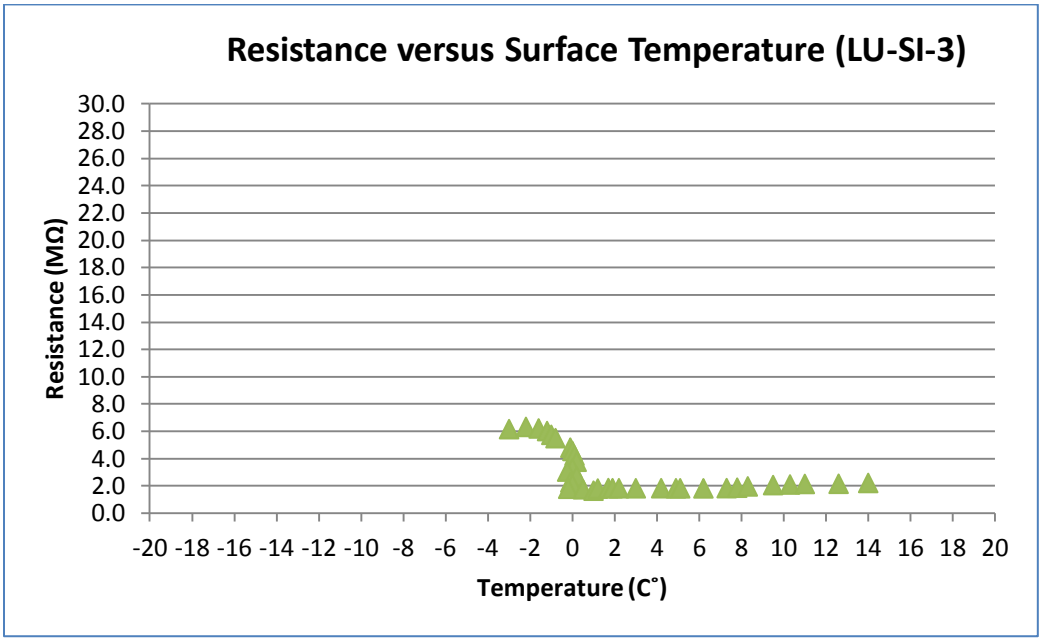

Figure 4.5-50: Resistance versus surface temperature for SP-II under surface ice condition (test2)

Results of all three tests together are combined in figures 4.5-51 and 4.5-52.

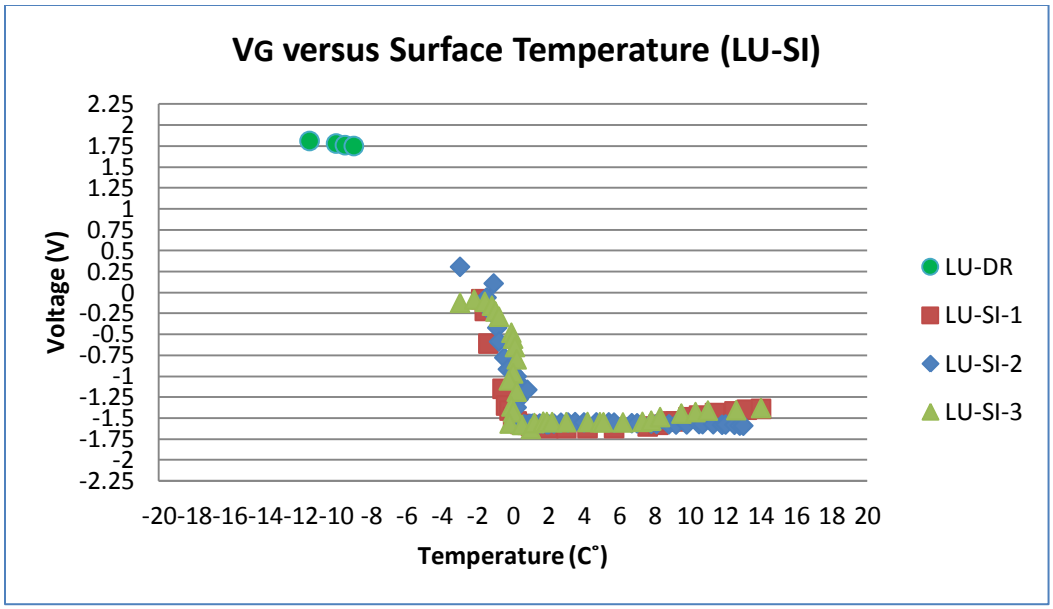

Figure 4.5-51: Output voltage versus surface temperature for SP-II under surface ice condition (all tests)

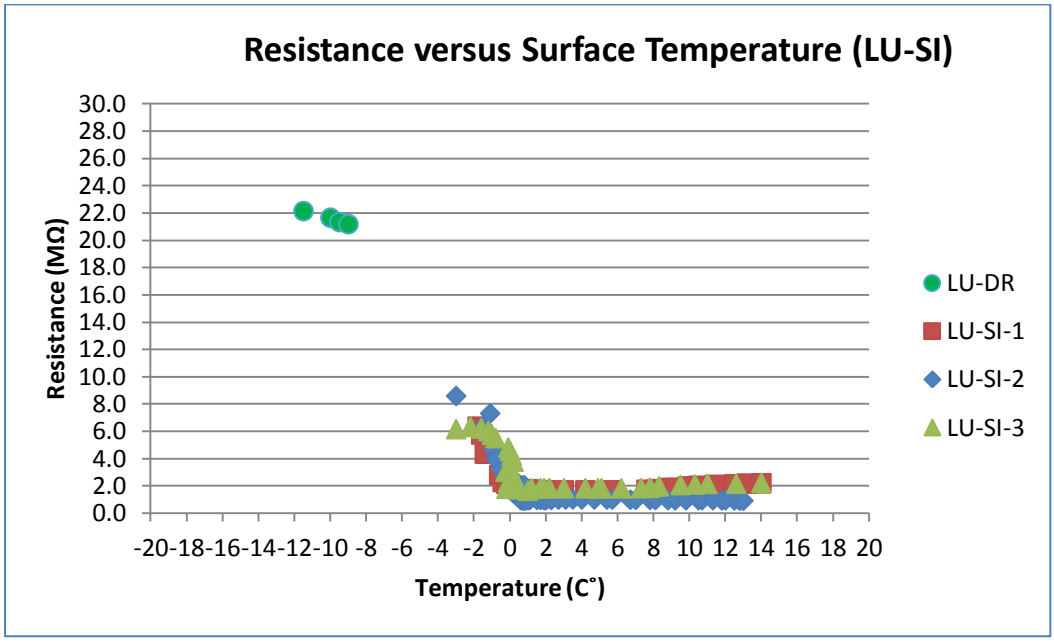

Figure 4.5-52: Resistance versus surface temperature for SP-II under surface ice condition (all tests)

The dry condition output voltage for LU poles is on the order of +1.75v. The surface ice condition results in an output voltage of approximately -0.5v to +0.5v, and the wet surface output voltage in the range of -1.4v to -.175v. The three tests have shown that when there is ice on the surface, the resistance tends to be higher,

and as the ice melts down and temperature increases, resistance gets lower until the ice totally melts the output voltage reduces. A resistance range could be set up for the dangerous case of surface ice formation. Output voltage ranges between 1.0v to -0.75v and resistance between 4MΩ-14MΩ could be basis for warning for surface ice presence, in LU poles.

Frozen test (LU-FR)

The LU poles were covered by insulation tape in order to avoid any moisture presence in the specimen. Water was sprayed on the surface several times for about an hour to make sure the pores were filled with water. The sensor was then put into the freezer for 24 hours, and then moved back to the lab to monitor the change in output voltages as temperature changed. Figures 4.5-53 and 4.5-54 show the output voltage and resistance of the sensor associated with the temperature changes. It can be observed that the output voltage of the sensor was essentially constant and not a function of the temperature. As expected the "Look-Up" poles are insensitive to the frozen condition of the concrete material between the two LU poles. Thus, LU poles will only be responsive to either surface ice condition, or wet conditions. This would overcome any uncertainties associated with surface ice and frozen condition in LUS poles discussed earlier.

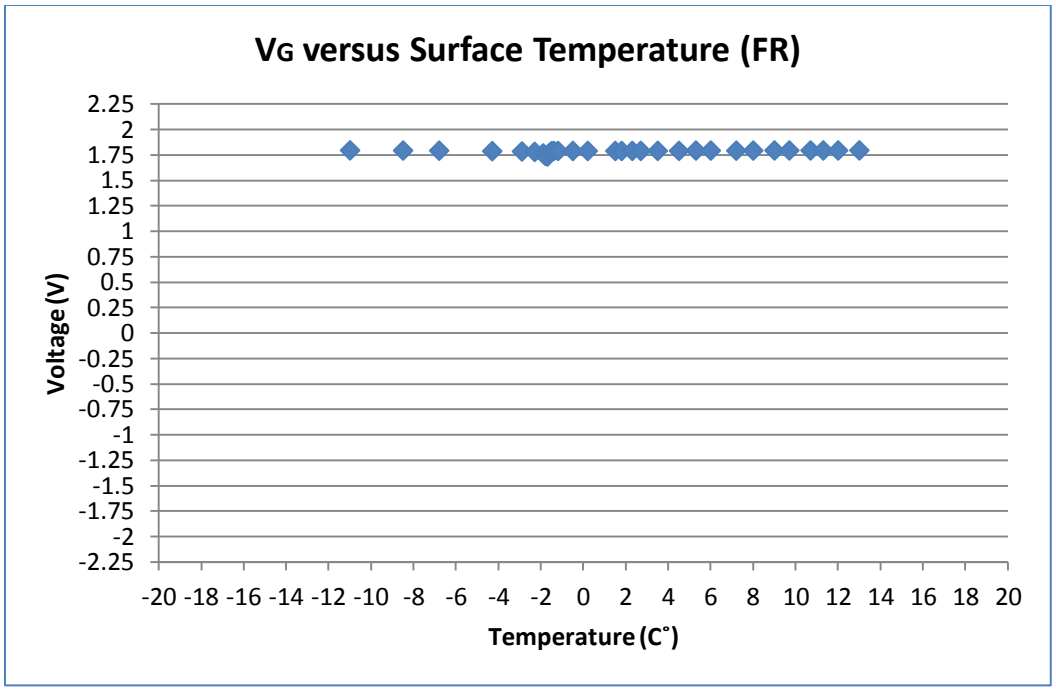

Figure 4.5-53: Output voltage versus surface temperature for SP-II under frozen condition

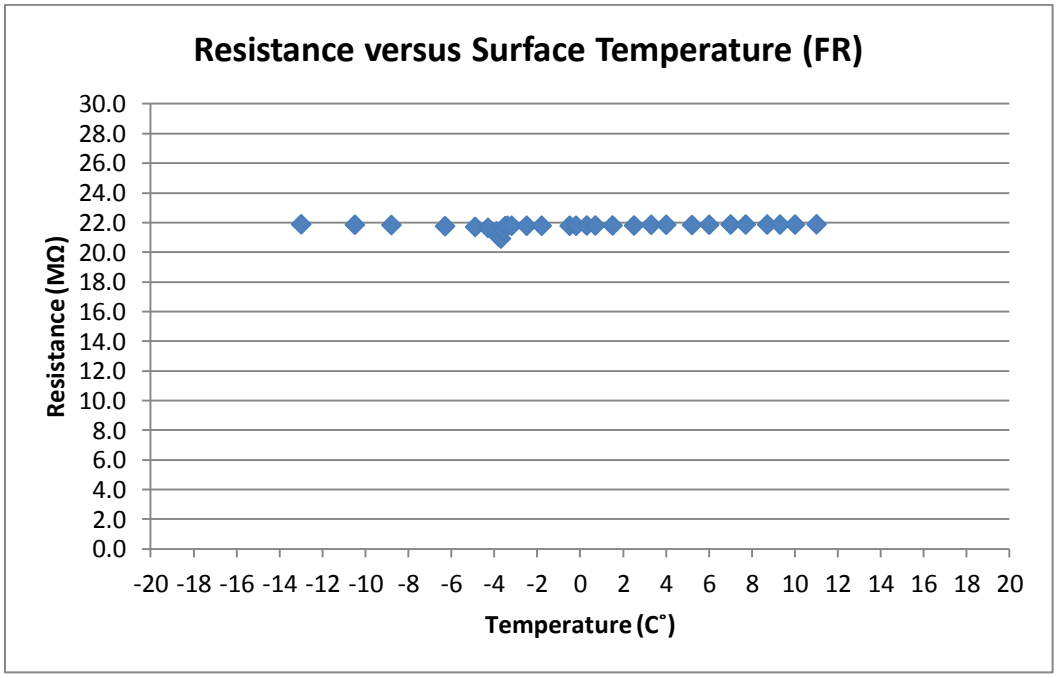

Figure 4.5-54: Resistance versus surface temperature for SP-II under frozen condition

4.6 Ice Test (without the sensor)

In an attempt to better understand the electrical properties of the ice and water at different thicknesses, tests have been performed as shown in Figure 4.7-9 and 4.6-10. A plastic container, which had served as a mold for casting of concrete sensors, was filled with a 1/16 inch or 1/8 inch thickness of water. Four stainless steel poles were created in each setup; only two were used for the test, as shown in Figure 4.6-11. The poles had the same arrangement as the poles used in the sensor. Figures 4.6-1 and 4.6-2 show results of 1/16-in-thick ice. A similar test was also performed on the 1/8-in-thick ice sample. The results are shown in figures 4.6-3 and 4.6-4.

The ice resistance has a linear relationship with temperature. This was seen in surface ice tests on the sensor as well. As the thickness of ice increases, the output voltage decreases. This can be explained as the effect of two parallel resistors. The 1/8-in-thick ice layer can be viewed as two 1/16-in-thick layers arranged as parallel resistors. Therefore, the resistance of the 1/8-in-thick ice would be expected to be roughly half of the corresponding value for the 1/16-in-thick layer, if other potential factors are neglected.

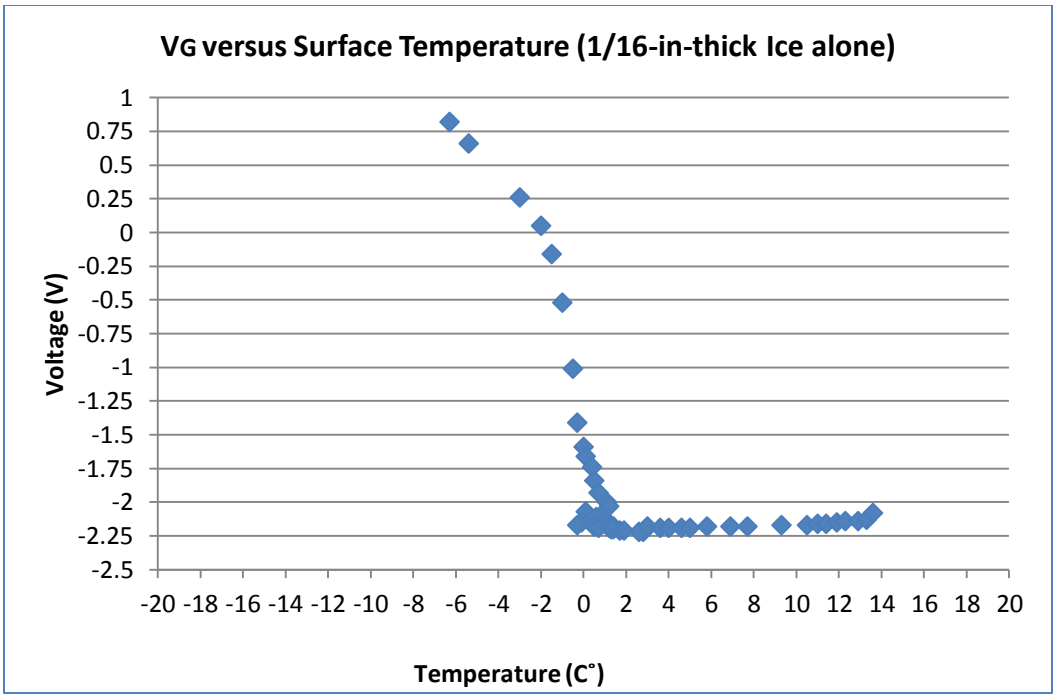

Figure 4.6-1: Output voltage versus surface temperature for 1/16-in-thick ice (without a sensor)

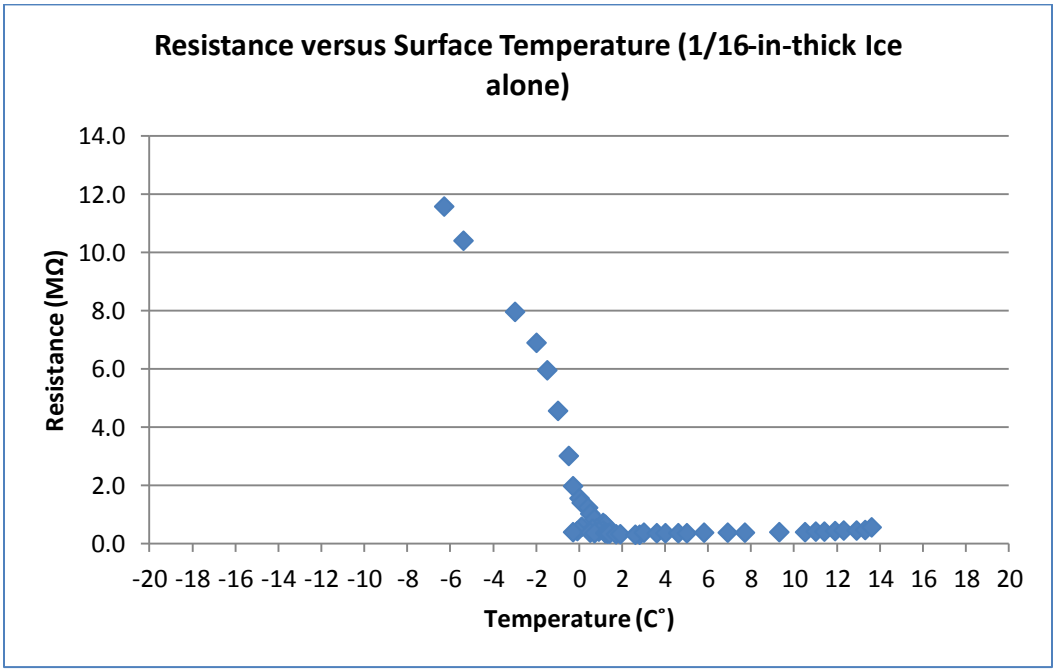

Figure 4.6-2: Resistance versus surface temperature for 1/16”-in-thick ice (without a sensor)

It is observed that at -6C˚ (21F˚), the 1/16-in-thick ice had a resistance of approximately 10.2 MΩ, while the resistance of the 1/8-in-thick layer at the same temperature was on the order of 7.5 MΩ.

Although the resistance of the 1/8-in-thick layer was not half the thinner layer's value, but the resistance was smaller. It can be concluded that a higher thickness of ice results in a lower voltage output and lower resistance.

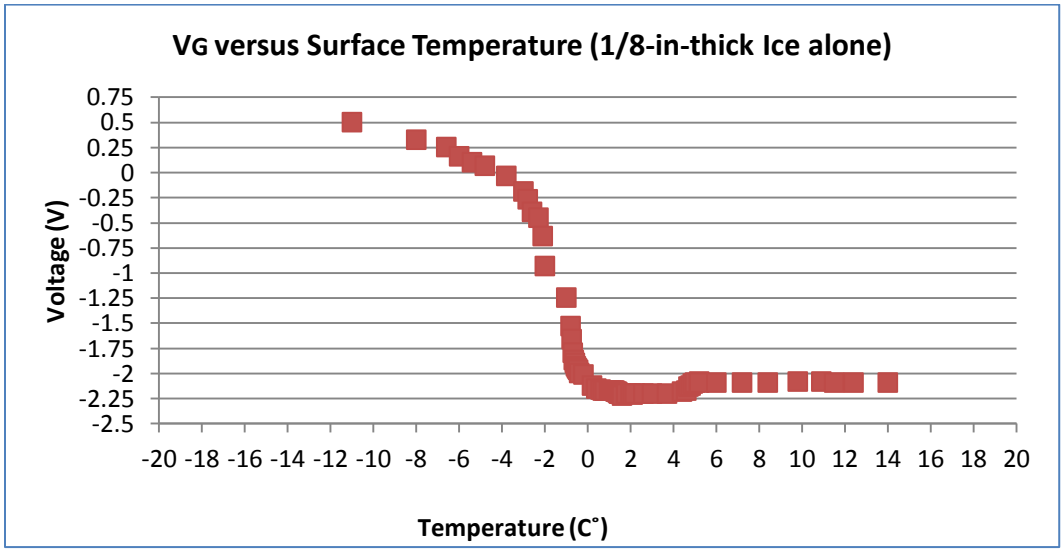

Figure 4.6-3: Output voltage versus surface temperature for 1/8"-in-thick ice (without a sensor)

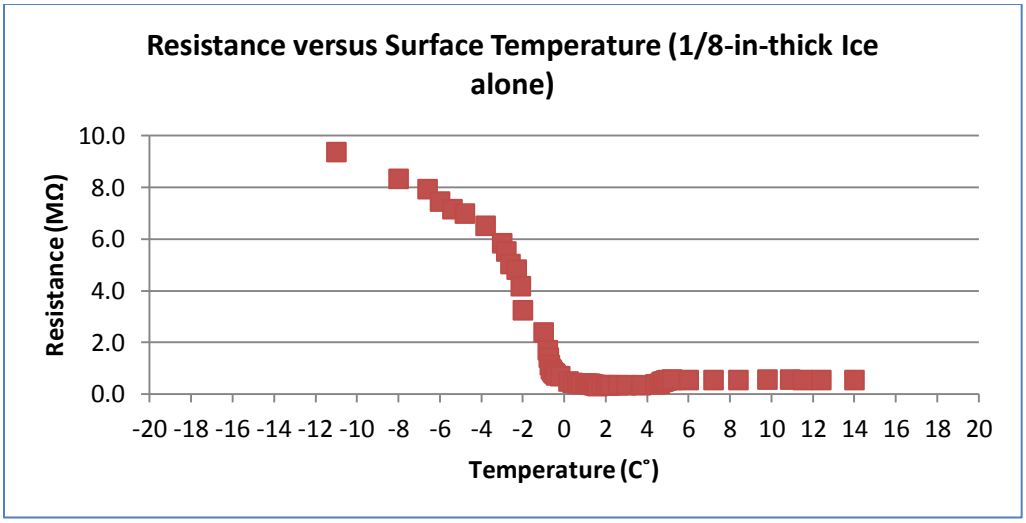

Figure 4.6-4: Resistance versus surface temperature for 1/8"-in-thick ice (without a sensor)

Also, a similar test was conducted on an ice sample that was made with 6% saltwater solution at a thickness of 1/16, Figures 4.6-5 and 4.6-6 show plots of these results. The results show a flat line across all temperatures, indicating that the very high alt content in the water reduced its resistance to the minimum possible value.

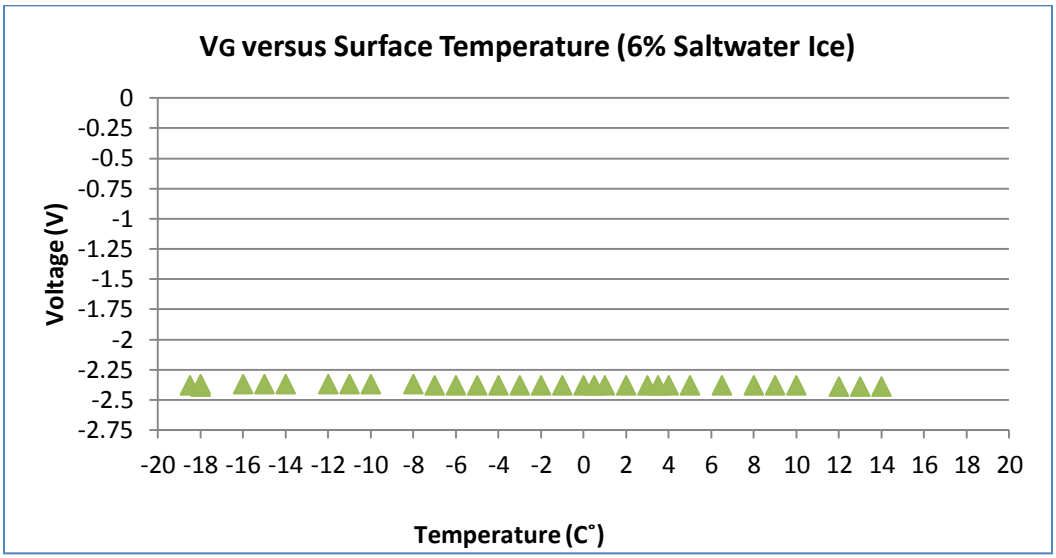

Figure 4.6-5: Output voltage versus surface temperature for 6% saltwater ice (without a sensor)

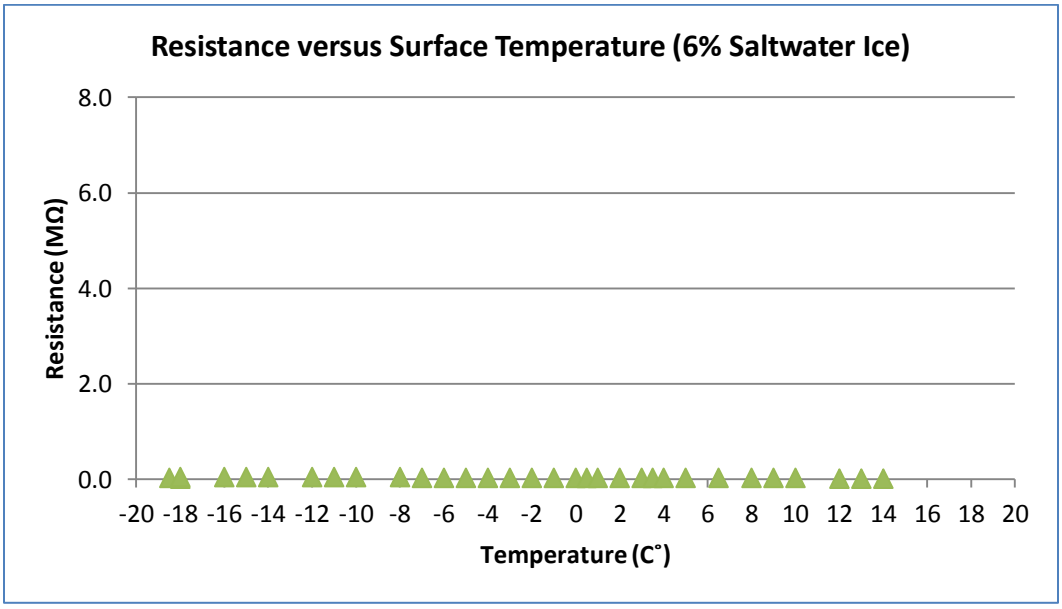

Figure 4.6-6: Resistance versus surface temperature for 6% saltwater ice (without a sensor)

The electrical resistance properties of ice could be deduced from the above test results. Figures 4.6-7 and 4.6-8 show results of all ice tests. For the conventional ice (tap water), tests show patterns similar to surface ice tests described earlier. As expected, the resistance of ice decreases as its thickness increases. As the temperature increases and ice melts, both ice tests (tap water) tend to have close results. Finally, it is very clear that the effect of salt presence in the ice (sample) drives the resistance to near zero.

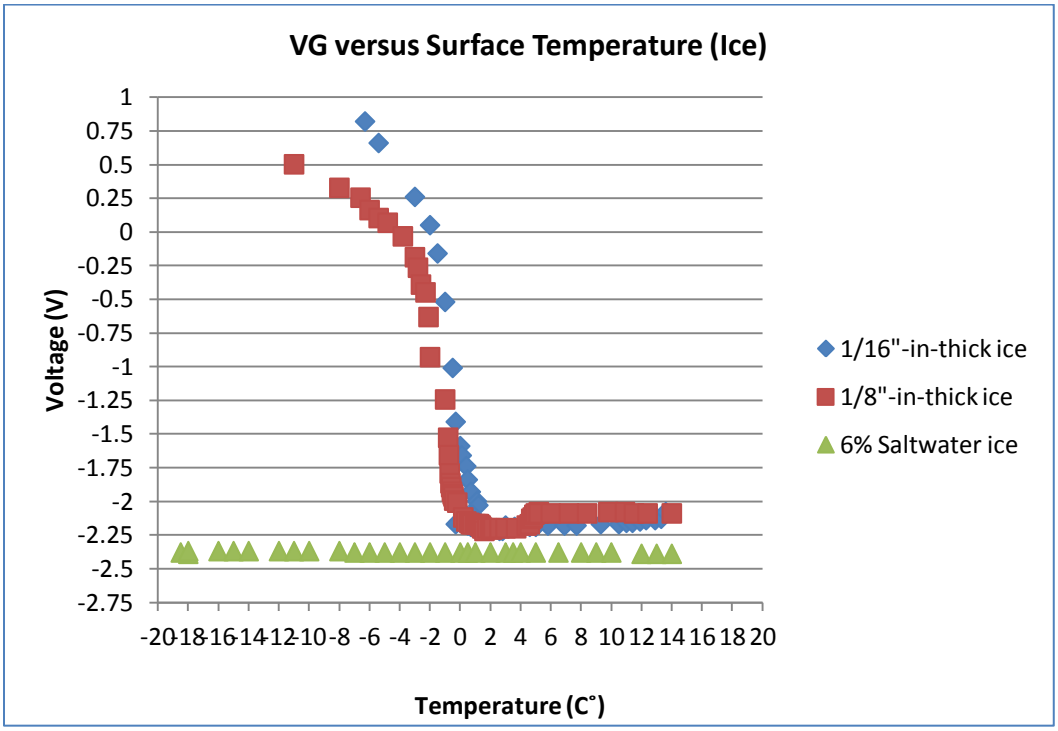

Figure 4.6-7: Output voltage versus surface temperature for ice

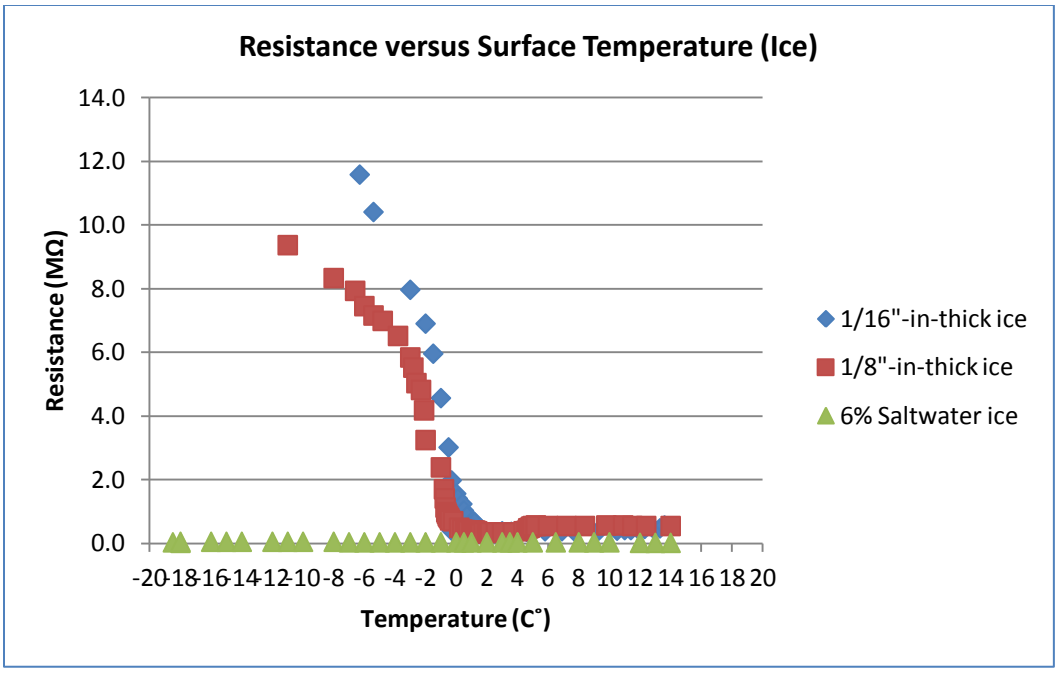

Figure 4.6-8: Resistance versus surface temperature for ice

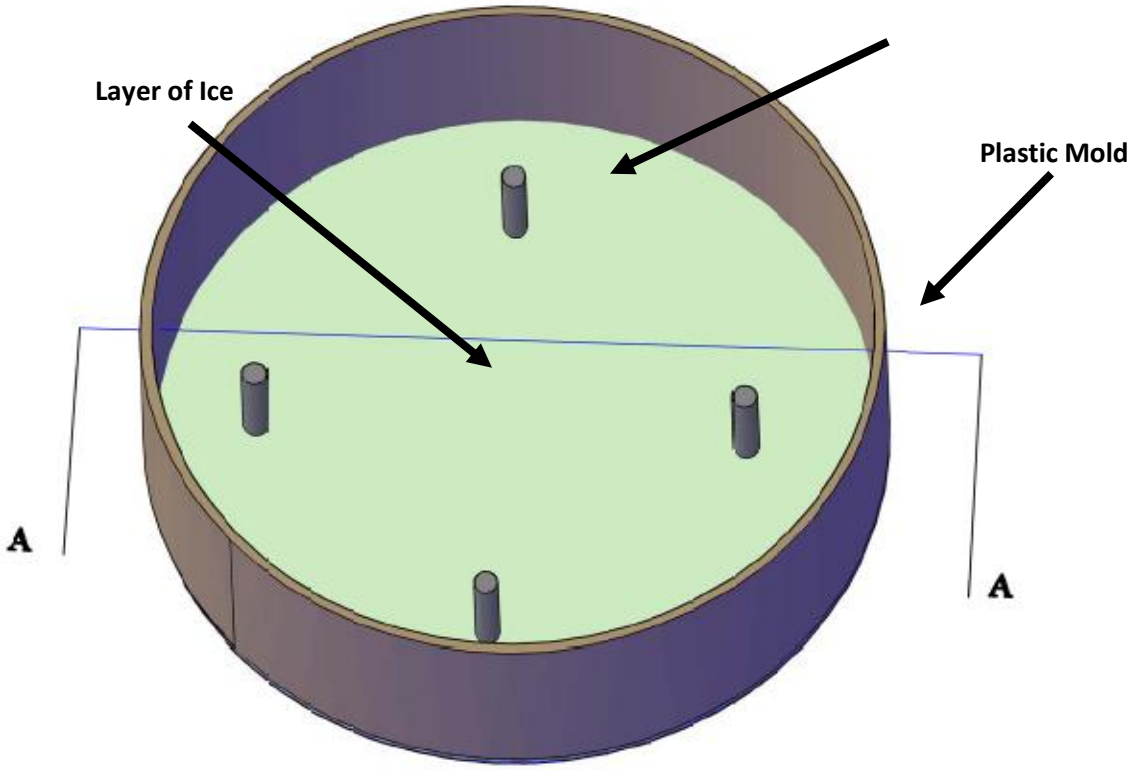

Figure 4.6-9: layer of ice in the mold

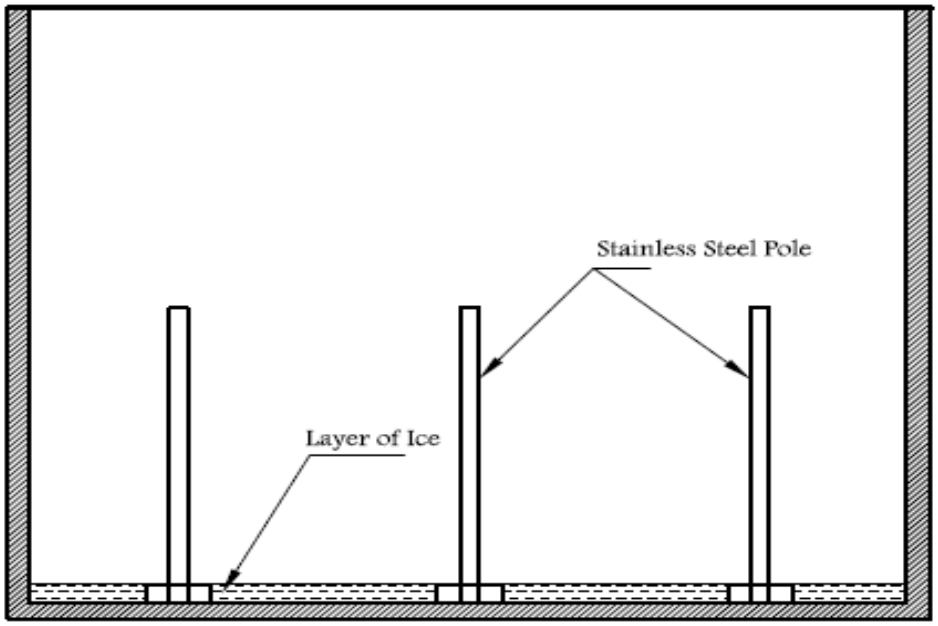

Figure 4.6-10: Section A-A of the ice test

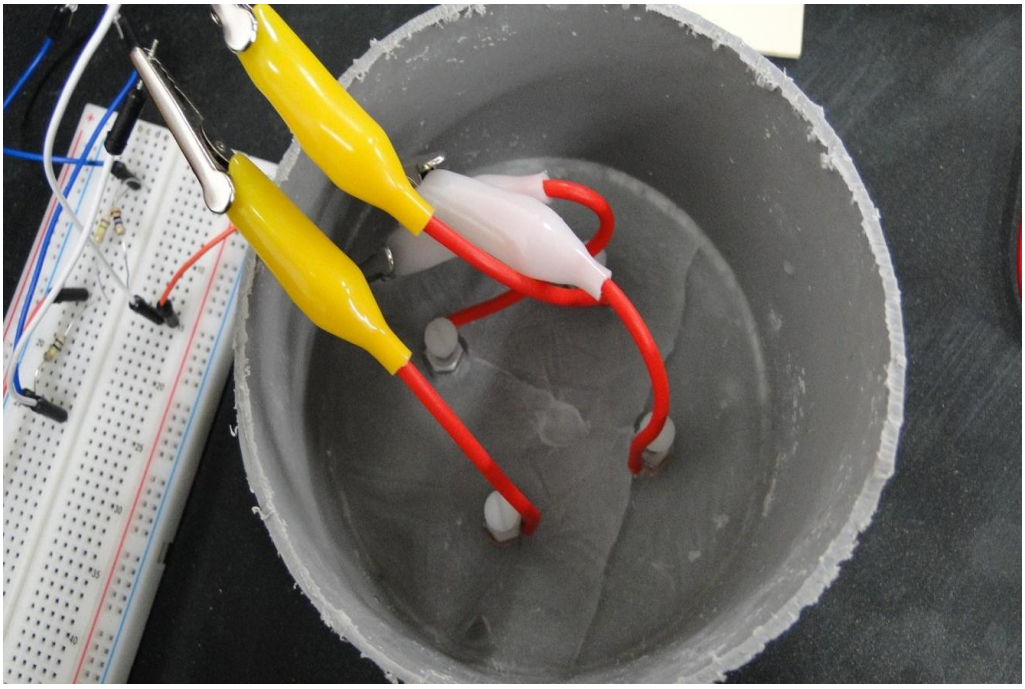

Figure 4.6-11: Ice test connections

4.7 Friction Tests

It is important to test the friction of the concrete surface under different test conditions, including surface ice, wet surface, dry surface, and when there is frozen water in the concrete pores that are near the surface. This is important because sensor outputs for different conditions can then be quantitatively related to road surface hazards. It is expected that friction would be at its lowest level when black ice condition exist. A Pendulum Friction Coefficient Meter (ASTM E303) was used for this test Figure 4.7-1. A Pendulum is released from a pre-determined height. The pendulum comes in contact with the surface and rises again. The friction is related to the difference between the height and after coming in contact with the surface. Basically the principle of the device is based on the loss of potential energy of the pendulum due to the work (energy) needed to overcome friction on the surface [29].

Tests on five different surface conditions were conducted; dry surface, wet surface, icy surface, frozen surface (i.e. frozen water in the concrete pores that are near the surface), and frozen-icy surface. A 1.5ftx1.5ft concrete slab was used for this test as shown in Figure 3-72. The concrete slab was first tested under dry conditions to obtain the baseline friction coefficient. The surface was then sprayed with water to achieve a wet surface condition, and friction test performed. The specimen was then moved into a freezer (-20C˚ (-4F˚)) and left there for approximately 24 hours. The specimen was removed from the freezer and water was sprayed on it to form surface ice. Specimen was then tested to find the friction coefficient under surface ice condition. For the frozen test, the slab was placed face down in a water-filled tray facing down for 24 hours. The specimen was then placed in the freezer for another 24 hours, after which the concrete slab was tested to

determine the friction coefficients under frozen condition. Finally, the process for the frozen condition was repeated, but this time water was sprayed on the surface of the concrete slab, and a Frozen-Icy surface condition was created for testing. The test in each condition was done by taking six readings, and an average was calculated, Table 4.7-1 shows the test results along with an average coefficient of friction for each tested condition.

Figure 4.7-1: Pendulum Friction Coefficient Meter

Table 4.7-1: Friction test results

Condition / Test Number	Dry	Wet	Icy Surface	Frozen	Frozen-Icy surface
1	62	66	30	60	20
2	62	64	28	55	12
3	60	60	24	58	12
4	66	60	30	55	18
5	66	66	30	54	16
6	70	64	28	60	18
Average	**64**	**63**	**28**	**57**	**16**

Figure 4.7-2 shows the relationship between surface condition and the friction coefficients in graphical form. As expected, the value of friction coefficient decreases as the ice forms on the surface. Finally, the worst friction value occurs when frozen water exists in the concrete pores near the surface together with a layer of surface ice. In this case, friction coefficient drops from 57% in case of frozen concrete (without surface ice) to 16% when there is ice on the surface of frozen slab. A reduction of almost 72% in the friction coefficient resulted from the combination of the presence of frozen water particles in the pores and the icy surface.

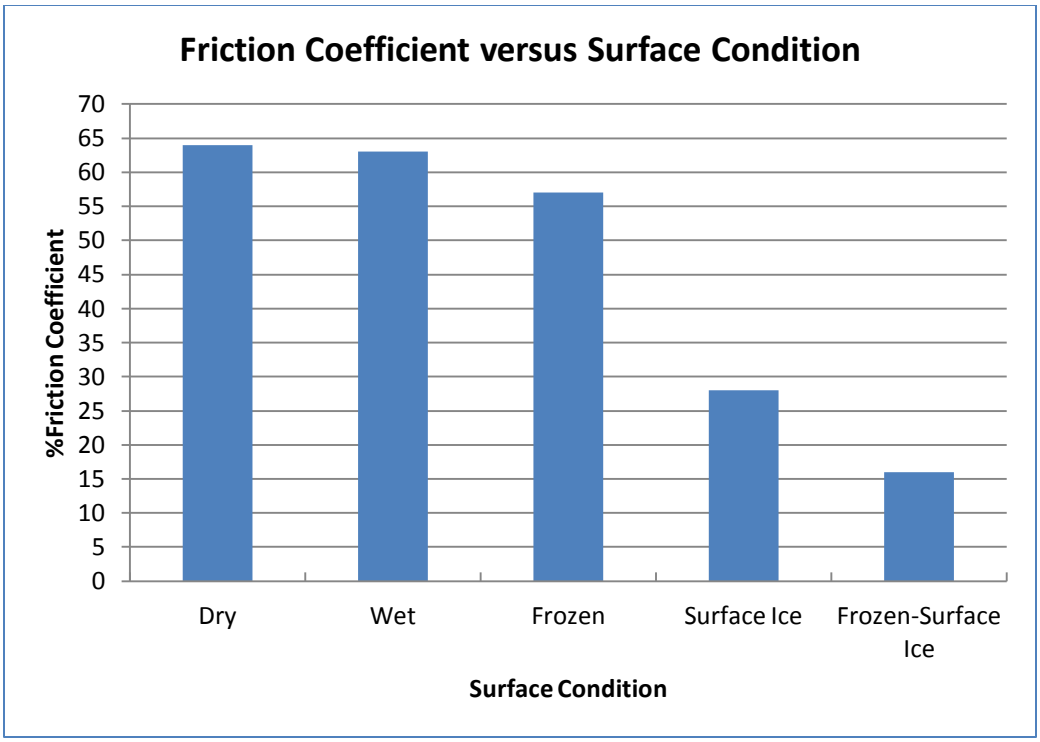

Figure 4.7-2: Friction results under different surface conditions

4.8 Discussion of SP-I results (LUS Poles)

Looking at all the 13 test results for LUS poles, it is clear that areas associated with ice formation could be isolated and detected, figures 4.8-1 and 4.8-2 show the plots for all the tests together. It could be noticed that results of cold dry sensor for example for a particular temperature or range of temperatures are well separated from results for conditions that have surface ice for the same temperature or range of temperatures. Output as voltage or resistance could be used to indicate to the condition of the surface. For instance, for temperature range

-8C˚ (18F˚) to -2C˚ (28F˚), if the output voltage ranges between +1.75v to +1.25v, it can be concluded that the surface is completely dry, while if the range is between +1.0v and 0v, there is ice on the surface. The output voltage response is linear with temperature in

this zone, and the slope is on the order of -0.1v/C˚. Similar overall response is observed if there is deicing salt on the surface. According to the results, salt presence did not affect the overall shape of the plots. However, it drove the resistance and voltage values lower. Therefore, a range of voltage or resistance should be found for the sensor's output that would include the effect of salt presence and the surface condition that is associated with it (dry, frozen, surface ice, etc). Also, there is no interference between the points of interest (surface ice, frozen, frozen-surface ice) with the dry condition under the same temperature or range of temperatures. There is however one potential interference area between surface ice and frozen condition when sale contamination exist. Since the friction test showed that the coefficient of friction for frozen surface is slightly lower than the dry condition, the frozen condition should be distinguish from surface ice or frozen-surface ice. Friction for the Frozen-Surface ice combined was the worst (lowest), so logic in the electrical circuit could be developed to separate between the frozen condition and the combination of Frozen-Surface ice condition. Since the LUS poles result in this zone of interference for salt-contaminated surfaces, the LU poles were developed to conclusively separate the two conditions.

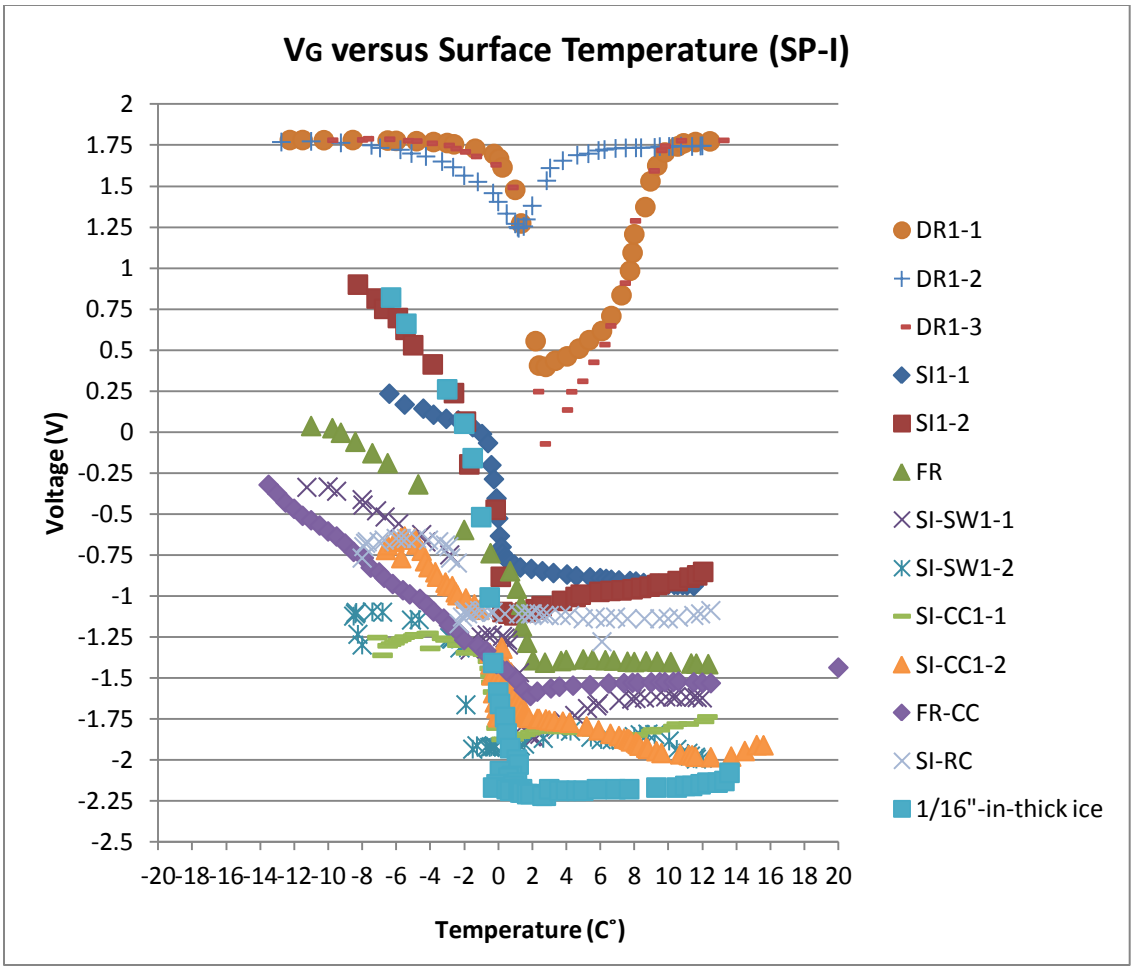

Figure 4.8-1: Output voltage versus surface temperature for SP-I all tests

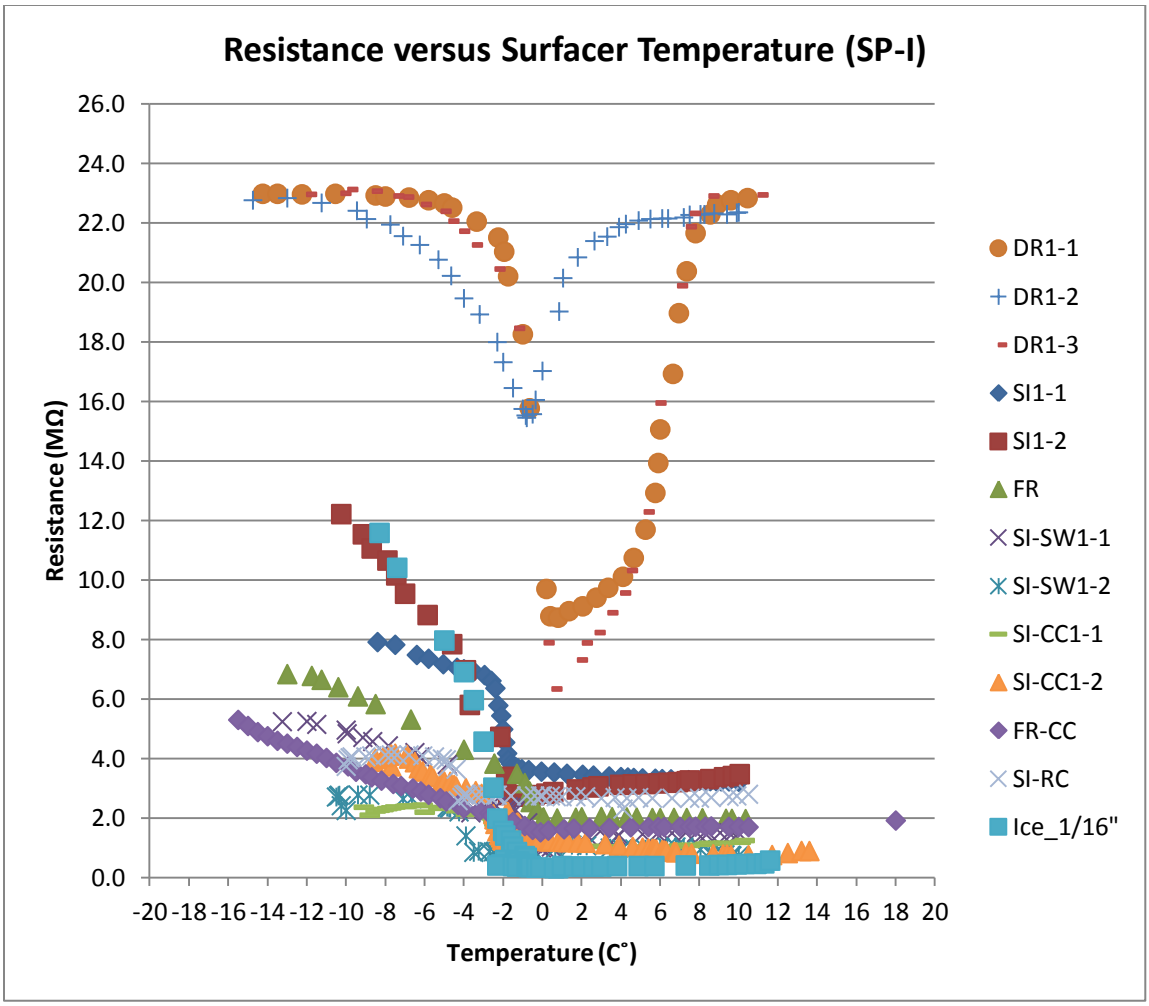

Figure 4.8-2: Resistance versus surface temperature for SP-I all tests

When surface temperature is above -2C˚ (28F˚) and the output voltage is the range of -2.25v to -0.75v, the surface condition is wet. As the output voltage approaches -2.25v, the wetness increases.

4.9 Discussion of SP-II results (LU Poles)

The primary reason for the addition of the LU poles is to conclusively distinguish between frozen and surface ice condition. The sensor prototype II has provided that as

shown in figures 4.9-1 and 4.9-2, for all surface ice tests and frozen tests. The output voltage of LU poles under frozen condition is similar to the cold dry results.

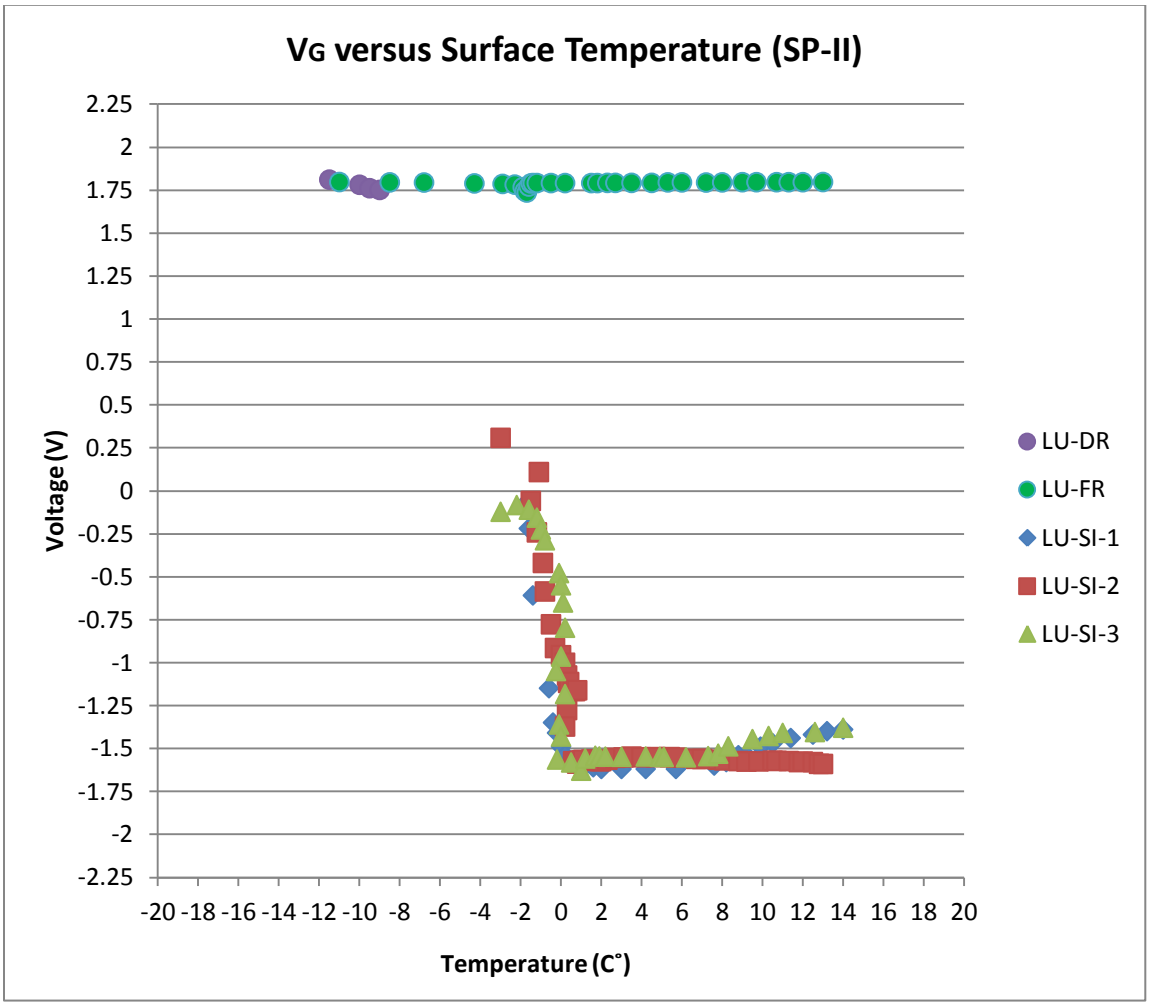

Figure 4.9-1: Output voltage versus surface temperature for SP-II all tests

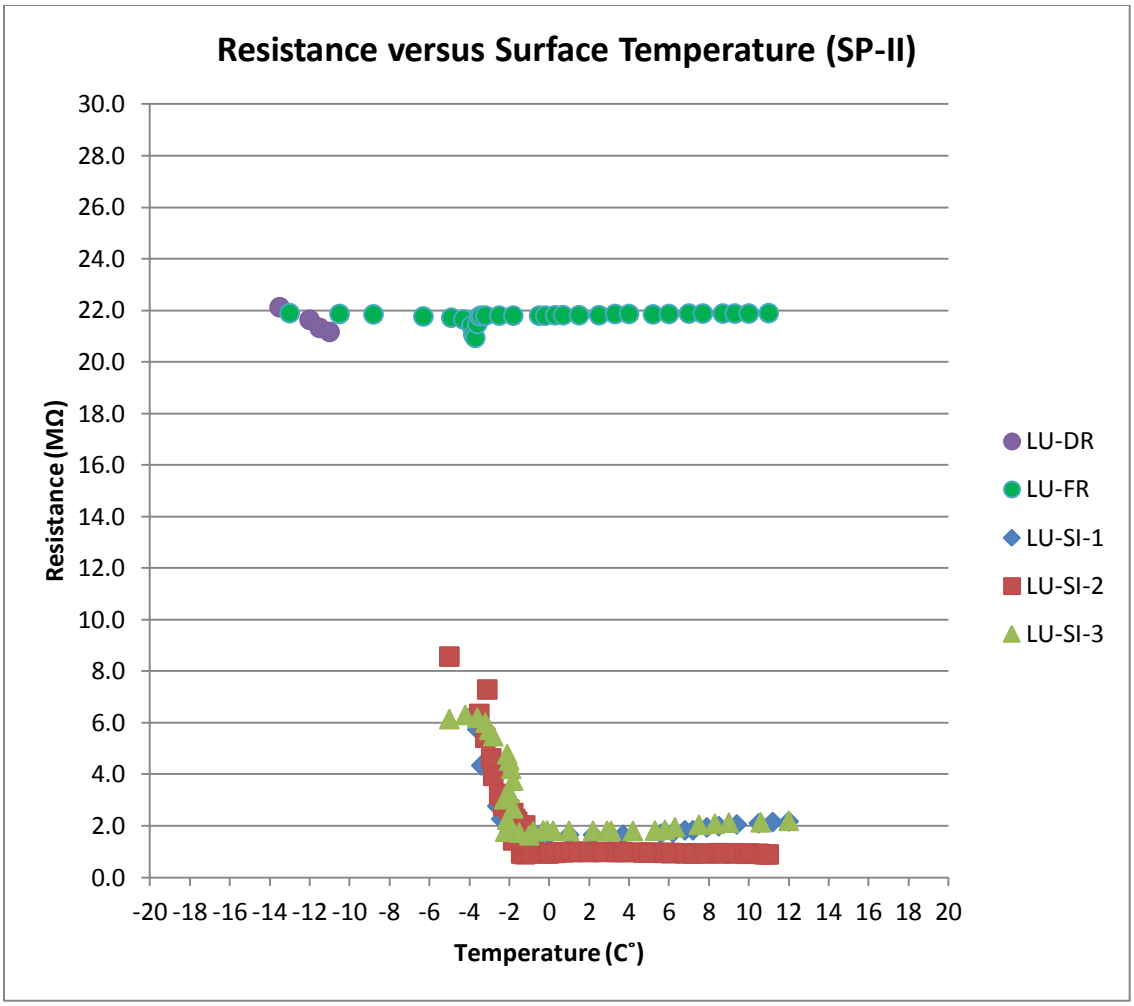

Figure 4.9-2: Resistance versus surface temperature for SP-II all tests

Therefore, frozen condition was successfully separated from the surface ice condition. With addition of the LU poles, there is no longer any ambiguity between the two outcomes. Logical algorithms can thus be developed based on these results to trigger a serious warning only when there is surface ice present. The frozen condition however could be detected by the LUS poles, and appropriate and less sever warning can be issued. As determined from the friction tests, the worst condition (most slippery) occurs when there is frozen concrete and surface ice combined.

4.10 Estimating Resistance

4.10.1 Surface Ice-Dry (SI-DR) condition

Results of Sensor Prototype I were used in these calculations. At temperature -6.4C˚ (20.5F˚), Surface resistance which is ice was measured at 11.6 MΩ, while the concrete resistance under same temperature 22.9 MΩ, as shown in Figure 4.10-1.

$$\frac{1}{R} = \frac{1}{11.6} + \frac{1}{22.9} = \frac{1}{7.7}$$

$$R = 7.7\ \text{MΩ}$$

The calculated resistance for surface ice on dry concrete is 7.7 MΩ. The measured value for surface ice on dry concrete under same temperature was 7.9 MΩ.

It should be noted that the thickness of ice affects the resistance of ice. As the thickness increases, more parallel resistors appear, and the overall resistance decreases.

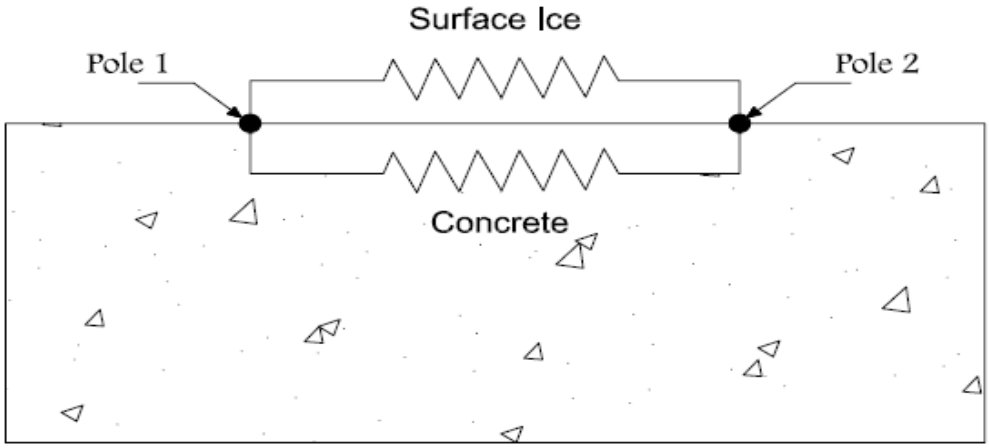

Figure 4.10-1: Dry Concrete-Surface Ice Resistance

The difference between estimated and measured resistance under surface ice condition was not significant. This way of calculation could be used if the surface and concrete resistance were known for certain condition and circumstances.

4.10.2 Frozen-Surface Ice (FR-SI)

At temperature -6.5C˚ (20.3F˚), concrete resistance under frozen (saturated) condition was 5.8MΩ. Surface resistance is equal to ice resistance which is 11.6MΩ, as shown in Figure 4.10-2.

Hence;

$$\frac{1}{R} = \frac{1}{5.8} + \frac{1}{11.6} = \frac{1}{3.9}$$

Which means that the resistance of frozen-black ice =3.9 MΩ. The test has shown that the measured resistance was 4.2, which is still close to what was measured.

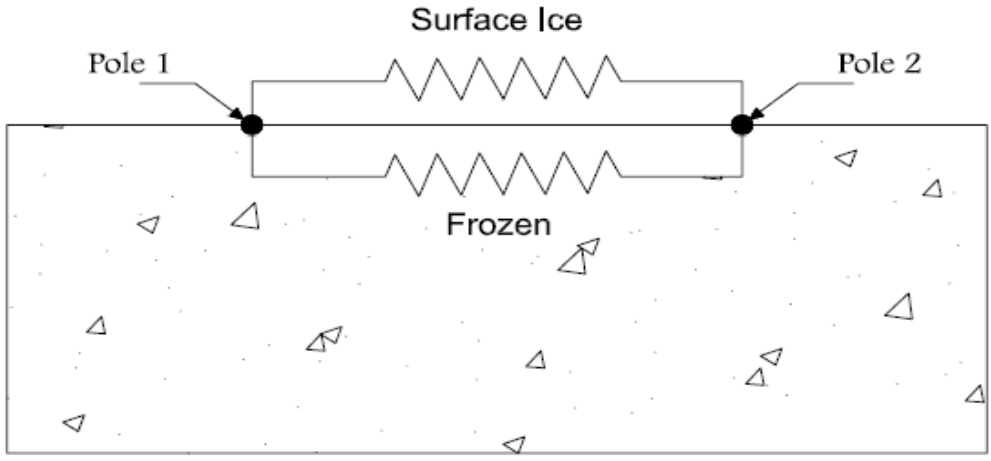

Figure 4.10-2: Frozen-Surface Ice Resistance

Chapter 5: Decision Algorithm

Results of the previous chapter's tests are listed in table (5-1). Figures 5-1 and 5-2 show zones of all tests (surface ice, frozen, dry, and wet) for both LU S and LU poles, respectively. Based on the tests results a decision algorithm was written.

Table 0-1: Diagnostic guide table

Poles	Surface Condition	Surface Temperature (˚C)	Output Voltage (v)
LUS	SI	-15 → -9	0 → +1.25
		-9 → 0	-0.8-0.1T → +0.13-0.14T
	FR	-15 → -8	-2.1-0.1T→ 0
		-8 → 0	-2.1-0.1T → 0.8-0.1T
	W	0 → 40	-1.0 → -2.0
	D	-15 → 40	+1.5 → +2.0
LU	SI	-15 → 0	-1.0 → +1.0
	FR	-15→ 0	+1.5 → +2.0
	W	0→ 40	-1.0 → -2.0
	D	-15 → 40	+1.5 → +2.0

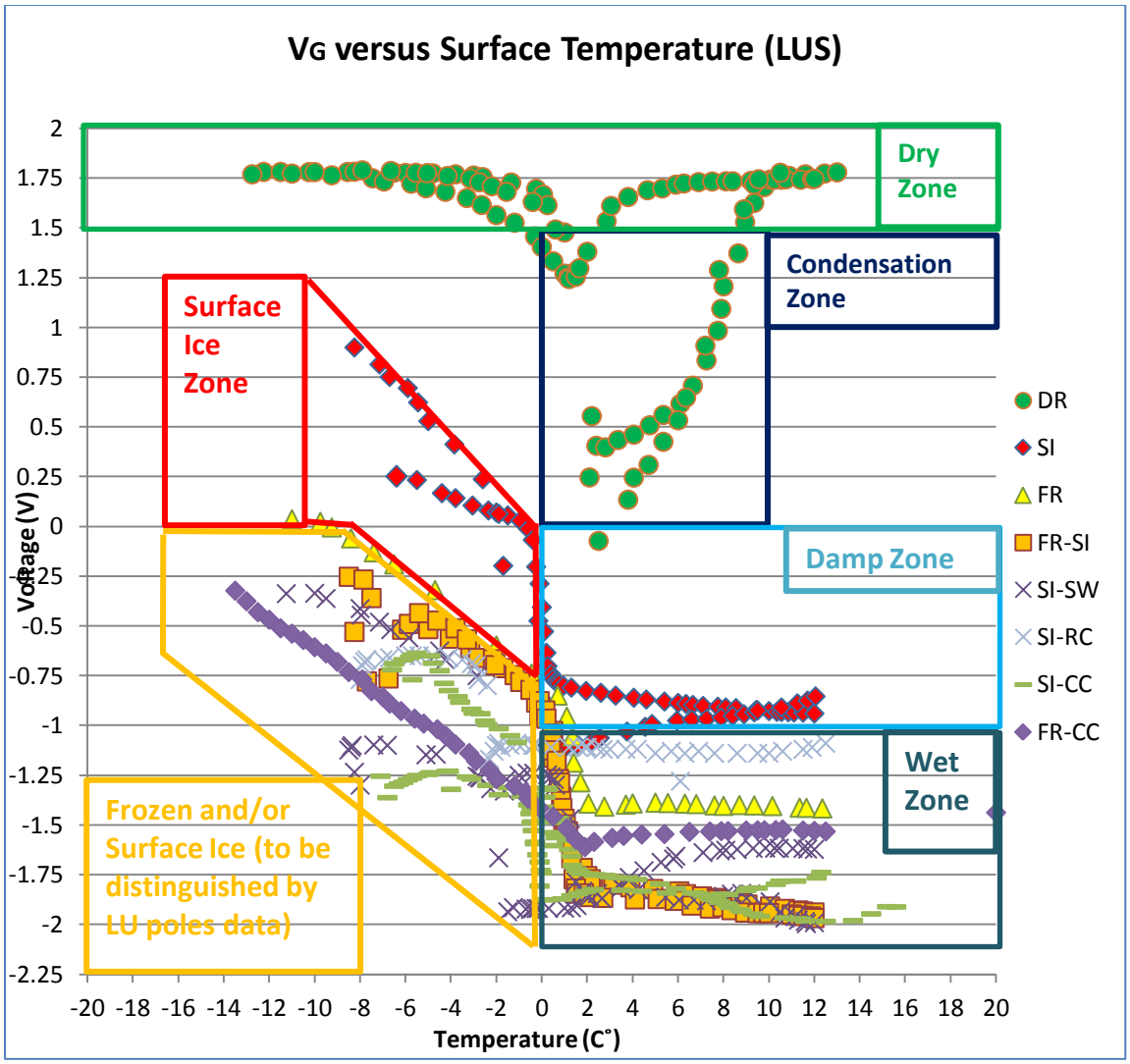

Figure 5-1: Zones of LUS tests results

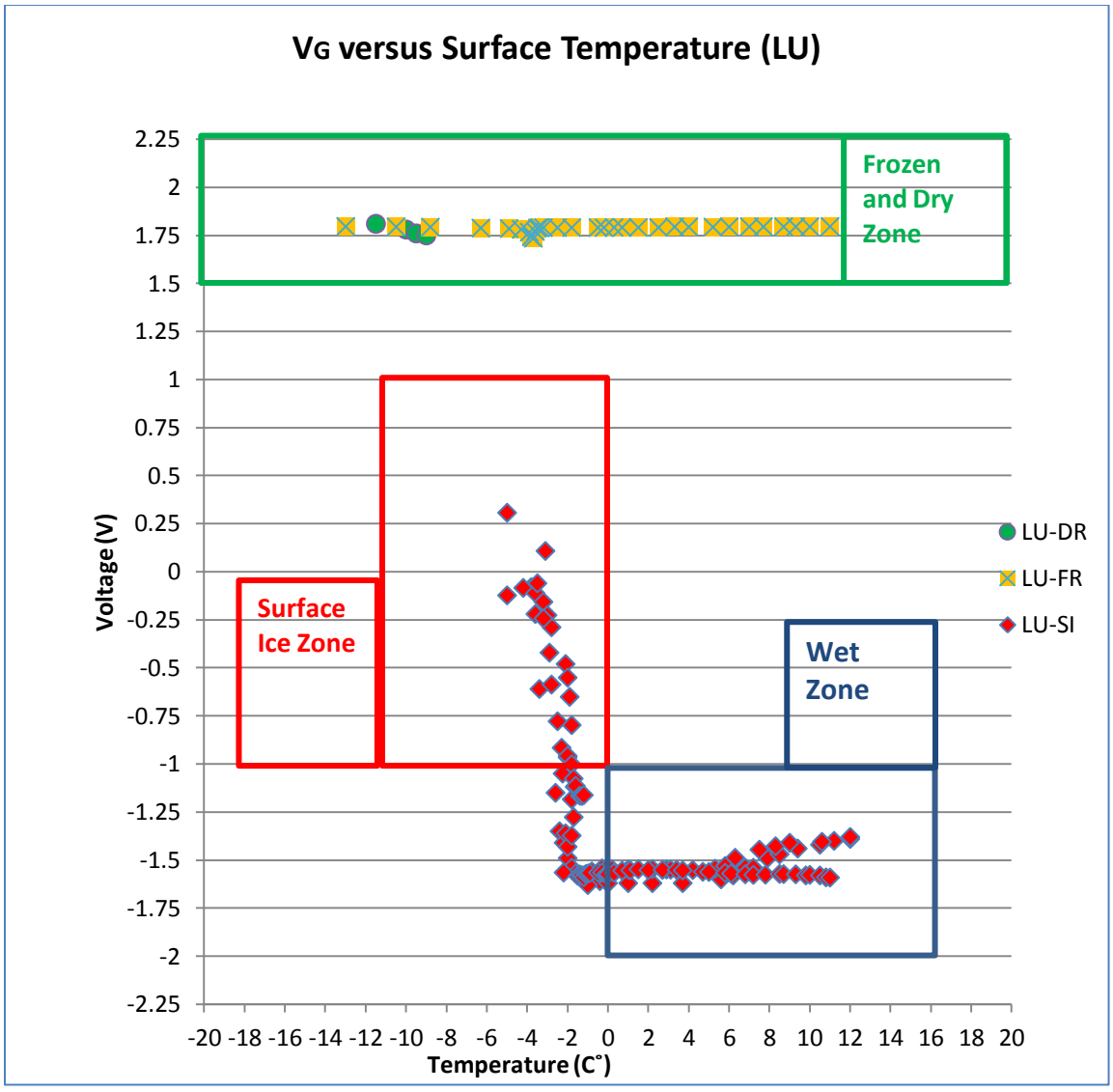

Figure 5-2: Zones of LU tests results

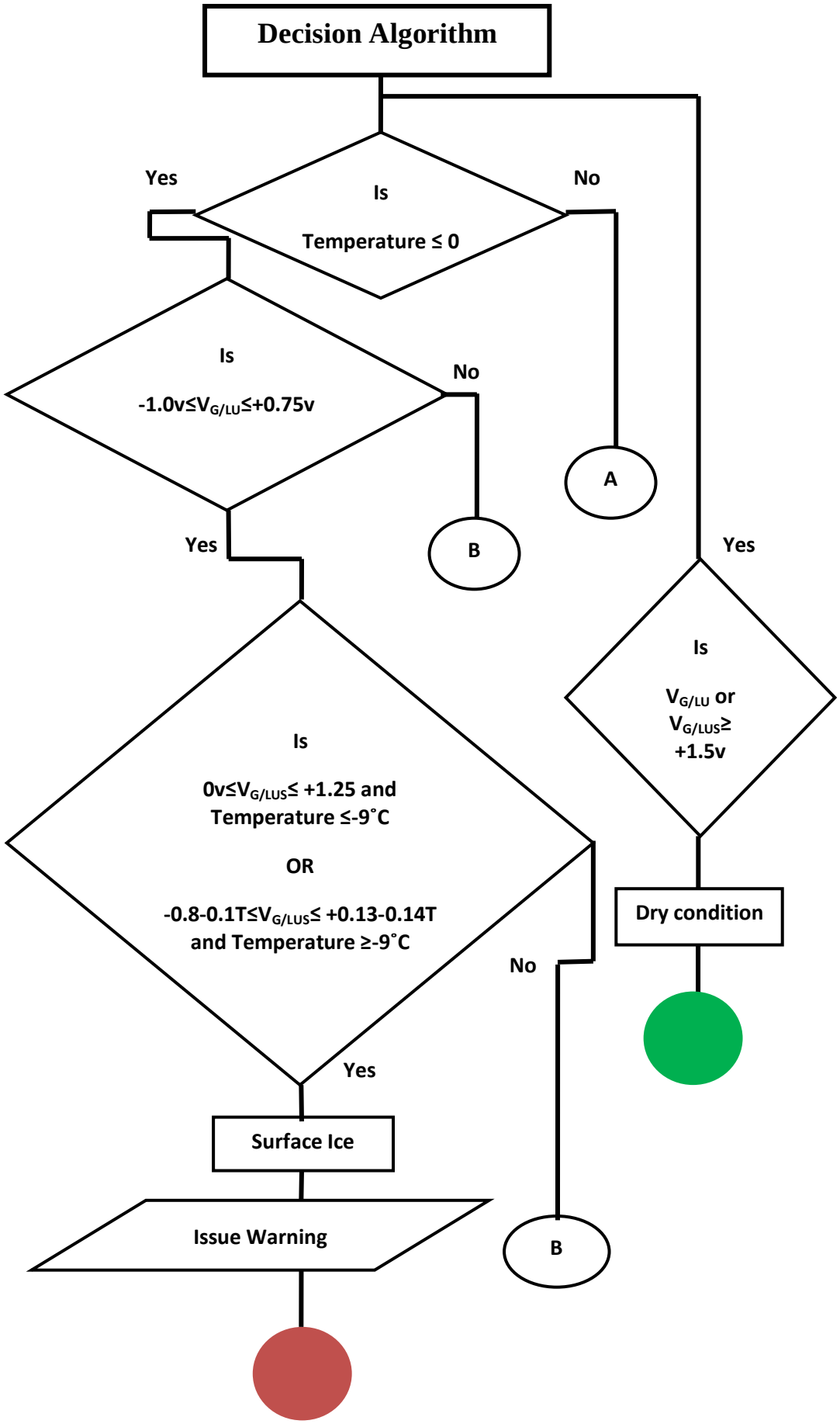
Decision Algorithm
Is
Temperature ≤ 0
Yes
No
Is
-1.0v≤V_G/LU≤+0.75v
No
Yes
A
B
Yes
Is
V_G/LU or
V_G/LUS≥
+1.5v
Is
0v≤V_G/LUS≤ +1.25 and
Temperature ≤-9˚C
OR
-0.8-0.1T≤V_G/LUS≤ +0.13-0.14T
and Temperature ≥-9˚C
No
Yes
Dry condition
Surface Ice
Issue Warning
B

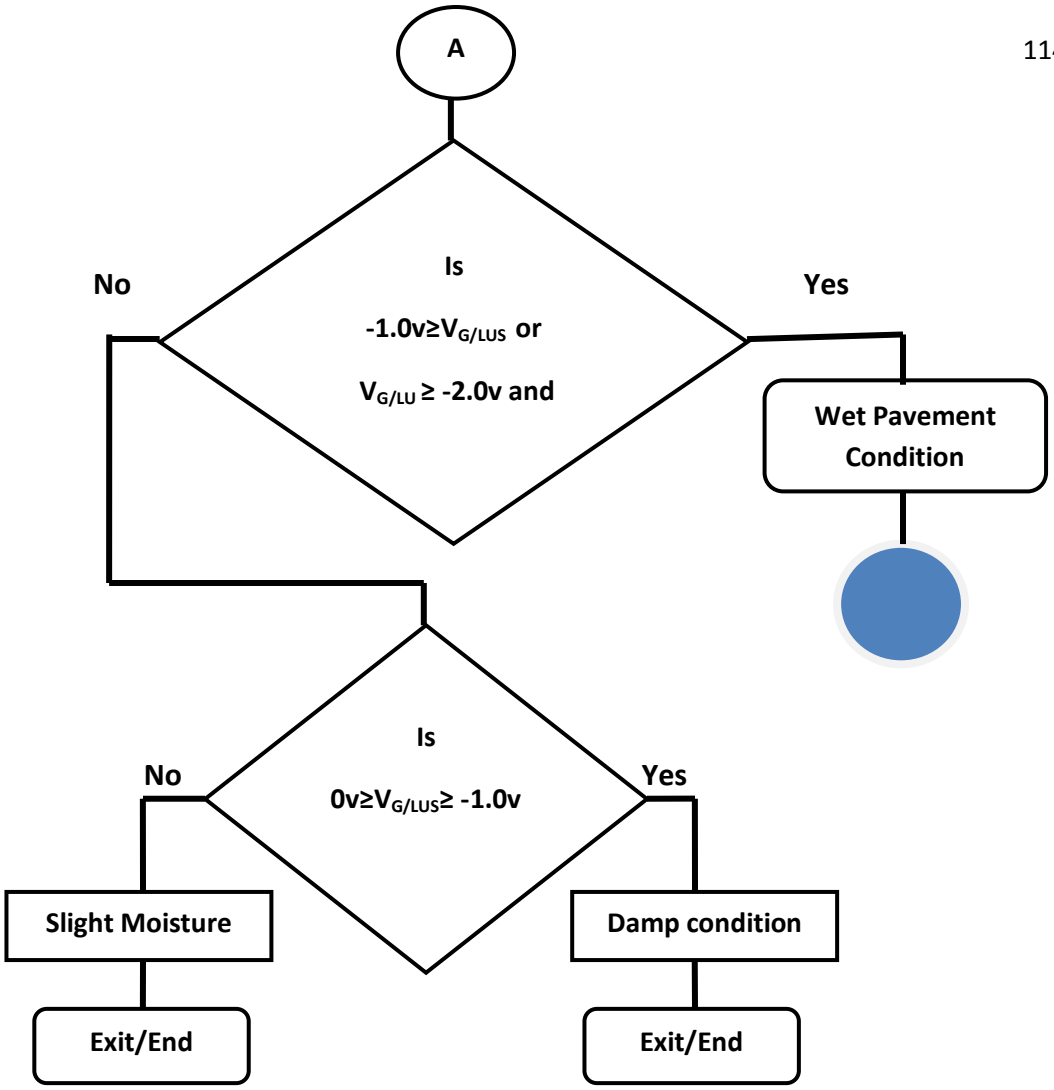
A
Is
-1.0v≥V_G/LUS or
V_G/LU ≥ -2.0v and
No
Yes
Wet Pavement Condition
Is
0v≥V_G/LUS≥ -1.0v
No
Yes
Slight Moisture
Damp condition
Exit/End
Exit/End

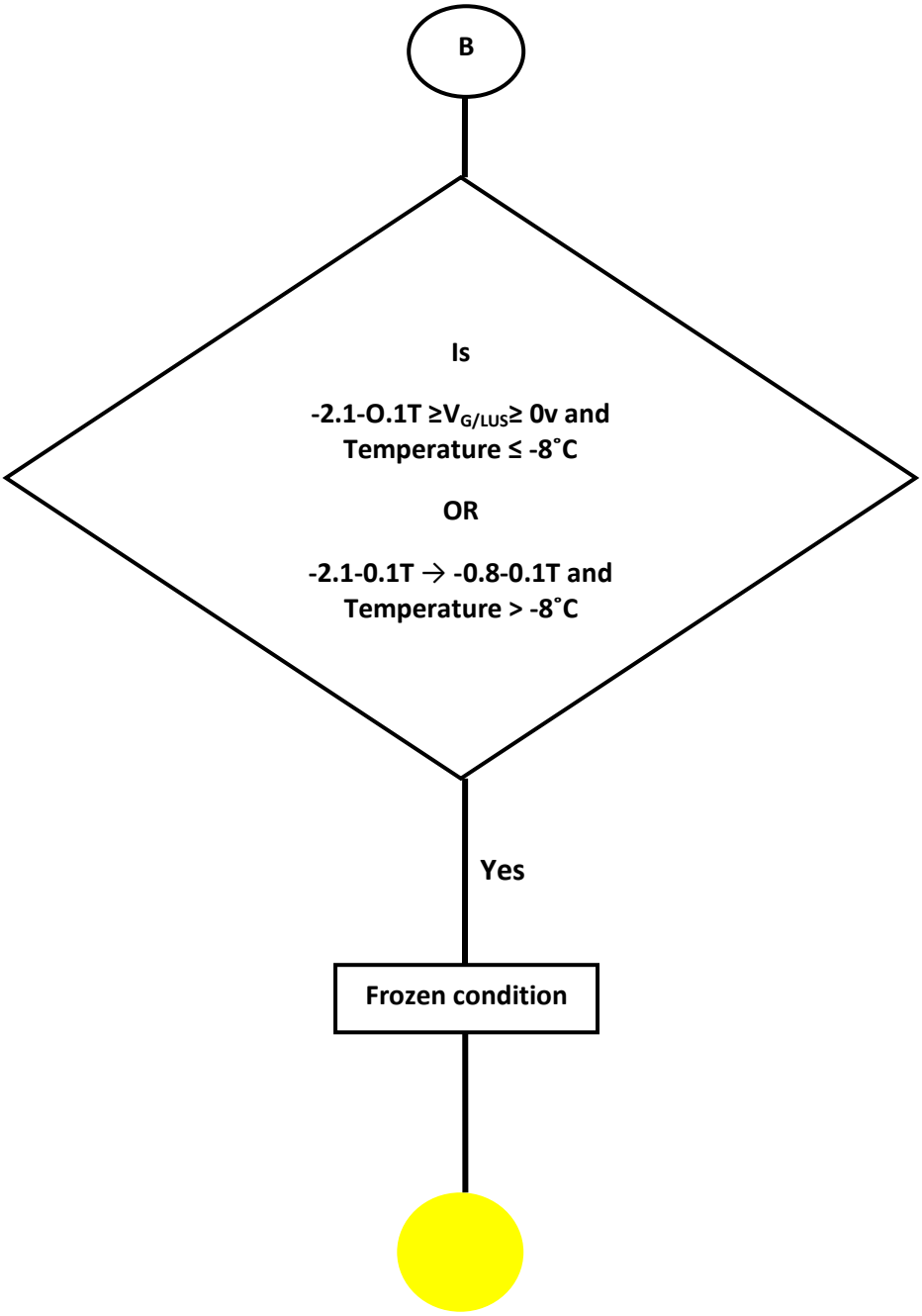
B
Is
-2.1-O.1T ≥$V_{G/LUS}$≥ 0v and
Temperature ≤ -8˚C
OR
-2.1-0.1T → -0.8-0.1T and
Temperature > -8˚C
Yes
Frozen condition

Chapter 6: Summary and Conclusions

This research aimed to develop an intelligent sensor system for detection of ice conditions on roadways, runways, bridge decks, and other surfaces. Several tests were done using two sensors prototypes under different conditions (e.g. dry, surface ice, frozen, wet, etc) to simulate the effect of weather conditions on sensor output. The resistance across two stainless steel poles, embedded at the surface of the concrete sensor, was monitored to develop a relationship between changes in surface temperature and the measured electrical resistance. Results have shown that the measured resistance could be an effective basis for detection and reporting of surface ice, frozen concrete and wet conditions.

Two sets of poles are used in each sensor; the LUS (Look-Up and Side) poles and LU (Look-Up) poles. Information from both poles is used to detect and confirm various conditions. Moisture presence drives the resistance (output voltage) lower, and the thickness of ice layer affects the resistance (resistance decreases when the thickness of the ice increases). On the other hand, chloride contamination from deicing salt reduces the resistance of the concrete.

Results of several tests have been conducted on LUS and LU poles under frozen and surface ice conditions have shown that these two conditions are distinguishable. A decision algorithm based on measured surface temperature and output voltage of both sets of poles has been developed. The findings of friction tests indicated that the most dangerous conditions (from the friction-standpoint) are surface ice and a combination of frozen concrete and surface ice condition. The decision algorithm is designed to distinguish and identify surface conditions and to issue different warning levels

accordingly. The proposed decision algorithm considers the effects of salt contamination on roadway surface.

The developed sensor system will have two embedded Wheatstone bridge circuits, a long-term battery, a logic controller, and a local-area signal transmission capability. The signal can either be used for local site warning signal/ lights/ messages, or can be relayed to a transportations control center, displayed on a web site, or communicated to vehicle information system. The sensor could also transmit coordinates of its location. The warnings could be received by drivers, transportations authorities, and vehicle control systems to warn drivers of surface ice formation.

Ultimately, the findings of this study could be used in many different fields and applications. The concepts presented in this study could be used in detecting ice presence on aircraft wings, cables of the cable-stayed bridges, or any other application where the ice formation may be an issue. Finally, the proposed sensor relies on low-cost and simple technologies that could be applied on a mass scale.

Recommendations for Future Research

The sensor system can be further developed through field testing and enhancement of the detection algorithm. An asphalt based sensor could be developed and a sensor with LU poles could be developed for aircraft and other applications. Communications systems for traffic operations centers and autonomous vehicles could be developed as well.

References

1- M. Clifford, R. Steed, “Roadway Icing and Weather” Department of Atmospheric Science, University of Washington, [online].

2- [http://www.atmos.washington.edu/cliff/Roadway2.htm] , (accessed Jan. 2014).

3- D. Robinson,” The Top 7 Icy roads Myths”, [http://www.icyroadsafety.com/blog/top_7_icy_road_myths.shtml], (accessed Feb. 2014).

4- D. Robinson, “Icy Road Fatality Statistics” , [http://www.icyroadsafety.com/fatalitystats.shtml], (accessed Jan 2014).

5- H. Yan, J. Sterling, “What other cities can learn from Atlanta ice debacle” [http://www.cnn.com/2014/01/30/us/atlanta-ice-how-it-happened/index.html?iref=allsearch], (accessed Jan. 2014).

6- D. Robinson, “Report: High Risk road icing event in south Texas/Louisiana”, [http://www.icyroadsafety.com/blog/jan2614a.shtml], (accessed Jan 2014).

7- A. Augenstein, “Hundreds of accidents reported on N.J. icy roads this Morning”, [http://www.nj.com/news/index.ssf/2014/01/hundreds_of_crashes_reported_on_nj_icy_roads_this_morning.html], (accessed Jan 2014).

8- D. Behm, “Snow makes mess of southeast Wisconsin roads, with crashes widespread”, [http://www.jsonline.com/weather/snowstorm-hits-southeast-wisconsin-could-drop-up-to-6-inches-b99159180z1-234958401.html], (accessed Jan 2014).

9- D. Robinson, “Road icing news for January-Feberuary 2012”,[www.icyroadsafety.com/blog/], (accessed Jan.2014).

10- G. A. Hoover, “Aircraft Ice Detectors and Onground and Inflight Applications”, (FAA Technical Center, Atlantic City International Airport), April 1993.

11- Magenheim, “Microwave Ice Detector” ,US patent 4054255, Oct. 18,1977.

12- Chamuel , “Ultrasonic Aircraft Ice Detector Using Flexural Waves”, US patent 4461178, Jul. 24, 1984.

13- Federow et al., “Laser Ice Detector” US patent 5296853, Mar. 22, 1994.

14- Kim, “Fiber Optic Ice Detector”, US patent 5748091, May 5, 1998

15- F. Rios-Gutierrez, M.A. Hassan. “Survey and Evaluation of Ice/Snow Detection Technologies”, (Northland Advanced Transportation Systems Research Laboratories), [http://www.d.umn.edu/natsrl/documents/FY2003reports/IRID_2003.pdf] (accessed Feb. 2014).

16- Anonymous, “Remote ice detection”, [www.sensice.com], (accessed Feb. 2014).

17- Anonymous, “VVT’s technology makes driving on black ice safer”, [http://www.vtt.fi/news/2013/23012013_liukkaudentunnistin.jsp?lang=en], (accessed Jan. 2014).

18- Anonymous, “Intelligent Ice Detector System”, [http://www.roadtraffic-technology.com/contractors/traffic_man/sernis/pressintelligent-ice-detector-system.html], (accessed Feb. 2014).

19- Rendon, “Method and System for Detecting Potential Icy Roads on Roads”, US Patent 5416476, May 16, 1995.

20- Decker, “Road Surface Ice Detector and Method for Vehicles” , US patent 4274091, June 16, 1981.

21- Anonymous, “Electrical resistivity of geologic materials” , “Geophysics foundations: physical properties”, [online].

22- [http://www.eos.ubc.ca/ubcgif/iag/foundations/properties/resistivity.htm], (accessed Dec. 2013).

23- G. E. Monfore, “The Resistivity of Concrete”, Journal of the PCA Research and Development Laboratories, vol. 20, P.35-48, May 1968.

24- A. Yazdanbakhsh, Z. Grasley, B. Tyson, and R.K. Abu Al-Rub, “Distribution of Carbon Nanofibers and Nanotubes in Cementitious Composites”, Transportation Research Record, P.89-95, 2010

25- Hammond, E., and Robson, T. D., “Comparison of Electrical Properties of Various Cements and Concretes” The Engineer (London), 199, No. 5165, 78-80, and No. 5166, 114-115 (January 21 and 28, 1955).

26- Dorsch, K. E., “Cement and Cement Manufacturing”.

27- Anonymous, “What Is Soil Resistivity Testing?”, [Online],”*E&S Grounding Solutions”* [http://www.esgroundingsolutions.com/about-electrical-grounding/what-is-soil-resistivity-testing.php], (accessed Feb. 2014).

28- Ali A. R., Amirreza P., Mahdi M., Faramarz M., “Practical evaluation of relationship between concrete resistivity, water penetration, rapid chloride penetration and compressive strength”, P. 2472-2479,Vol. 25, May 2011.

29- Daintith, John Martin, Elizabeth (2010). Dictionary of Science (6th Edition), Oxford University Press, [Online].

30- [http://app.knovel.com/hotlink/toc/id:kpDSE00001/dictionary-science-6th, (pp. 874).

31- M.M.S. Anand, “Electrical Instruments and Instrumentation Technology”, P190-192, March, 2006.

32- Pendulum Friction Coefficient Meter, Operation manual, Shanghai Civil& Road Instrument Co., Ltd. P(2-3).